課程博士

学位授与年月：2019 年 3 月

関西大学審査学位論文

博士論文

Buta-1,3-diene production via oxidative dehydrogenation of n-butene with metal oxide catalyst

理工学研究科・総合理工学専攻

エネルギー工学領域

16D6005

清川　貴康

博士論文要旨

理工学研究科総合理工学専攻
エネルギー工学領域
16D6005
清川　貴康

＜論題＞

Buta-1,3-diene production via oxidative dehydrogenation of n-butene with metal oxide catalyst

（金属酸化物触媒を用いる n-ブテンの酸化的脱水素反応によるブタ-1,3-ジエン生成）

＜概要＞

ブタ-1,3-ジエン（BD）は合成ゴムや樹脂などの原料として用いられており、その需要は年々増加している。現在、BD のほとんどはナフサのスチームクラッキングにより製造されている。しかし、このプロセスは主にエチレンを製造しており、BD は副生成物として製造されるため選択性が低い。また、この反応は吸熱反応であり、高い反応温度を必要とするエネルギー多消費プロセスでもある。それゆえ、BD の生産効率が低いことが問題である。一方で近年、エチレンを安価に製造するために、スチームクラッキングの原料がナフサから、シェールガス由来の安価なエタンに代わってきている。原料がナフサからエタンに代わることで、BD の生産量が低下し、今後の BD 供給が懸念されている。そのため、BD 製造の代替技術の開発が求められている。

その代替技術の一つとして、金属酸化物触媒を用いる n-ブテンや n-ブタンの酸化的脱水素反応（ODH）がある。この反応は BD のみを選択的に製造でき、発熱反応であるため、省エネルギープロセスとして注目されている。本反応に有効な触媒として、酸化鉄系や Bi-Mo 系などの金属酸化物触媒が数多く報告されている。しかし、ODH は酸素共存下で反応を行うため、CO_2 への完全酸化反応が容易に進行する。これを抑制するために、大過剰のスチーム共存下で反応が行われているが、余分なエネルギー投入を生む問題がある。他の方法として、金属酸化物の格子酸素のみを用いて、BD を高選択的に製造する方法も検討もされているが、使用された格子酸素の再生工程が必要であるため、多段階なプロセスとなる。以上より、酸素共存下で選択的に BD を合成できる触媒の開発が求められている。

本研究では、n-ブテンと酸素共存下で高効率に BD を製造できる金属酸化物触媒の検討を行った。完全酸化反応を進行させないためにも、低温で反応を進行させる触媒に着目し、高 BD 選択性を得ることができる触媒の開発を行った。低温下の ODH では、酸化銅系触媒に着目した。また、既存の酸化鉄系触媒に代わる新規かつ高性能な酸化鉄触媒の開発も行った。

第 1 章　＜**General introduction**＞

第 1 章では、本研究の背景、目的をまとめた。

第 2 章　＜**Oxidative dehydrogenation of but-1-ene with lattice oxygen in ferrite catalysts**＞

第 2 章は、フェライト触媒の格子酸素を用いる 1-ブテンの ODH について記述している。初めに、様々なフェライト系触媒の格子酸素の有効利用に着目した。種々のフェライト触媒の格子酸素の反応性を検討した結果、銅フェライト触媒が、300 ºC 以下の低温で ODH を進行させた。この触媒を用いて、1-ブテンの ODH に及ぼす反応温度の影響を検討したところ、270 ºC で 39.9%の BD 選択率、8.5%の高い BD 収率を得ることができた。また、反応前後の XRD および XPS 分析により、ODH はフェライト中の Cu に結合する格子酸素で進行することが明らかとなった。一方で、繰り返し ODH 反応（格子酸素による ODH と酸素による再生のサイクル）を行った際、10 回の繰り返し試験において BD 収率は維持された。この結果から、銅フェライト触媒の格子酸素は容易に再生でき、1-ブテンの ODH に対して再利用できることを明らかにした。

第 3 章　＜**Oxidative dehydrogenation of but-1-ene at low temperature with copper ferrite catalysts**＞

第 3 章では、銅フェライト触媒を用いる 1-ブテンの ODH について述べている。第 2 章で、銅フェライト触媒の格子酸素は 1-ブテンの ODH に有効に用いられることを明らかにした。そこで、本章では酸素と 1-ブテンを同時に供給し、連続的な BD 生成を試みた。1-ブテンの ODH に及ぼす、触媒の調製条件、反応条件の影響について検討を行ったところ、活性炭共存下、Cu/Fe=1/2 で調製を行った銅フェライト触媒が、270 ºC、1-ブテン/O_2=5/5 (mL/min) の条件下において、45.6%の BD 選択率、15%の高い BD 収率を示した。また、BD 収率は 100 分間維持されたため、長時間にわたる BD 製造が可能であることも示された。反応前後の XRD および XPS 分析により、完全酸化反応は、反応中に生成した Cu_2O に起因し、ODH には銅フェライトの結晶構造と価数（Cu^{2+}）の維持が必要であることも示された。

第 4 章　＜**Selective buta-1,3-diene production via oxidative dehydrogenation of but-1-ene with CuO-loaded catalyst**＞

第 2 および 3 章で得られた結果より、低温下における 1-ブテンの ODH は銅酸化物種上のみで進行することが示された。そこで本章では、活性種として銅酸化物種を多く有する酸化銅担持触媒に着目し、ODH 活性、BD 選択性の向上を目指した。種々の担体に CuO を担持した触媒を用いて 1-ブテンの ODH を行ったところ、高比表面積を有する SiO_2 に担持した CuO 触媒が高い BD 収率（8.1%）を示した。次に、担持量ならびに焼成温度の影響について検討を行ったところ、700 ºC で焼成した 5 wt%CuO 担持 SiO_2 触媒が、最も高い BD 選択率（92.8%）および高い BD 収率（11.4%）を与えた。CuO 担持 SiO_2 触媒はスチームなしの酸

素下の反応において、高選択的な BD 製造を可能にする触媒であることが示唆された。N_2O パルス、XRD および XPS を用いて触媒の分析を行ったところ、選択的に BD を製造するためには、高い銅比表面積を有し、結晶性 CuO や mono-(μ-oxo)-dicopper のような銅酸化物種を含まない銅酸化物種が必要であることが示された。

第 5 章　＜**Oxidative dehydrogenation of n-butene with novel iron oxide based catalyst**＞

n-ブテンの ODH に及ぼす金属酸化物触媒の結晶構造の影響はよく検討されており、その広範な研究は ODH に高活性を示す触媒の開発に重要であると考えられる。一方、酸化鉄はα-、β-、γ-、ε-Fe_2O_3 など多様な結晶相を持つことが知られている。しかし、酸化鉄の結晶相が ODH に及ぼす影響は未だ検討されていない。そこで第 5 章では、酸化鉄の結晶相が n-ブテンの ODH に及ぼす影響について詳細な検討を行った。また、長時間の反応における活性維持の検討も行った。種々の酸化鉄系触媒（α-、β-、γ-、ε-Fe_2O_3、Fe_3O_4、$ZnFe_2O_4$）を用いて 1-ブテンの ODH を行った結果、ε-Fe_2O_3 が 39.3%の BD 選択率、最も高い BD 収率（17.1%）を与えた。ε-Fe_2O_3 が本反応系に用いられた報告例はなく、新規な触媒として提案した。しかし、ε-Fe_2O_3 相の安定性が低く、BD 収率は反応時間に伴い低下した。そこで、安定性向上を目的に SiO_2 を添加したε-Fe_2O_3 を用いて反応を行ったところ、4 h の間、65%以上の高い BD 選択率ならびに、18%以上の高い BD 収率が維持された。SiO_2 の存在により、ε-Fe_2O_3 構造の安定化および触媒の酸化還元特性が向上し、これらが ODH 活性の維持に寄与したと考えられた。また、本触媒は *cis*-2-ブテンの ODH にも適用でき、n-ブテンの ODH における新規かつ高性能な触媒として提案した。

第 6 章　＜**General conclusions**＞

本研究で得られた結果を総括した。

以上

Contents

Chapter 1

General introduction

Usefulness of buta-1,3-diene

Buta-1,3-diene (BD) is one of important petrochemical materials for producing styrene butadiene rubber (SBR), butadiene rubber (BR), styrene butadiene latex, acrylonitrile butadiene styrene resins (ABS), and nitrile rubber. Among them, synthetic rubbers such as SBR and BR are mainly produced, and more than 50% of BD is used for the production of SBR and BR. These demands tend to increase because of the development of the automotive industry in emerging economies such as China, India, and Brazil. In 2012, 10 million tons of BD are produced, and the global BD demand is expected to reach 14 million tons in 2020 [1-3].

BD production

Steam cracking of naphtha

The world's BD of over 98% is supplied by the steam cracking of naphtha. Since this process can produce the light olefins such as ethene and propylene, BD is produced as a byproduct, and it is included in one of the C4 fraction (n-butane, n-butene, and BD). Then, BD is obtained by extracting from C4 fraction. For the above reasons, this process can not produce BD efficiently. Moreover, the steam cracking process needs a high temperature and is an energy consuming process, because this reaction is endothermic. The formation of coke by the thermal decomposition of organic compounds is also a problem [1, 4].

There are other problems with stem cracking of naphtha. Recently, ethane is cheaply obtained due to the shale gas revolution. In order to reduce ethene production cost, the substrate used for the steam cracking tends to transfer from naphtha to light parafins such as ethane. Since the steam cracking of ethane can produce almost only ethene, this trend affects the production of BD. If the feedstock of steam cracking changes from naphtha to ethane, the BD productivity seems to decline from 0.13 to 0.02 (BD kg/ethene kg) [2]. Although ethene is cheaply produced over a long period, the supply of BD in the near future is worried. Hence, the development of an alternative process is required.

BD production with direct dehydrogenation

As an alternative process of steam cracking of naphtha, direct dehydrogenation of n-butane and n-butene has been investigated (Eq. (1)) [5].

$$C_4H_8 \rightarrow C_4H_6 + H_2 \qquad \Delta H^o = 109.7 \text{ kJ/mol} \quad (1)$$

In this process, the high BD selectivity and BD yield can be obtained [6]. However, catalytic dehydrogenation process has some problems; supplying heat due to endothermic reaction, deep cracking to light organic compounds, the formation of coke and the deactivation of catalyst with the coke deposition [7-9]. Since the excessive step is necessary to regenerate the deactivated catalyst, the production of BD for a long term is difficult [10].

BD production with oxidative dehydrogenation

Oxidative dehydrogenation (ODH) of n-butane and n-butene with O_2 has also attracted much attention as an alternative process of BD production (Eq. (2)) [1, 10].

$$C_4H_8 + 1/2O_2 \rightarrow C_4H_6 + H_2O \qquad \Delta H^o = -132.1 \text{ kJ/mol} \quad (2)$$

The ODH reaction does not need the supply of excess energy because of exothermic process. Moreover, since the formation of coke is inhibited by reacting with O_2, the ODH has a possibility which can continuously produce BD for a long time. This process is very useful from a viewpoint of efficiency BD production. However, the ODH reaction contains the serious problem. The deep oxidation reaction of C4 compounds to CO_2 can easily proceed (Eq. (3), (4)).

$$C_4H_8 + 6O_2 \rightarrow 4CO_2 + 4H_2O \qquad \Delta H^o = -2540.8 \text{ kJ/mol} \quad (3)$$

$$C_4H_8 + 4O_2 \rightarrow 4CO + 4H_2O \qquad \Delta H^0 = -1409.0 \text{ kJ/mol} \quad (4)$$

The excessive oxidation as a side reaction must be inhibited. For the ODH of n-butene, in order to inhibit the complete oxidation, a large amount of steam is supplied with the substrate and O_2 [11]. An excessive energy is necessary because steam has the high latent heat. Therefore, the inhibition of the complete oxidation without the supply of steam is desirable.

As a new attempt, the ODH of propane or butene without oxidant has been reported [12, 13]. In these studies, only lattice oxygen of the metal oxide catalyst was used for the ODH to inhibit the complete oxidation of the reactant and the product. Furthermore, molecular O_2 was supplied after the reaction to regenerate the used lattice oxygen (Eqs. (5), (6)). Moreover, the catalytic activity was maintained throughout the repeated ODHs. As an industrial process, moving bed type reactor or fluidized bed reactor to this ODH process will be preferable to give the good performance.

$$C_4H_8 + MO_x \rightarrow C_4H_6 + H_2O + MO_{x-1} \qquad (5)$$

$$MO_{x-1} + 1/2O_2 \rightarrow MO_x \quad (6)$$

BD synthesis

Recently, synthesis of chemicals from biomass has attracted attention from a viewpoint of realization of a low-carbon society. As one of technologies, BD synthesis from bio-ethanol as a renewable resource with catalysts has been investigated [14, 15]. Since this reaction can efficiently produce BD without depending on petroleum resources, BD synthesis using bio-ethanol is an effective technology to realize the sustainable society. However, in order to contend with dehydrogenation of C4 derived from oil and gas, this technology has to overcome many problems such as BD selectivity, productivity, and the stability of catalytic performance [2]. Therefore, the extensive study seems to be desired to advance this technology in the future.

Among these BD production technologies, the ODH reaction of C4 fraction has the potential which can more efficiently produce BD, because this process does not have the problems in the steam cracking, direct C4 dehydrogenation, and BD synthesis from bio-ethanol. Hence, this process is expected as the technology that can early respond for the shortage of BD in the near future.

Oxidative dehydrogenation catalysts

Various composite metal oxides, metal oxides, and metal-supported catalysts have been investigated for the ODH of many hydrocarbons, including ethane [16-18], propane [19, 20], n-butane [21, 22], n-butene [23, 24], ethylbenzene [25-27], and cyclohexane [28, 29]. For the ODH of n-butene and n-butane, it is reported that Pt-In catalyst [30], V-containing catalysts [21, 22, 31, 32], CuO/Al_2O_3 catalyst [13], Bi-Mo catalyst [24, 33-40], and ferrite-type catalysts [23, 41-54] exhibited the high ODH activity.

Among various catalysts, Bi-Mo catalysts have been widely studied. According to the literatures, the reaction mechanism for the ODH of n-butene with Bi-Mo catalyst is known to proceed through the Mars-van Krevelen mechanism [6, 24, 33]. The Mars-van Krevelen mechanism is related to the oxidation and reduction cycle (redox cycle) with the lattice oxygen in the metal oxide catalyst. Therefore, the redox property of catalyst via the lattice oxygen is often discussed to determine the catalytic activity. For example, the effect of crystalline structure of Bi-Mo composite oxide on the ODH of n-butene has been reported. The Bi-Mo composite oxide catalyst has the various crystalline structures such as α-$Bi_2Mo_3O_{12}$, β-$Bi_2Mo_2O_9$, and γ-Bi_2MoO_6, and each structure shows the different lattice oxygen mobility [55]. J.C. Jung, *et al.* reported the catalytic activity for the ODH of n-butene is the order of γ>α, and this result is related to the reactivity of lattice oxygen [35]. γ-Bi_2MoO_6 showed the high BD yield of ca.50% at 420 ºC under following conditions; the feed composition of n-butene:oxygen:steam = 1:0.75:15, GHSV (gas hourly space velocity) of 300 h^{-1} on the basis of n-butene [35]. β-$Bi_2Mo_2O_9$ is inappropriate for use in the ODH, because it decomposes to α and γ at the reaction temperature of 400–550 ºC [34]. They also reported that mixture of α and γ showed the higher catalytic performance than that of single Bi-Mo phase because of the high lattice oxygen reactivity of γ-Bi_2MoO_6 and the high adsorption ability of α-$Bi_2Mo_3O_{12}$ to butene [36]. On the other hand, the ODHs of n-butene with multicomponent Bi-Mo catalyst including Fe [37], V [38], La [39], and Zr [40] have been also reported. The role of additional metal is to improve the catalytic performance through the lattice oxygen reactivity for butenes and the redox property of catalyst [39].

As another catalyst for the ODH of n-butene, ferrite-type catalysts have been investigated. Ferrite has the spinel structure. This chemical formula is $A^{2+}Fe^{3+}{}_2O_4$, and all

of A^{2+} and Fe^{3+} occupy either the tetrahedral or octahedral sites.

Zinc ferrite-type catalysts such as Zn-Fe [23, 41-46, 52, 53], Zn-Fe-Cr [48], and Zn-Fe-Al [49] have been widely studied for the ODH of C4 fraction. It is reported that the ODHs with ferrite catalysts proceed by the Mars-van Krevelen mechanism just like that for the ODH of n-butene with the Bi-Mo catalyst [36-38]. The reactivity of the lattice oxygen and the regeneration of the used lattice oxygen are very important for producing BD with the ODH of n-butene. However, it is also reported that the ferrite-type catalyst is deactivated as a result of the increase in Fe^{2+} produced by reducing Fe^{3+} and its isolation from the spinel phase [53, 54]. In order to maintain the reactivity of lattice oxygen to produce BD and the spinel structure, Sb_2O_4, $BiPO_4$, or SnO_2 was added as an oxygen donor to the zinc ferrite catalyst. These catalysts maintained the high ODH activity for a long time [52, 53]. On the other hand, it was reported that the zinc ferrite catalyst modified by heteropoly acid or sulfonic acid showed good catalytic performance for the ODH of but-1-ene [44, 45]. This shows that the surface acidity of the catalyst is related to the adsorption of butene in the first step of the ODH reaction, and this contributes the improvement of catalytic performance for the ODH of but-1-ene. The effect of catalyst preparation conditions on the ODH is also examined. For the zinc ferrite preparation by the co-precipitation method, it has been found that pH control was important to obtain the high but-1-ene conversion and the high BD selectivity [46]. H. Lee, *et al*., [46] reported that $ZnFe_2O_4$ prepared at pH=9 showed the high BD yield (80.2%) at 420 ºC under the following conditions; the feed composition of n-butene:oxygen:steam = 1:0.75:15, GHSV of 475 h^{-1} on the basis of n-butene.

Purpose of this study

The ODH with the metal oxide catalyst has been discussed, and a large number of catalysts that could exhibit the good performance have been proposed. However, in current reports, the ODHs of n-butene using these catalysts are mostly the energy consuming process because of the reaction conditions under excessive steam flow.

In this study, I studied metal oxide catalysts which could efficiently produce BD under the reaction conditions without steam. In order to inhibit the excessive oxidation of substrate and product, I focused on the copper oxide-based catalyst that could show the ODH activity at the low temperature. On the other hand, the effect of crystalline structure of iron oxide catalyst on the ODH of n-butene was also investigated.

The considerations in this study are given below.

Considerations

I focused on the effective utilization of the lattice oxygen in various ferrite type catalysts at the beginning, and it was founded that the copper ferrite catalyst showed the relatively high ODH activity at the low temperature of 270 ºC (Chapter 2).

Copper ferrite was used for the ODH under O_2 flow to produce BD continuously at 270 ºC. BD could be produced for a long time by optimizing the preparation conditions of catalyst and the reaction conditions. Furthermore, it was found that the ODH could be progressed on copper oxide species coordinated to ferrite structure (Chapter 3).

To improve the ODH activity and the BD selectivity during the ODH of but-1-ene at 270 ºC with the copper oxide-based catalyst, CuO-loaded various metal oxide catalysts were used for the ODH. Among various supports, CuO loaded on SiO_2 having a high specific surface area showed the high ODH activity and the high BD selectivity. It was

found that this catalyst has the potential to produce BD more efficiently (Chapter 4).

Extensive study on the effect of the crystalline structure of the metal oxide catalyst on the ODH is important to development of the catalyst which can show the high catalytic performance. Iron oxide has various crystalline structures such as α-, β-, γ-, and ε-Fe_2O_3. However, the detailed investigation of crystallite phase of iron oxide on ODH of n-butene is not conducted yet. Hence, I investigated the effect of the crystalline structure of iron oxide on the ODH of n-butene, and ε-Fe_2O_3 was proposed as the novel iron oxide catalyst that had the high ODH activity (Chapter 5).

The summary of this thesis is described in general conclusions (Chapter 6).

References

[1] E. Hong, J.H. Park, C.H. Shin, *Catal. Surv. Asia*, **20** (2016) 23-33

[2] E.V. Makshina, M. Dusselier, W. Janssens, J. Degreve, P.A. Jacobs, B.F. Sels, *Chem. Soc. Rev.,* **43** (2014) 7917-7953

[3] Global 1,3 Butadiene (BD) Market By Application, Grand View Research, Inc., September 2015, SBR (Styrene Butadiene Rubber) Market Worth $9.9 Billion By 2025, Grand View Research, Inc., May 2017

[4] W.C. White, *Chem. Bio. Interact.*, **166** (2007) 10-14

[5] M.M. Bhasin, J.H. Cain, B.V. Vora, T. Imai, P.R. Pujado, *Appl. Catal. A: Gen.,* **221** (2001) 397-419

[6] Y. Xu, J. Lu, M. Zhong, J. Wang, *J. Nat. Gas Chem.,* **18** (2009) 88-93

[7] F.J. Dumez, G.F. Froment, *Ind. Eng. Chem. Process Des. Dev.,* **15** (1976) 291-301

[8] R. Hughes, C. L. Koon, *Appl. Catal. A: Gen.,* **119** (1994) 153-162

[9] L.A. Boot, A.J.v. Dillen, J.W. Geus, F.R.v. Buren, *J. Catal.*, **163** (1996) 195-203

[10] L.M. Madeira, M.F. Portela, *Catal. Rev.,* **44** (2002) 247-286

[11] J.H. Park, C.H. Snin, *Appl. Catal. A: Gen.,* **495** (2015) 1-7

[12] K. Fukudome, N. Ikenaga, T. Miyakke, T. Suzuki, *Catal. Sci. Technol.,* **1** (2011) 987- 998

[13] S. Gong, S. Park, W.C. Choi, H. Seo, N.Y. Kang, M.Wan. Han, Y.K. Park, *J. Mol. Catal. A: Chem.,* **391** (2014) 19-24

[14] S. Chung, C. Angelici, S.O.M. Hinterding, M. Weingarth, M. Baldus, K. Houben, B.M. Weckhuysen, P.C.A. Bruijnincx, *ACS Catal.,* **6** (2016) 4034-4045

[15] Y. Sekiguchi, S. Akiyama, W. Urakawa, T. Koyama, A. Miyaji, K. Motokura, T. Baba, *Catal. Commun.,* **68** (2015) 20-24

[16] I.A. Bakare, S.A. Mohamed, S. Al-Ghamdi, S.A. Razzak, M.M. Hossain, H.I. de Lasa, *Chem. Eng. J.,* **278** (2015) 207-216

[17] J. Liu, V. Fung, Y. Wang, K. Du, S. Zhang, L. Nguyen, Y. Tang, J. Fan, D. Jiang, F.F. Tao, *Appl. Catal. B: Environ.,* **237** (2018) 957-969

[18] Z. Zhang, G. Zhao, R. Chai, J. Zhu, Y. Liu, Y. Lu, *Catal. Sci. Technol.,* **8** (2018) 4383-4389

[19] F. Ma, S. Chem, Y. Li, H. Zhou, A. Xu, W. Lu, *Appl. Surf. Sci.,* **313** (2014) 654-659

[20] Q.X. Luo, X.K. Zhang, B.Li. Hou, J.G. Chen, C. Zhu, Z.W. Liu, Z.T. Liu, J. Lu, *Catal. Sci. Technol.,* **8** (2018) 4864-4876

[21] M. Setnicka, R. Bulanek, L. Capek, P. Cicmanec, *J. Mol. Catal. A: Gen.,* **344** (2011) 1-10

[22] A. Dejoz, J.M. LoÂpez Nieto, F. MaÂrquez, M.I. VaÂzquez, *Appl. Catal. A: Gen.,* **180** (1999) 83-94

[23] J.A. Toledo, N. Nava, M. Martinez, X. Bokhimi, *Appl. Catal. A: Gen.,* **234** (2002) 137-144

[24] M.F. Portela, *Top. Catal.,* **15** (2001) 241-245

[25] H. Fan, J. Feng, X. Li, Y. Guo, W. Li, K. Xie, *Chem. Eng. Sci.,* **135** (2015) 403-411

[26] S. Jarczewski, M. Drozdek, P. Michorczyk, C.C. Collados, J.G. Loe, J.S. Albero, P. Kuśtrowski, *Microporous Mesoporous Mater.,* **271** (2018) 262-272

[27] J. Wanga, J. Diaoa, J. Zhang, Y. Zhang, H. Liu, D.S. Su, *Catal. Today,* **301** (2018) 32-37

[28] S. Lee, M.D. Vece, B. Lee, S. Seifert, R.E. Winans, S. Vajda, *Phys. Chem. Chem. Phys.,* **14** (2012) 9336-9342

[29] S.L. Nauert, F. Schax, C. Limberg, J.M. Notestein, *J. Catal.,* **341** (2016) 180-190

[30] S. Furukawa, M. Endo, T. Komatsu, *ACS catal.,* **4** (2014) 3533-3542

[31] J.K. Lee, H. Lee, U.G. Hong, J. Lee, Y.-J. Cho, Y. Yoo, H.S. Jang, I.K. Song, *J. Ind. Eng. Chem.,* **18** (2012) 1096-1101

[32] J.M. Lopez Nieto, P. Concepci, A. Dejoz, H. Knozinger, F. Melo, M.I. Vazquez., *J. Catal.,* **189** (2000) 147-157

[33] J.C. Jung, H. Lee, H. Kim, Y.M. Chung, T.J. Kim, S.J. Lee, S.H. Oh, Y.S. Kim, I.K. Song, *Catal. Lett.,* **124** (2008) 262-267

[34] J.C. Jung, H. Kim, Y.M. Chung, T.J. Kim, S.J. Lee, S.H. Oh, Y.S. Kim, I.K. Song, *J. Mol. Catal. A: Chem.,* **264** (2007) 237-240

[35] J.C. Jung, H. Lee, I.K. Song, *Catal. Surv. Asia,* **13** (2009) 78-93

[36] J.C. Jung, H. Lee, H. Kim, Y.M. Chung, T.J. Kim, S.J. Lee, S.H. Oh, Y.S. Kim, I.K. Song, *J. Mol. Catal. A: Chem.,* **271** (2007) 261-265

[37] J.H. Park, H. Noh, J.W. Park, K. Row, K.D. Jung, C.H. Shin. *Appl. Catal. A: Gen.,* **431-432** (2012) 137-143

[38] J.C. Jung, H. Kim, Y.S. Kim, Y.M. Chung, T.J. Kim, S.J. Lee, S.H. Oh, I.K. Song, *Appl. Catal. A: Gen.,* **317** (2007) 244-249

[39] C. Wan, D. Cheng, F. Chen, X. Zhan, *Chem. Eng. Sci.,* **135** (2015) 553-558

[40] C. Wan, D. Cheng, F. Chen, X. Zhan, *J. Chem. Technol. Biotechnol.,* **91** (2016) 353-358

[41] H. Armendariz, G. Aguilar-Rios, P. Salas, M.A. Valenzuela, I. Schifter, H. Arriola, N. Nava, *Appl. Catal. A: Gen.,* **92** (1992) 29-38

[42] H. Lee, J.C. Jung, H. Kim, Y.M. Chung, T.J. Kim, S.J. Lee, S.H. Oh, Y.S. Kim, I.K. Song, *Catal. Lett.,* **131** (2009) 344-349

[43] Y.M. Chung, Y.T. Kwon, T.J. Kim, S.J. Lee, S.H. Oh, *Catal. Lett.,* **130** (2009) 417-

423

[44] H. Lee, J.C. Jung, I.K. Song, *Catal. Lett.,* **133** (2009) 321-327

[45] H. Lee, J.C. Jung, H. Kim, Y.M. Chung, T.J. Kim, S.J. Lee, S.H. Oh, Y.S. Kim, I.K. Song, *Korean J. Chem. Eng.,* **26** (2009) 994-998

[46] H. Lee, J.C. Jung, H. Kim, Y.M. Chung, T.J. Kim, S.J. Lee, S.H. Oh, Y.S. Kim, I.K. Song, *Catal. Commun.,* **9** (2008) 1137-1142

[47] J.A. Toledo, P. Bosch, M.A. Valenzuela, A. Montoya, N. Nava, *J. Mol. Catal.,* **125** (1997) 53-62

[48] H. Armendariz, J.A. Toledo, G. Aguilar-Rios, M.A. Valenzuela, P. Salas, A. Cabral, H. Jimenez, I. Schifter, *J. Mol. Catal.,* **92** (1994) 325-332

[49] R.J. Rennard, W.L. Kehl, *J. Catal.,* **21** (1971) 282-293

[50] B.J. Liaw, D.S. Cheng, B.L. Yang, *J. Catal.,* **118** (1989) 312-326

[51] W.Q. Xu, Y.G. Yin, G.Y. Li, S. Chen, *Appl. Catal. A: Gen.,* **89** (1992) 131-142

[52] F.Y. Qiu, L.T. Weng, E. Sham, P. Ruiz, B. Delmon, *Appl. Catal.,* **51** (1989) 235-253

[53] Y.M. Chung, Y.T. Kwon, T.J. Kim, S.J. Lee, S.H. Oh, *Catal. Lett.,* **131** (2009) 579-586

[54] M.A. Gibson, J.W. Hightower, *J. Catal.,* **41** (1976) 431-439

[55] E. Ruckenstein, R. Krishnan, K.N. Rai, *J. Catal.,* **45** (1976) 270-273

Chapter 2

Oxidative dehydrogenation of but-1-ene with lattice oxygen in ferrite catalysts

1. Introduction

Buta-1,3-diene (BD) has attracted interest as a monomer of petrochemical products such as polybutadiene rubber, styrene butadiene rubber, and ABS resin. About 90% of BD is produced by purifying C4 fraction containing BD, n-butene, and n-butane obtained from the endothermic steam-cracking of naphtha. However, this process produces many chemical materials such as ethylene and propylene at the same time and needs a temperature higher than 700 ^{o}C. Therefore, this process consumes a large amount of energy and can not produce BD efficiently.

Recently, oxidative dehydrogenation (ODH) of n-butene with molecular O_2 (Eq. (1)) has attracted attention from the viewpoint of energy saving, because it is an exothermic process and can more efficiently produce BD at lower temperatures than the current process. Moreover, as BD is the sole C4 product of ODH of n-butene, BD can be produced with high selectivity without by-products such as ethylene and propylene.

$$1\text{-}C_4H_8 + 1/2O_2 \rightarrow C_4H_6 + H_2O \quad \Delta H^o = -132.1 \text{ kJ/mol} \qquad (1)$$

Various composite metal oxides and supported catalysts have been investigated for the ODH of many hydrocarbons, such as propane [1], ethylbenzene [2], ethane [3], n-butane [4], and n-butene [5]. For the ODH of n-butene and n-butane, ferrite-type catalysts

[5-19], V-containing catalysts [20-22], and Bi-Mo catalysts [23-27] exhibited the high activity. It was reported that the Bi-Mo catalyst progressed the ODH through the Mars-van Krevelen mechanism and gave the high catalytic activity for the ODH of but-1-ene to BD at 440 ºC [26]. The Mars-van Krevelen mechanism is a redox cycle with lattice oxygen in the metal oxide catalyst [23, 24].

Among these catalysts for the ODH of the C4 compounds, ferrite-type (spinel) catalysts have been widely studied. Spinel structures, such as Zn-Fe [5-11, 17, 18], Zn-Fe-Cr [13], Zn-Fe-Al [12], and γ-Fe_2O_3 [15, 16], is necessary to obtain high activity. The presence of α-Fe_2O_3 in the ferrite catalysts decreased the conversion and the BD selectivity [8]. Among ferrite catalysts, zinc ferrite has been widely investigated. For example, it was reported that a zinc ferrite catalyst modified by heteropoly acid or sulfonic acid was effective for the ODH of but-1-ene [9, 10]. In addition, when zinc ferrite was prepared by the co-precipitation method, pH control was important to obtain high but-1-ene conversion and high BD selectivity [11].

The reaction mechanism for the ODH of n-butene with the zinc ferrite catalyst is known to proceed through the Mars-van Krevelen mechanism, the same as that of the Bi-Mo catalyst [7-9]. However, it was proposed that the ferrite-type catalyst deactivated as a result of an increase in Fe^{2+} generated by reducing Fe^{3+} and its isolation [18, 19]. In order to maintain high oxygen mobility and inhibit change in the spinel structure, Sb_2O_4, $BiPO_4$, or SnO_2 as an oxygen donor was added to the zinc ferrite catalyst. These catalysts showed high oxygen mobility and high ODH activity for a long time [17, 18].

On the other hand, the deep oxidation reaction (Eqs. (2), (3)) proceeds easily during the ODH under O_2 atmosphere.

$$1\text{-}C_4H_8 + 6O_2 \rightarrow 4CO_2 + 4H_2O\ \Delta H^o = -2717\ \text{kJ/mol} \qquad (2)$$

$$C_4H_6 + 11/2O_2 \rightarrow 4CO_2 + 3H_2O\ \Delta H^o = -2540\ kJ/mol \quad (3)$$

To inhibit the complete oxidation, the ODH with the zinc ferrite catalyst has been carried out under a lot of steam and O_2 flow. However, because the latent heat of steam is large, excessive energy is necessary. Supplying the steam consumes excessive energy.

In another viewpoint, it was proposed that the lattice oxygen in metal oxide catalyst could be used to restrict the deep oxidation of the reactant and the product, and that the catalyst that lost the lattice oxygen could be re-oxidized by introducing molecular O_2 after the reaction (Eqs. (4), (5)) [28].

$$1\text{-}C_4H_8 + MO_x \rightarrow C_4H_6 + H_2O + MO_{x-1} \quad (4)$$

$$MO_{x-1} + 1/2O_2 \rightarrow MO_x \quad (5)$$

Our laboratory, on the other hand, found that various ferrites could be prepared at a low temperature, such as 500 ^oC, in the presence of activated carbon as the novel preparation method of ferrite [29].

In this chapter, the ODH of but-1-ene with the lattice oxygen in various ferrite catalysts prepared with activated carbon was examined. In order to inhibit complete oxidation, the lattice oxygen in the catalyst was used as a mild oxidant, and then the catalytic activity of the ferrite catalyst for the ODH of but-1-ene was investigated.

2. Experimental

2.1 Materials

$Fe(NO_3)_3{\cdot}9H_2O$ (assay = min. 99.0%), $Ni(NO_3)_2{\cdot}6H_2O$ (assay = 99.0%), $Zn(NO_3)_2{\cdot}6H_2O$ (assay = 99.0%), $Co(NO_3)_2{\cdot}6H_2O$ (assay = 98.0%), $Cu(NO_3)_2{\cdot}3H_2O$ (assay = min. 99.0%), and activated carbon (AC) were purchased from Wako Pure Chemical Industry and were used for the preparation of ferrite catalysts. But-1-ene (1-C_4H_8) (assay = min. 99.0%) was supplied from Sumitomo Seika Chemical.

2.2 Catalyst preparation

Preparation by impregnation method

Various ferrite catalysts were prepared by the impregnation method at a weight ratio of AC:composite metal oxides=4:1. AC was impregnated with a mixed aqueous solution of $Fe(NO_3)_3{\cdot}9H_2O$ and $Ni(NO_3)_2{\cdot}6H_2O$, $Zn(NO_3)_2{\cdot}6H_2O$, $Co(NO_3)_2{\cdot}6H_2O$, or $Cu(NO_3)_2{\cdot}3H_2O$ as Ni, Zn, Co, or Cu:Fe=1:2 in molar ratio. After the mixture was allowed to stand at room temperature overnight, excess water was evaporated to dryness at 70 ºC under reduced pressure of 1 kPa. The solid was then dried at 70 ºC overnight in vacuo. Nickel, zinc, and cobalt ferrites were prepared by calcination at 500 ºC for 2 h in air. Copper ferrite was prepared by calcination at 280-500 ºC for 2 h in air. For comparison, CuO was prepared in same method at 500 ºC. Hereafter, the notation is $NiFe_2O_4$(AC)-500, $ZnFe_2O_4$(AC)-500, $CoFe_2O_4$(AC)-500, $CuFe_2O_4$(AC)-280, -300, -400, -500, and CuO(AC).

2.3 Catalyst test

ODH of but-1-ene using lattice oxygen in ferrite catalyst

The ODH of but-1-ene was carried out using a fixed-bed flow quartz reactor at various temperatures under atmospheric pressure. After 200 mg of the catalyst was placed in the reactor, 5 mL/min (STP) of but-1-ene and 25 mL/min (STP) of Ar were introduced for 8 min. The re-oxidation after ODH was performed under 5 mL/min of O_2 and 25 mL/min of Ar for 8 min at the same temperature as the reaction temperature. The relative error of the experimental operation is within 5%.

The C4 compounds (1-C_4H_8, *cis*-2-C_4H_8, *trans*-2- C_4H_8, and C_4H_6) were analyzed by a flame ionization detector (FID) gas chromatograph (Shimadzu GC14B, column: Unicarbon A-400). CO and CO_2 were also analyzed by the FID gas chromatograph (column: Activated carbon) equipped with a methanizer (Shimadzu MTN-1). H_2 was analyzed by a thermal conductivity detector (TCD) gas chromatograph (Shimadzu GC8A, column: Activated carbon).

2.4 Catalyst characterization

X-ray diffraction (XRD) patterns were obtained by the powder method with a Shimadzu XRD-6000 diffractometer using monochromatic Cu Kα radiation. X-ray photoelectron spectra (XPS) analyses were carried out with a JEOL model JPS-9010MX using Mg Kα radiation as an energy source. The surface area of the catalyst was measured by the Brunauer-Emmett-Teller (BET) method at -196 ºC using N_2 as an adsorbate with a MicrotracBEL (BELSORP-mini II-ISP). Thermogravimetry and differential thermal analysis (TG-DTA) (Shimadzu DTG-60) was used to measure the burning point of AC. The reactor was heated to 800 ºC at a rate of 10 ºC /min under 100 mL/min (STP) of air and was maintained at 800 ºC for 10 min. A temperature-programmed reaction of but-1-ene (1-C_4H_8-TPR) was carried out under but-1-ene/Ar=5/25 mL/min using a fixed-bed

flow reactor in which 200 mg of catalyst was placed. To remove water, the catalyst was pretreated at 200 °C under an Ar atmosphere, and then the reactor was heated to 500 °C at a rate of 5 °C/min under but-1-ene and Ar flow. The products (H_2, H_2O, C_4H_6, CO, CO_2) were continuously analyzed by a Q-mass mass spectrometer (Hiden Analytical, HAL 201) fitted at the outlet of the reactor.

3. Results and Discussion

3.1 Activity test of various ferrite catalysts by but-1-ene-TPR measurement

Figure 2-1 shows XRD patterns of various ferrite catalysts. $NiFe_2O_4$(AC)-500, $ZnFe_2O_4$(AC)-500, $CoFe_2O_4$(AC)-500, and $CuFe_2O_4$(AC)-500 catalysts showed the spinel diffraction peaks. Therefore, these catalysts could be used for but-1-ene-TPR.

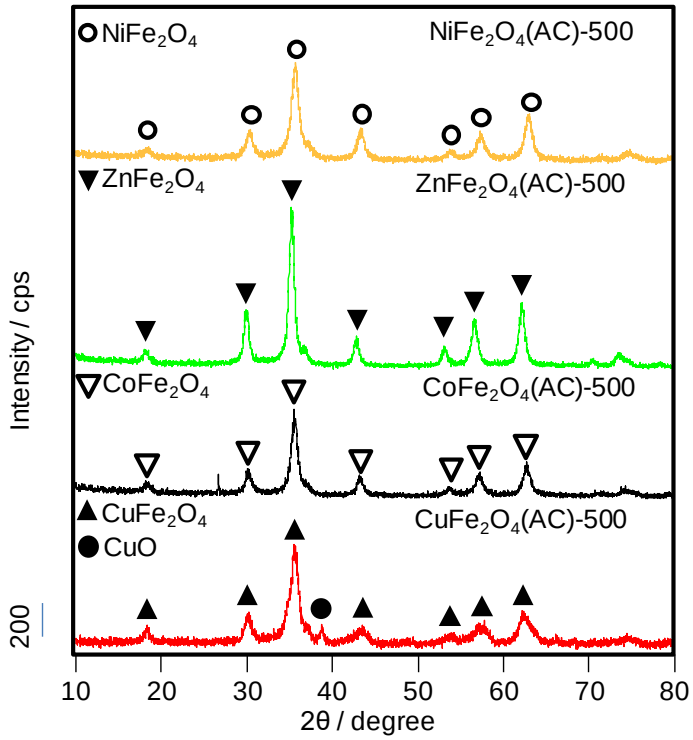

Fig.2-1 XRD patterns of various ferrite catalysts

But-1-ene-TPR was measured in order to confirm the lattice oxygen mobility of ferrite catalysts; $NiFe_2O_4$(AC)-500, $ZnFe_2O_4$(AC)-500, $CoFe_2O_4$(AC)-500, and $CuFe_2O_4$(AC)-500. The results are shown in Fig. 2-2. Since H_2O and CO_2 were seen at 380 ºC, $NiFe_2O_4$(AC)-500 progressed the complete oxidation of but-1-ene. At about 400 ºC, $NiFe_2O_4$(AC)-500 progressed the decomposition of but-1-ene to produce H_2. The formation of CO_2 increased from about 460 ºC. However, the production of H_2O was not seen. Therefore, carbon produced by the decomposition of but-1-ene seemed to be oxidized by the lattice oxygen (Fig. 2-2 a)). On the other hand, $CoFe_2O_4$(AC)-500 and $ZnFe_2O_4$(AC)-500 produced BD, although the latter produced BD and H_2 at over 400 ºC. Since H_2O was not observed, $ZnFe_2O_4$(AC)-500 catalyst progressed the simple dehydrogenation of but-1-ene (Fig. 2-2 b)). $CoFe_2O_4$(AC)-500 catalyst produced BD, H_2O, CO_2, and H_2 over 400 ºC. Therefore, this catalyst promoted the ODH, the complete oxidation, and the simple dehydrogenation of but-1-ene at the same time (Fig. 2-2 c)). When $CuFe_2O_4$(AC)-500 was used for but-1-ene-TPR, BD and H_2O were produced over 200 ºC (Fig. 2-2 d)). At 300 ºC, CO_2 and H_2O were formed by the complete oxidation of but-1-ene. Since H_2 formed over 400 ºC, the decomposition of but-1-ene progressed. These results indicate that $CuFe_2O_4$(AC)-500 catalyst is the most suitable for ODH at a lower temperature. Since $CuFe_2O_4$(AC)-500 produced CO_2 at 300 ºC and H_2 at 400 ºC, the ODH using $CuFe_2O_4$(AC)-500 was carried out at a temperature range of 200-300 ºC.

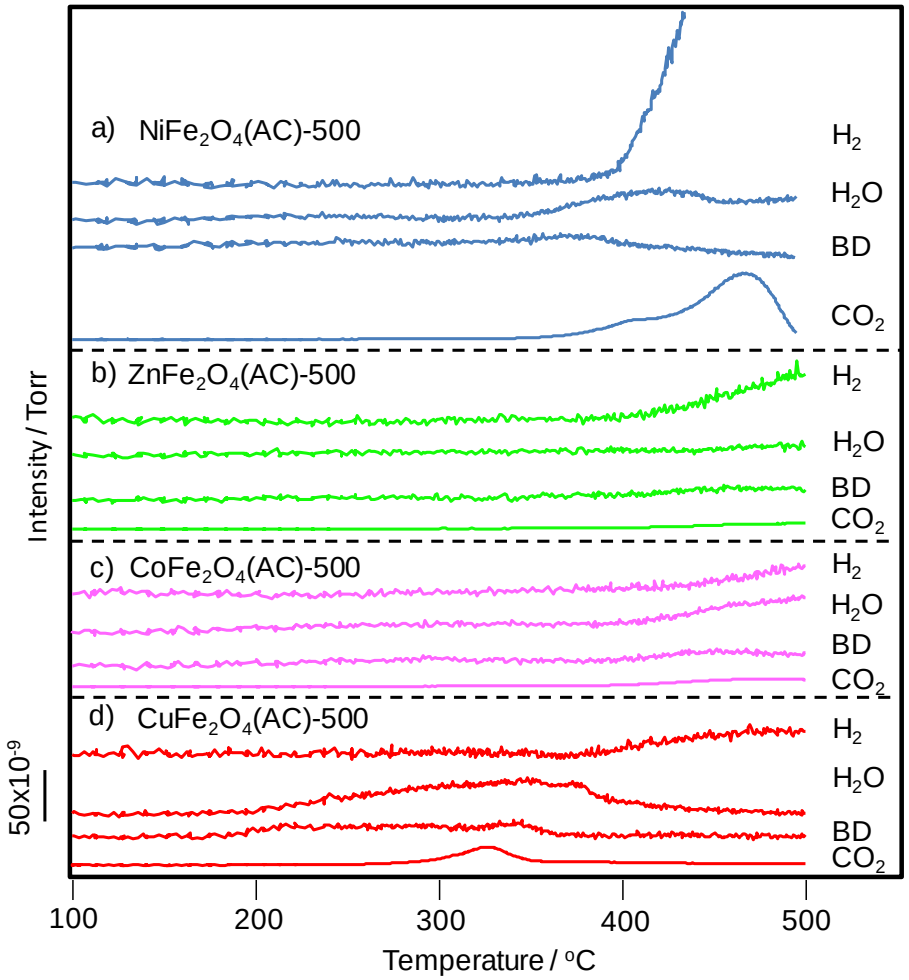

Fig.2-2 But-1-ene-TPR profiles with various ferrite catalysts

Catalyst weight: 200 mg, 1-C_4H_8=/Ar=25/5 mL/min,
Heating rate: 5 ^oC/min

3.2 Effect of reaction temperature on ODH with lattice oxygen of $CuFe_2O_4$(AC)-500

The ODHs with lattice oxygen of $CuFe_2O_4$(AC)-500 were carried out between 200-300 °C. The results are illustrated in Fig. 2-3. When the ODH was conducted at 200 °C, $CuFe_2O_4$(AC)-500 indicated the highest conversion of 25.6% mainly by the isomerization reaction. Low BD selectivity of 17.9% and low BD yield of 4.6% were obtained. In the ODHs at 250-270 °C, this catalyst exhibited higher conversion, BD selectivity, and BD yield. At 270 °C, $CuFe_2O_4$(AC)-500 gave a conversion of 21.3%, high BD selectivity of 39.9%, and the highest BD yield of 8.5%. At 300 °C, this catalyst showed low conversion of 12.8% due to less isomerization reaction, high CO_2 selectivity of 14.2%, and a low yield of 6.5%. Since the catalyst gave the highest BD yield and low CO_2 formation at 270 °C, 270 °C was the most suitable reaction temperature for the ODH with $CuFe_2O_4$(AC)-500.

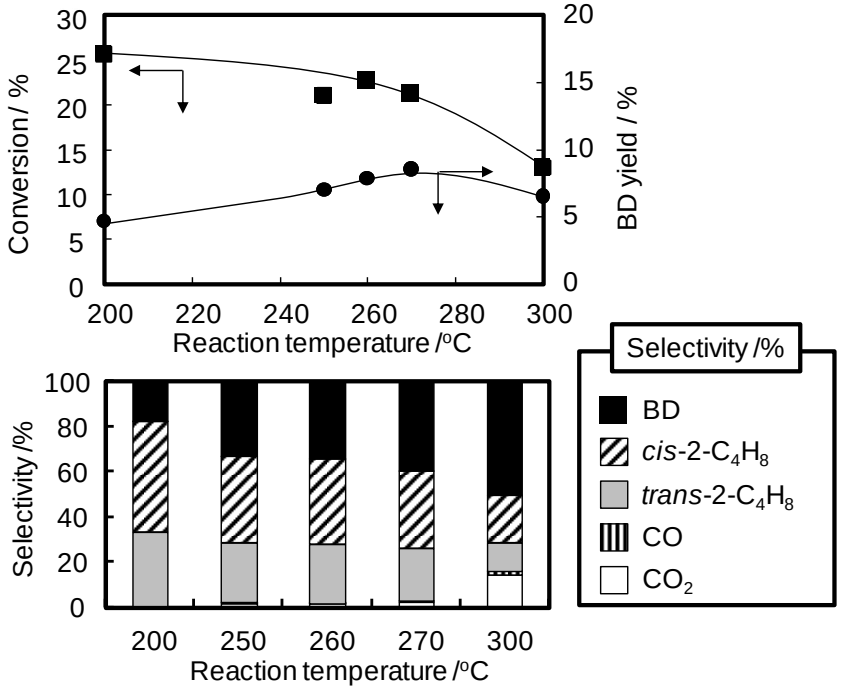

Fig. 2-3 Oxidative dehydrogenation of but-1-ene with copper ferrite catalyst

Catalyst: $CuFe_2O_4$(AC)-500, Catalyst weight: 200 mg,
Flow rate: 1-C_4H_8/Ar=5/25 mL/min, reaction time: 8 min

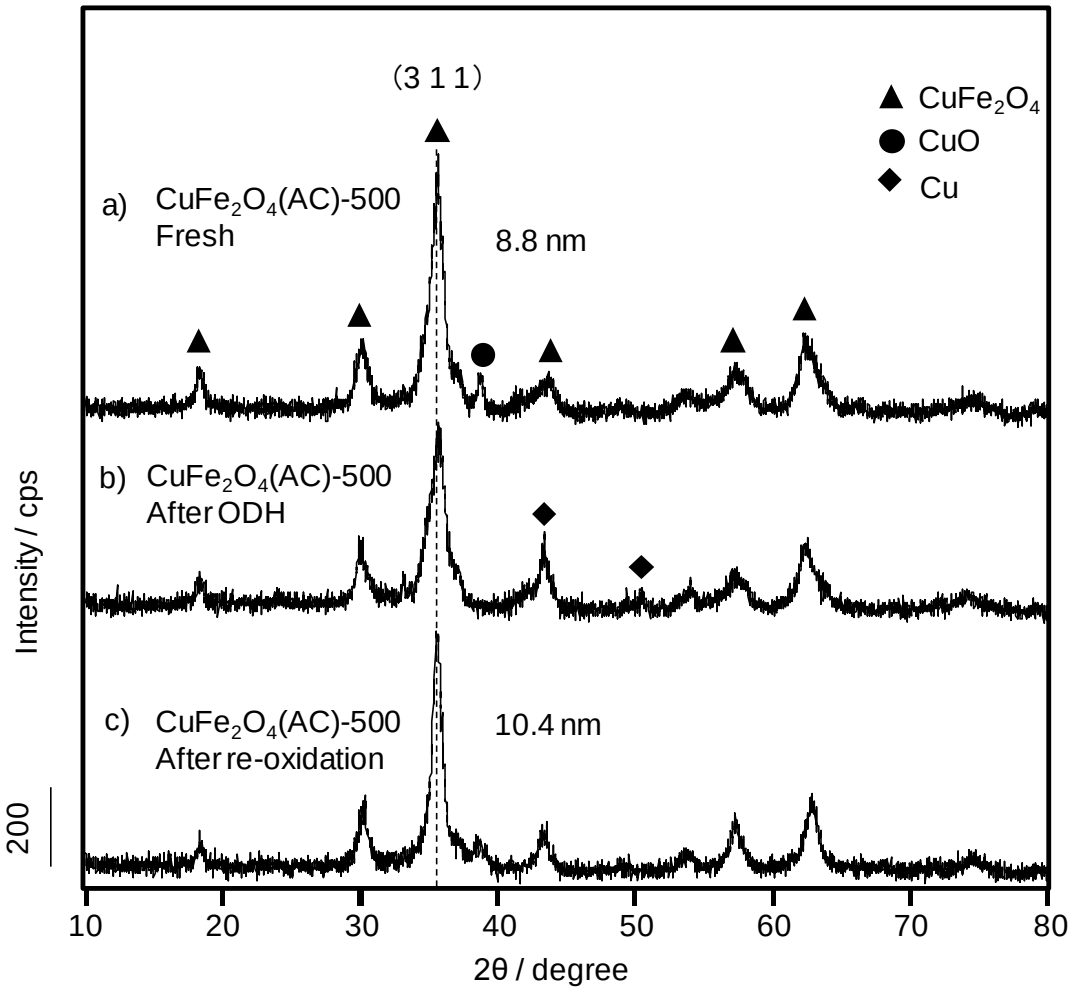

Fig. 2-4 XRD patterns of copper ferrite after ODH and re-oxidation

XRD analyses were carried out to examine the change in the crystalline structure of the catalyst before and after the ODH and after the re-oxidation at 270 °C. XRD patterns are shown in Fig. 2-4. $CuFe_2O_4$ and CuO diffraction peaks were seen in $CuFe_2O_4$(AC)-500 before the ODH (Fig. 2-4a)). $CuFe_2O_4$(AC)-500 after the reaction exhibited diffraction peaks of metallic copper in addition to copper ferrite, and CuO diffraction peak intensity was clearly decreased as compared to that of the fresh catalyst (Fig. 2-4b)). The lattice oxygen in CuO may also be used for the ODH of but-1-ene. In order to confirm the reactivity of the lattice oxygen, CuO(AC) catalyst was used for the ODH of but-1-ene.

When the CuO(AC) was used for the ODH, CuO(AC) indicated the lower conversion of 1.9%, the higher CO_2 selectivity of 36.9%, and the lower BD yield of 0.9% than those of $CuFe_2O_4$(AC) catalyst. In other words, the reducibility of the lattice oxygen in CuO is very low. Therefore, it was suggested that the lattice oxygen in $CuFe_2O_4$ was more effective than that of CuO for the ODH. After the re-oxidation, $CuFe_2O_4$ and CuO diffraction peaks were similar to those of the catalyst before the reaction. Furthermore, since the crystallite sizes of $CuFe_2O_4$ in $CuFe_2O_4$(AC)-500 before and after the reaction calculated by the Scherrer equation were 8.8 nm and 10.4 nm, respectively (Fig. 2-4c)), the $CuFe_2O_4$ crystallite barely grew. Thus, the crystal structure in the used $CuFe_2O_4$(AC)-500 could be recovered by re-oxidation.

To investigate the active species for the ODH with $CuFe_2O_4$(AC)-500 and the change in valences of iron and copper, XPS analyses were used for $CuFe_2O_4$(AC)-500 before and after the reaction at 270 °C. XPS spectra of Fe and Cu species are shown in Fig. 2-5. In general, the XPS spectra of Fe and Cu species of $CuFe_2O_4$ can be ascribed to two peaks of octahedral and tetrahedral sites [30, 31]. Fe 2p3/2 peak at 713.6 eV is related to Fe^{3+} species in tetrahedral (Fe^{3+}_T) site, and the peak at 710.5 eV is related to Fe^{3+} species in octahedral (Fe^{3+}_O) site. Cu 2p3/2 peak at 935.8 eV is related to Cu^{2+} species in tetrahedral (Cu^{2+}_T) site, and the peak at 934.1 eV is related to Cu^{2+} species in octahedral (Cu^{2+}_O) site. XPS spectra of $CuFe_2O_4$(AC)-500 before the reaction indicated $Fe^{3+}_{T,O}$ and $Cu^{2+}_{T,O}$ (Fig. 2-5 a), b)). According to the XPS analysis of $CuFe_2O_4$(AC)-500 after the ODH, because XPS spectra of reduced Fe species were not observed in the catalyst after the reaction, lattice oxygen in the Fe-O bond was not used for the ODH (Fig. 2-5 a)).

On the other hand, $Cu^{0,+}$ appeared at 932.1 eV after the reaction in addition to two peaks with Cu^{2+} related to tetrahedral and octahedral sites in the catalyst (Fig. 2-5 b)). Moreover,

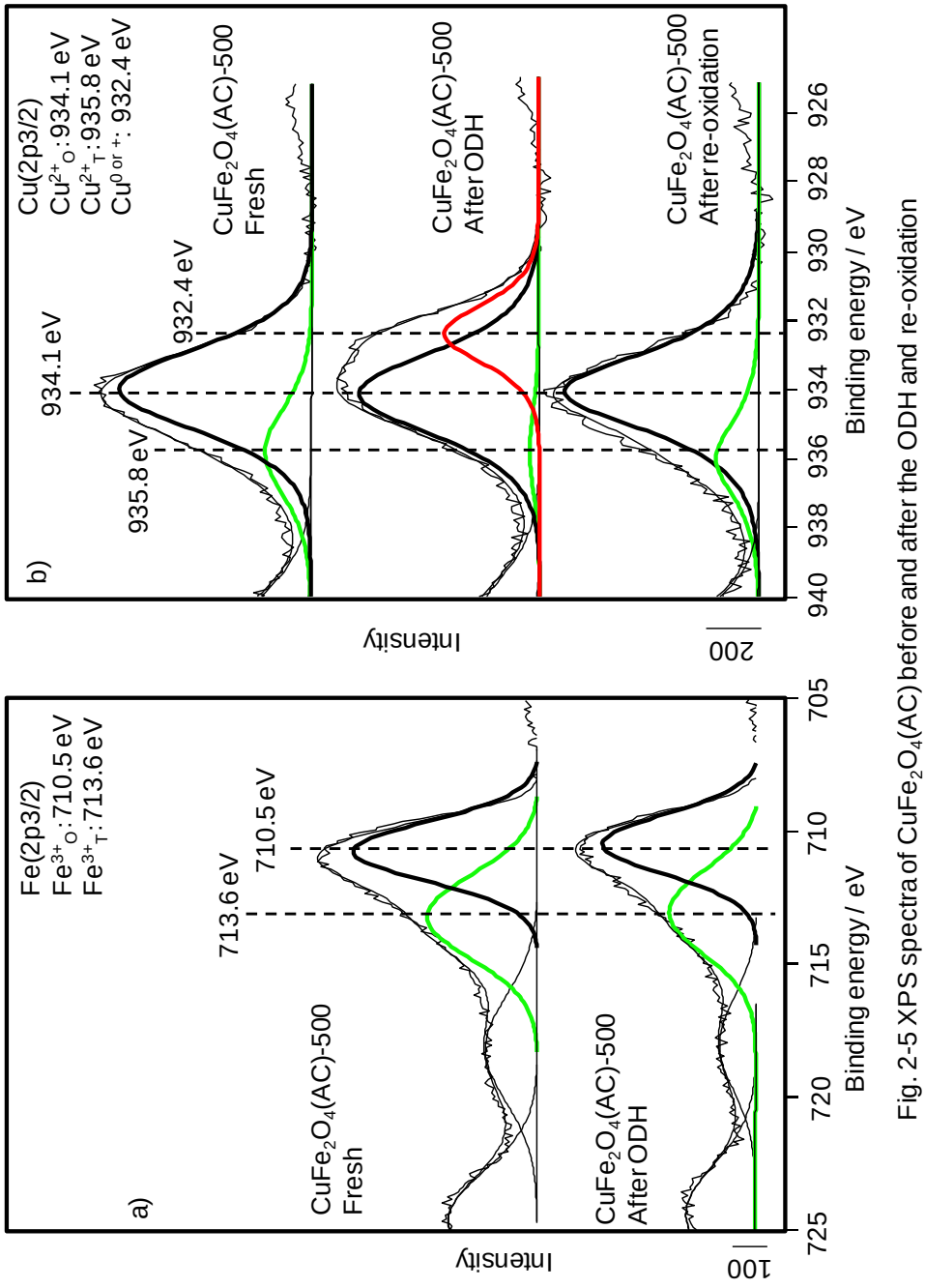

Fig. 2-5 XPS spectra of $CuFe_2O_4$(AC) before and after the ODH and re-oxidation

Cu^{2+}_{T} in $CuFe_2O_4$(AC)-500 clearly decreased after the ODH. XPS spectrum of $CuFe_2O_4$(AC)-500 after the re-oxidation showed Cu^{2+}_{T} in addition to Cu^{2+}_{O} similar to those of the catalyst before the reaction. In addition, Cu species rates of $Cu^{2+}_{T, O}$ and $Cu^{0, +}$ were calculated from the result of XPS spectra (Table 2-1). Cu^{2+}_{T} ratio decreased from 20.5% to 4.1% after the ODH. Cu^{2+}_{O} ratio decreased from 79.5% to 69.5% after the ODH. Therefore, the both oxygen species bonded to Cu^{2+}_{T} and/or Cu^{2+}_{O} would be used for the ODH of but-1-ene. In order to investigate in detail, the amount of lattice oxygen related to $Cu^{2+}_{T, O}$ used in the ODH were estimated from the amount of lattice oxygen based on CuO in $CuFe_2O_4$ and $Cu^{2+}_{T, O}$ ratio (Table 2-2). The amount of lattice oxygen related to Cu^{2+}_{T} used in the reaction (136.9 μmol) was mostly consistent with BD amount (139 μmol) generated in the ODH. Therefore, it was suggested that oxygen species bonded to Cu^{2+}_{T} seems to be related to the ODH. The oxygen species bonded to Cu^{2+}_{O} may generate CO and/or CO_2. On the other hand, the both oxygen species after the ODH could be recovered because Cu^{2+}_{T} after re-oxidation increased from 4.1 to 17.9% and Cu^{2+}_{O} after re-oxidation recovered from 69.5% to 82.1%. Although oxygen species bonded to Fe^{3+} did not relate to the ODH, it was thought that the iron species is necessary to form $Cu^{2+}_{T, O}$.

Table 2-1 Cu species ratio of $CuFe_2O_4$(AC)-500 catalyst before and after ODH calculated from XPS analysis

Catalyst	Cu^{2+}_{T} (%)	Cu^{2+}_{O} (%)	$Cu^{0 \text{ or } +}$ (%)
	935.8 eV	934.1 eV	932.4 eV
$CuFe_2O_4$(AC)-500 fresh	20.5	79.5	0.00
$CuFe_2O_4$(AC)-500 after ODH	4.1	69.5	26.4
$CuFe_2O_4$(AC)-500 after re-oxidation	17.9	82.1	0.00

Table 2-2 Amount of lattice oxygen bonded to $Cu^{2+}_{T,O}$ and product

Catalyst	Cu^{2+}_{T} lattice oxygen (μmol)	Cu^{2+}_{O} lattice oxygen (μmol)	BD (μmol)	CO, CO_2, H_2O (μmol)
$CuFe_2O_4$(AC)-500	136.9	83.2	139.0	112.6

The atomic ratio of Cu and O on $CuFe_2O_4$(AC)-500 surface before and after the reaction and after the re-oxidation calculated from XPS analyses are shown in Table 2-3. Cu species/O atomic ratio on the catalyst surface after the ODH increased from 0.37 (fresh catalyst) to 0.46 (Table 2-3a,b)). For the catalyst after the re-oxidation, Cu species/O ratio decreased from 0.46 (after the ODH) to 0.4. As indicated in Fig. 2-5, the change in the valence of Fe species was not seen. Therefore, the lattice oxygen bonded to Cu^{2+} in $CuFe_2O_4$ structure can be used for the ODH of but-1-ene, and the used lattice oxygen can be regenerated by the re-oxidation. According to the results of XRD and XPS analyses, because the used $CuFe_2O_4$(AC)-500 catalyst could be regenerated by re-oxidation with oxygen, the re-oxidized $CuFe_2O_4$(AC)-500 can be used for the ODH of but-1-ene again.

Table 2-3 Cu and O atomic ratio of $CuFe_2O_4$/AC-500 catalyst before and after ODH and after re-oxidation calculated from XPS analysis

Fresh, used, and re-oxidized catalysts	$Cu^{2+, 0}$/O
a) $CuFe_2O_4$(AC)-500 fresh	0.37
b) $CuFe_2O_4$(AC)-500 after ODH	0.46
c) $CuFe_2O_4$(AC)-500 after re-oxidation	0.40

3.3 Effect of calcination temperature on ODH

The effects of the specific surface area and the crystallite size of $CuFe_2O_4$ in $CuFe_2O_4$(AC)-500 catalyst with a change in the calcination temperature on the ODH were examined.

In order to confirm the burning point of AC, TG-DTA measurement of $CuFe_2O_4$(AC) before calcination was carried out. The results are illustrated in Fig. 2-6. Remarkable weight loss and exothermic peak in DTA were observed at 300 °C with burning of AC. Therefore, $CuFe_2O_4$(AC) catalyst was prepared by calcination at 280-500 °C. Their XRD patterns

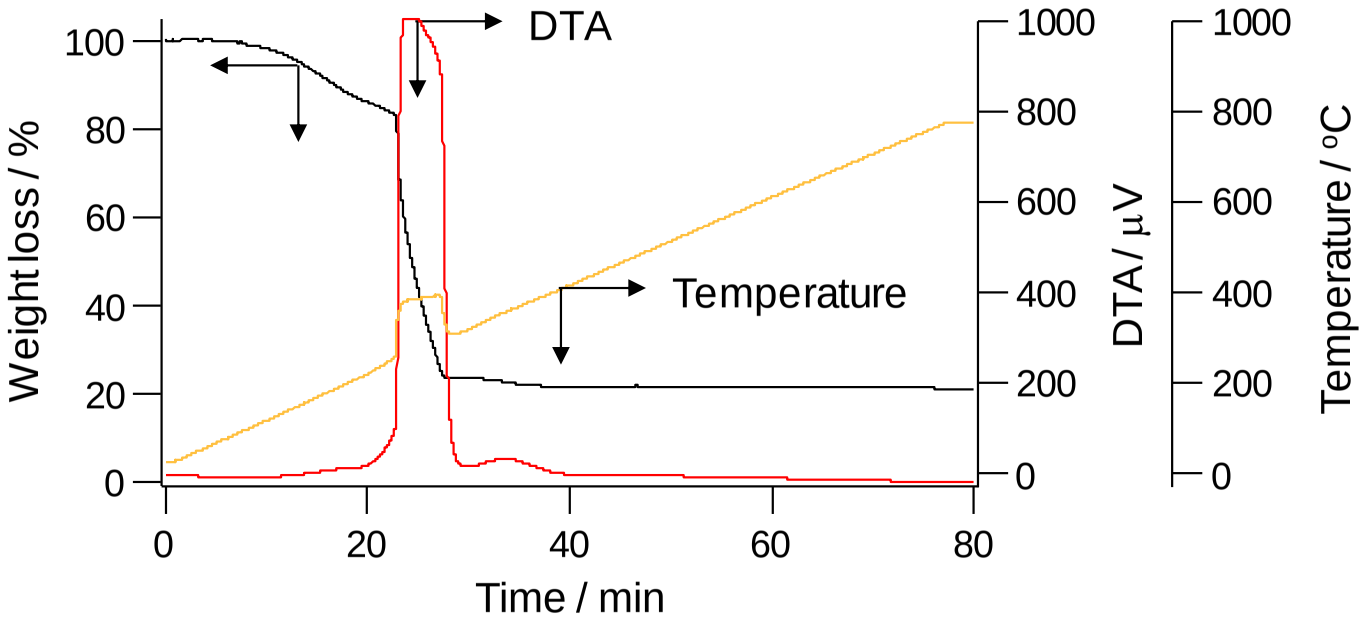

Fig. 2-6 Weight loss and DTA of precursor before calcination by TG-DTA

Substance: precursor of $CuFe_2O_4$(AC)-500 before calcination,
Flow rate: air=100 mL/min,
Heating rate: 5 °C/min

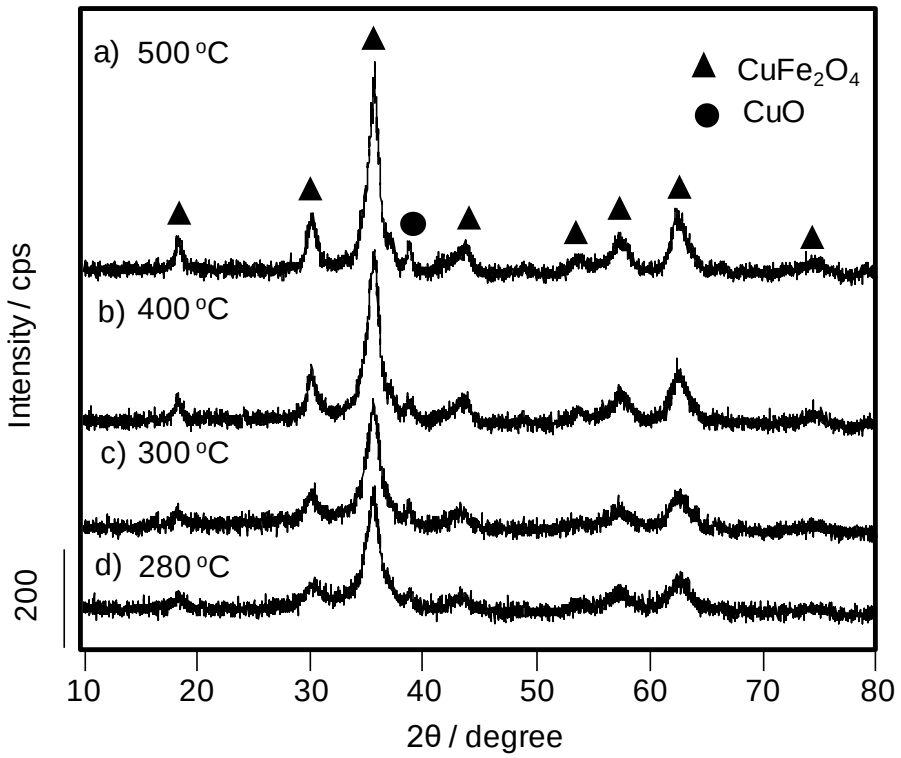

Fig. 2-7 XRD patterns of copper ferrite calcined at various temperatures
Catalyst notice: a) $CuFe_2O_4$(AC)-500, b) $CuFe_2O_4$(AC)-400,
c) $CuFe_2O_4$(AC)-300, d) $CuFe_2O_4$(AC)-280

are shown in Fig. 2-7, and the specific surface area and crystallite size are shown in Table 2-2. $CuFe_2O_4$ diffraction peaks were observed for all catalysts (Fig. 2-7 a)-d)). Therefore, it was considered that the crystal structure of $CuFe_2O_4$ would be formed by burning of AC, because no DTA increase, which are related to the formation of iron and copper oxide after AC burning, was seen (Fig. 2-6). On the other hand, the specific surface area decreased in the order of $CuFe_2O_4$(AC)-280>300>400>500=105>76>59>34 m^2/g and the crystallite size tended to increase in the order of $CuFe_2O_4$(AC)-280<300<400<500=6.8<7.4<8.1<8.8 nm as the calcination temperature (Table 2-4). When the catalyst was calcined at 280 °C, it showed a higher specific surface area of 105 m^2/g and a smaller crystallite size of 6.8 nm than those of catalysts calcined at the other

Table 2-4 Specific surface area and crystallite size of $CuFe_2O_4$/AC catalyst prepared at different calcination temperatures

Sample	Specific surface area (m^2/g)	Crystallite size (nm)
$CuFe_2O_4$(AC)-500	34	8.8
$CuFe_2O_4$(AC)-400	59	8.1
$CuFe_2O_4$(AC)-300	76	7.4
$CuFe_2O_4$(AC)-280	105	6.8

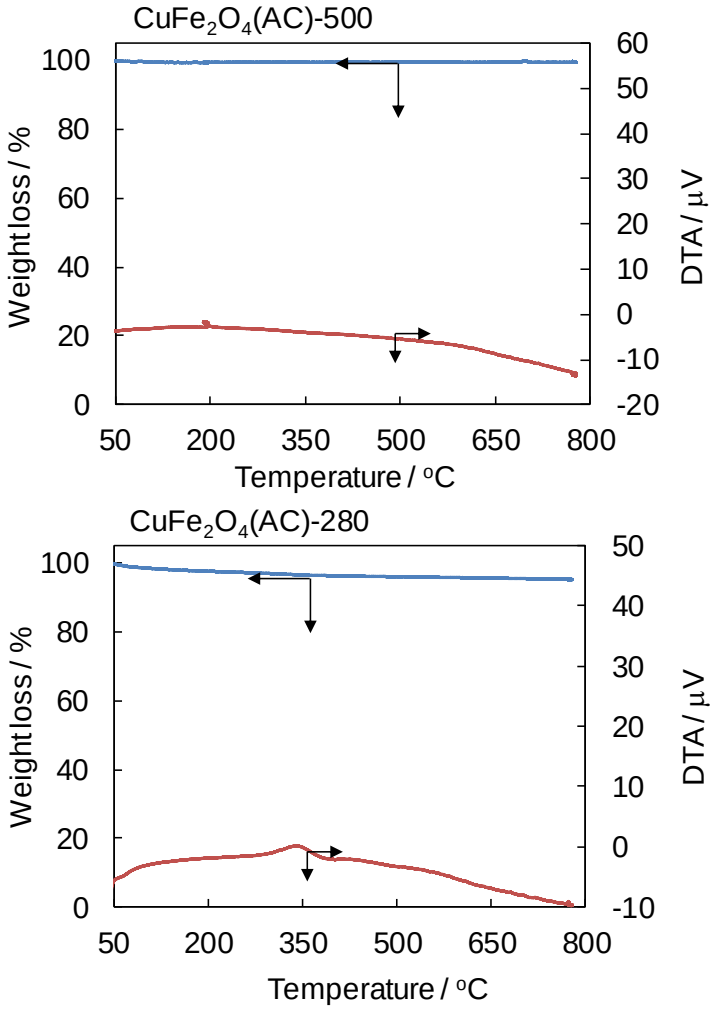

Fig. 2-8 Weight loss and DTA of $CuFe_2O_4$(AC)-500 and -280 by TG-DTA

Substance: $CuFe_2O_4$(AC)-500, -280,
Flow rate: air=100 mL/min, Heating rate: 5 °C/min

temperatures. Here, TG-DTA analyses of $CuFe_2O_4$(AC)-500 and- 280 were conducted to confirm remaining AC (Figure 2-8). $CuFe_2O_4$(AC)-500 did not show the weight loss and the rise of DTA. Therefore, the deposited carbon did not exist. On the other hand, the results of TG-DTA of $CuFe_2O_4$(AC)-280 showed the weight loss of 2% and the small rise of DTA at around 350 °C. Therefore, the high specific surface area (105 m^2/g) might be due to remaining AC.

The effects of the calcination temperature on the ODH are shown in Fig. 2-9. $CuFe_2O_4$(AC)-400 and $CuFe_2O_4$(AC)-500 gave quite similar BD yields of about 8.5%. $CuFe_2O_4$(AC)-300 showed a higher conversion, 24.4%, and a higher BD yield, 8.8%. When the ODH was carried out using $CuFe_2O_4$(AC)-280, conversion of 27.6% and a BD yield of 9.2% were obtained. $CuFe_2O_4$(AC), which has a high specific surface area, tended to give a high BD yield because of the larger contact area with but-1-ene.

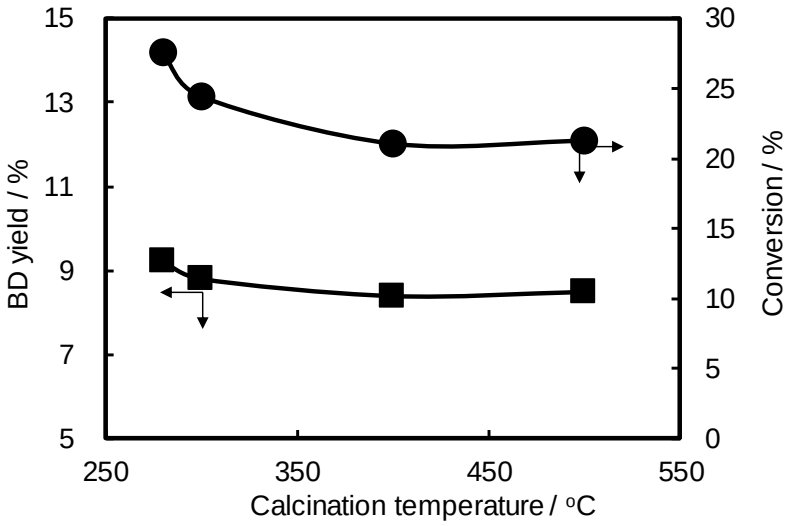

Fig. 2-9 Effect of calcination temperature on ODH of but-1-ene

Catalyst: $CuFe_2O_4$(AC)-500, -400, -300, -280,
Catalyst weight: 200 mg, Reaction temperature: 270 °C,
Flow rate: 1-C_4H_8/Ar=5/25 mL/min, Reaction time: 8 min

3.4 Evaluation of activity maintenance in repeated ODH

ODHs and re-oxidation were repeated using $CuFe_2O_4$(AC)-500 and $CuFe_2O_4$(AC)-280. The results are shown in Figs. 2-10 and -11, respectively. For $CuFe_2O_4$(AC)-500 (Fig. 2-10), the second reaction gave a lower conversion, 8.8% and a lower BD yield, 4.7%, and higher CO_2 selectivity, 11.3%, than those of the first reaction. The increase in the CO_2 selectivity after the second ODH indicated that the complete oxidation of C4 compounds such as but-1-ene and BD progressed. Thereafter, the conversion and the BD selectivity gradually increased from the third to the eighth ODH. After the seventh ODH, lower conversion of 15%, BD yield of 7.5%, higher BD selectivity of 48.2%, and CO_2 selectivity of 4.2% were maintained. The BD yield was stabilized at the eighth ODH, and $CuFe_2O_4$(AC)-500 stably produced BD in the repeated ODH. When $CuFe_2O_4$(AC)-280 was used for the repeated ODH (Fig. 2-11), in the second ODH, the conversion decreased from 26.9% to 17.0%, similar to that of $CuFe_2O_4$(AC)-500. Even at the tenth ODH, the conversion increased from 26.9% to 32.6% by the isomerization reaction. BD selectivity of about 35% was maintained, and CO_2 selectivity decreased relative to that at the second ODH. The BD yield then increased from 9.3% to 11.3%.

To examine the change in the crystal structure during the repeated ODHs, XRD analyses of $CuFe_2O_4$(AC)-500 and -280 were carried out after the repeated ODHs. The XRD patterns are shown in Fig. 2-12.

CuO diffraction peaks in both catalysts after the repeated ODHs were larger than those before the reaction (Fig. 2-12 a), b)). As already mentioned in section 3.2, since CuO(AC) showed the lower conversion, the high CO_2 selectivity, and the low BD yield, the results after the second ODH (Figs. 2-10, -11) show that $Cu_{1-x}Fe_2O_{4-x}$ produced by losing Cu species from the spinel phase hardly promoted the complete oxidation of C4 compounds

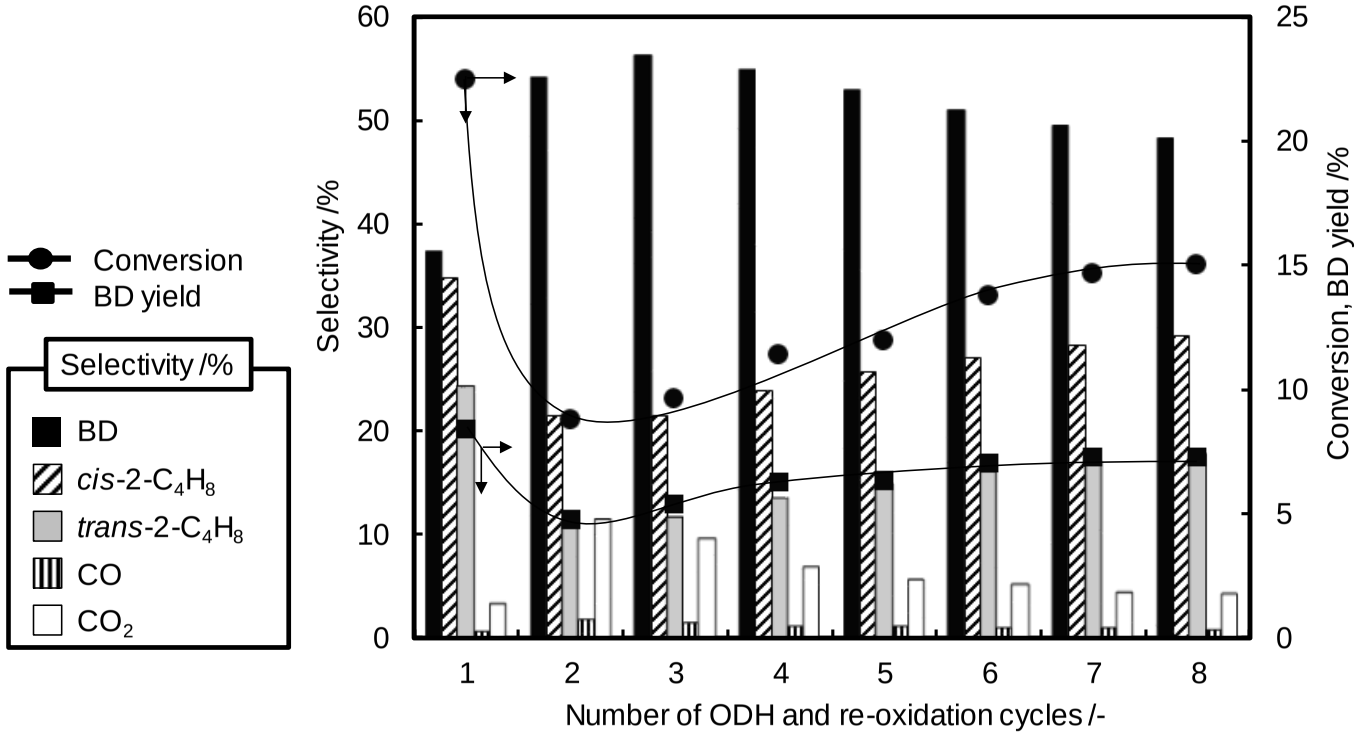

Fig. 2-10 Repeated ODH of but-1-ene and re-oxidation with $CuFe_2O_4$(AC)-500

Catalyst: $CuFe_2O_4$(AC)-500, Catalyst weight: 200 mg,
Flow rate: 1-C_4H_8/Ar=5/25 mL/min, Reaction temperature: 270 °C,
Reaction time: 8 min,
Re-oxidation: O_2/Ar=5/25 mL/min, Re-oxidation temperature: 270 °C,
Re-oxidation time: 8 min

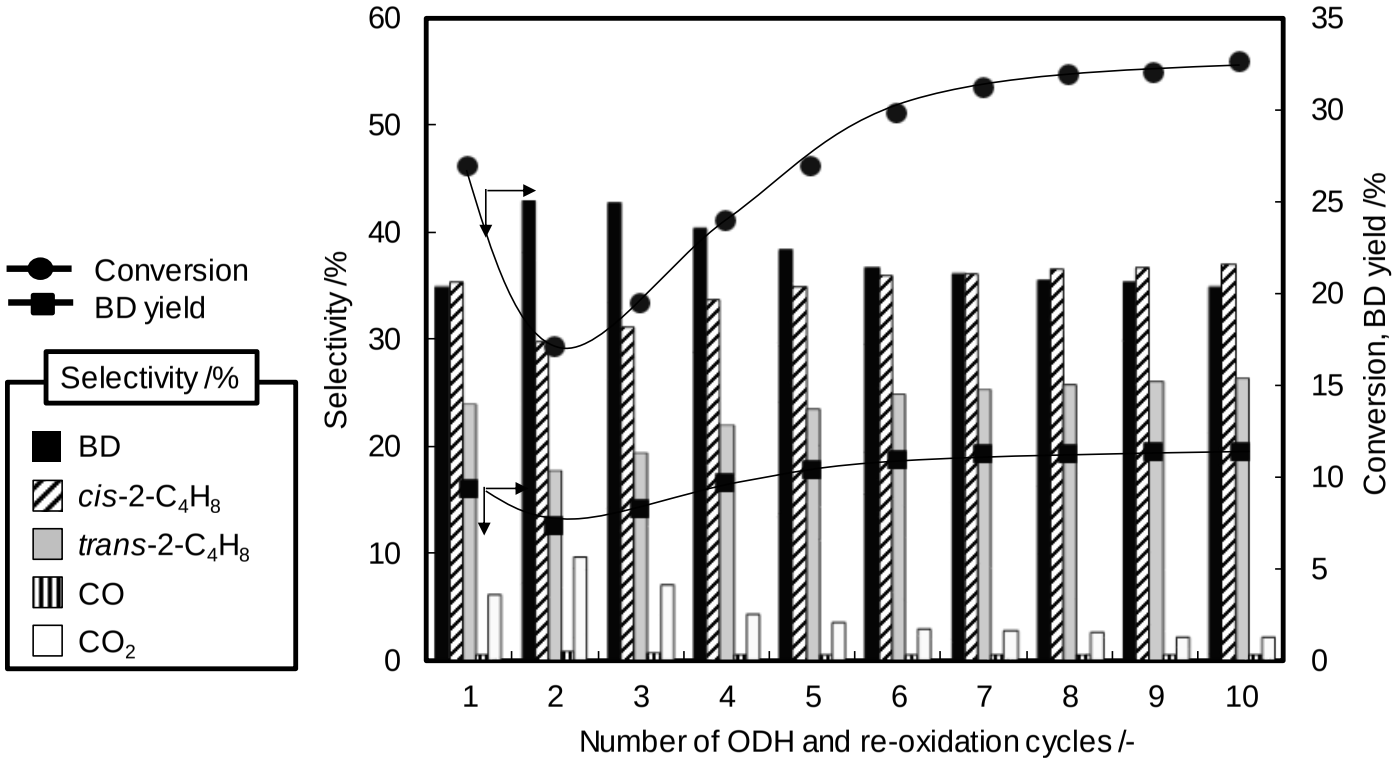

Fig. 2-11 Repeated ODH of but-1-ene and re-oxidation with $CuFe_2O_4$(AC)-280

Catalyst: $CuFe_2O_4$(AC)-280, Catalyst weight: 200 mg,
Flow rate: 1-C_4H_8/Ar=5/25 mL/min, Reaction temperature: 270 °C,
Reaction time: 8 min,
Re-oxidation: O_2/Ar=5/25 mL/min, Re-oxidation temperature: 270 °C,
Re-oxidation time: 8 min

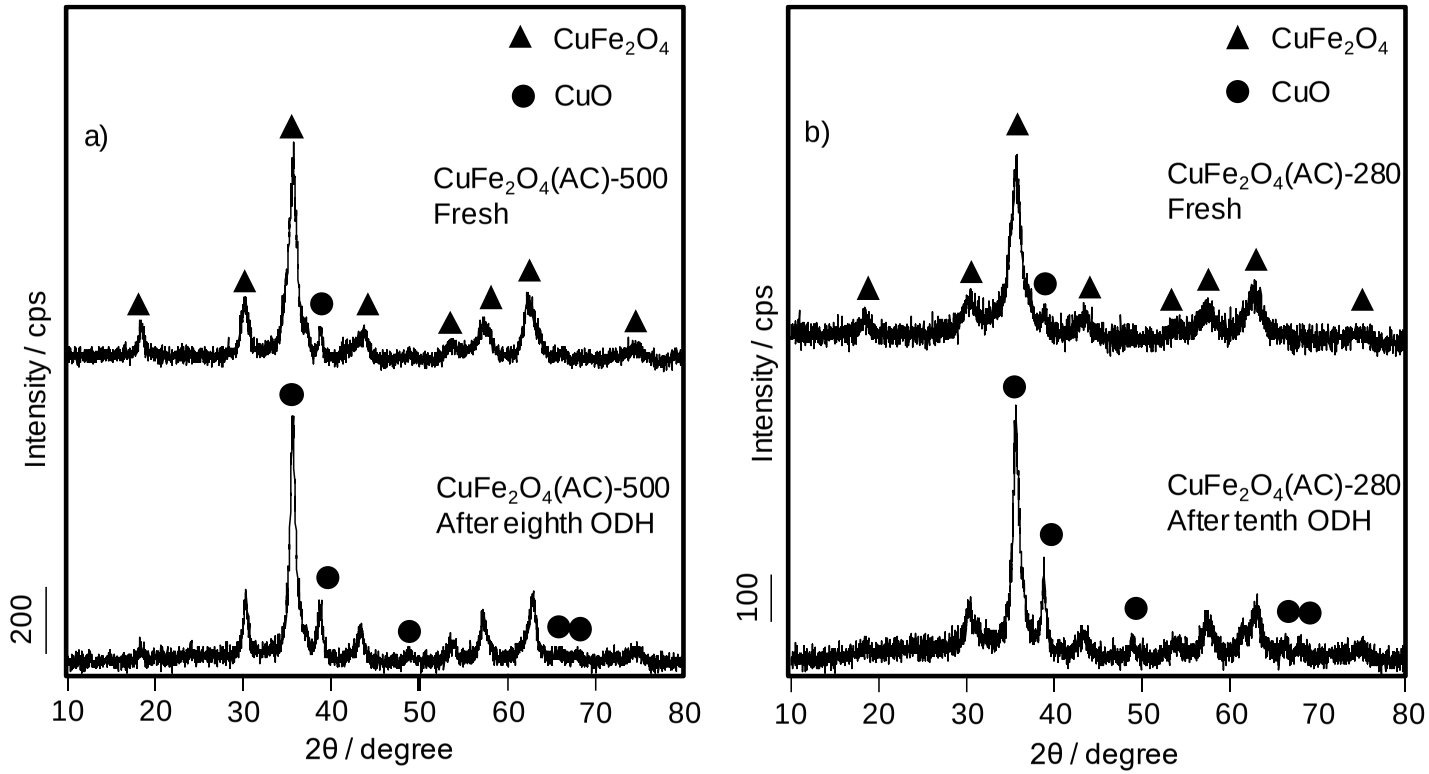

Fig.2-12 XRD patterns of $CuFe_2O_4$(AC)-500 and $CuFe_2O_4$(AC)-280 before and after repeatedly ODH

and promoted the isomerization reaction.

In order to evaluate the effects of Cu species such as tetrahedral and octahedral sites on the repeated ODHs, XPS analyses were used for the $CuFe_2O_4$(AC)-500 and -280 after the repeated ODHs. The ratios of Cu^{2+}_T/Cu^{2+}_O calculated from XPS analyses are shown in Table 2-5. The ratio of Cu^{2+}_T/Cu^{2+}_O of $CuFe_2O_4$(AC)-500 after the first ODH was lower than that of the fresh catalyst (Table 2-5 a), b)). Hence, decline of BD yield in second ODH would be due to the decrease of Cu^{2+}_T rate, and an increase in CO_2 selectivity was related to an increase in Cu^{2+}_O rate. On the other hand, the Cu^{2+}_T/ Cu^{2+}_O ratio after the eighth ODH was higher than that after the first re-oxidation (Table 2-5 b), c)), and the BD yield gradually recovered and stabilized at the eighth ODH. In the case of $CuFe_2O_4$(AC)-280, the Cu^{2+}_T/ Cu^{2+}_O ratio in $CuFe_2O_4$(AC)-280 after the first re-oxidation was lower than that of the fresh catalyst (Table 2-5 d), e)). However, the Cu^{2+}_T/ Cu^{2+}_O ratio after the tenth ODH increased from 0.26 to 0.36 compared to the fresh catalyst (Table 2-5 d), f)). Therefore, BD yield recovered at the tenth ODH.

Although the role of Cu^{2+}_T phase is not clear, its existence might be the most important factor for BD production in the ODH of but-1-ene.

Table 2-5 Cu^{2+}_T/Cu^{2+}_O ratio of $CuFe_2O_4$/AC catalyst before and after ODH calculated from XPS analysis

Fresh and used catalyst	Cu^{2+}_T (%)	Cu^{2+}_O (%)	Cu^{2+}_T/Cu^{2+}_O
a) $CuFe_2O_4$(AC)-500 fresh	20.5	79.5	0.26
b) $CuFe_2O_4$(AC)-500 after first re-oxidation	17.9	82.1	0.22
c) $CuFe_2O_4$(AC)-500 after 8th ODH	20.2	79.8	0.25
d) $CuFe_2O_4$(AC)-280 fresh	20.8	79.2	0.26
e) $CuFe_2O_4$(AC)-280 after first re-oxidation	18.4	81.6	0.23
f) $CuFe_2O_4$(AC)-280 after 10th ODH	26.7	73.3	0.36

4. Conclusions

$CuFe_2O_4$(AC)-500 gave a BD yield of 8.5% at 270 ºC, and the used catalyst was regenerated by re-oxidation with molecular O_2. The results of XRD and XPS analyses of $CuFe_2O_4$(AC)-500 after the ODH showed that the ODH progressed by using the lattice oxygen of Cu-O relating to Cu^{2+}_T. The $CuFe_2O_4$(AC) catalyst that had a higher specific surface area was more efficient for the ODH, and $CuFe_2O_4$(AC)-280, which had the highest specific surface area of 105 m^2/g, gave the highest BD yield, 9.3%.

For the repeated ODHs using $CuFe_2O_4$(AC)-500 and $CuFe_2O_4$(AC)-280, $CuFe_2O_4$(AC)-500 maintained a BD yield of about 8% until the eighth ODH and regeneration cycle. When $CuFe_2O_4$(AC)-280 was used for the repeated ODHs, BD was formed until the tenth ODH and the BD yield increased from 9.5% to 11.3%. From the XRD and XPS analyses of $CuFe_2O_4$(AC)-500 and $CuFe_2O_4$(AC)-280 after the repeated ODHs, $Cu_{1-x}Fe_2O_{4-x}$ generated by losing Cu species did not progress complete oxidation of but-1-ene. In addition, the increase in Cu^{2+}_T species seemed to increase the BD yield in the ODH of but-1-ene.

5. References

[1] F. Ma, S. Chem, Y. Li, H. Zhou, A. Xu, W. Lu, *Appl. Surf. Sci.,* **313** (2014) 654-659

[2] H. Fan, J. Feng, X. Li, Y. Guo, W. Li, K. Xie, *Chem. Eng. Sci.,* **135** (2015) 403-411

[3] I.A. Bakare, S.A. Mohamed, S. Al-Ghamdi, S.A. Razzak, M.M. Hossain, H.I. de Lasa, *Chem. Eng. J.,* **278** (2015) 207-216

[4] M. Setnicka, R. Bulanek, L. Capek, P. Cicmanec, *J. Mol. Catal. A: Gen,* **344** (2011) 1-10

[5] J.A. Toledo, N. Nava, M. Martinez, X. Bokhimi, *Appl. Catal. A: Gen.,* **234** (2002) 137-144

[6] H. Armendariz, G. Aguilar-Rios, P. Salas, M.A. Valenzuela, I. Schifter, H. Arriola, N. Nava, *Appl. Catal. A: Gen.,* **92** (1992) 29-38

[7] H. Lee, J.C. Jung, H. Kim, Y.M. Chung, T.J. Kim, S.J. Lee, S.H. Oh, Y.S. Kim, I.K. Song, *Catal. Lett.,* **131** (2009) 344-349

[8] Y.M. Chung, Y.T. Kwon, T.J. Kim, S.J. Lee, S.H. Oh, *Catal. Lett.,* **130** (2009) 417-423

[9] H. Lee, J.C. Jung, I.K. Song, *Catal. Lett.,* **133** (2009) 321-327

[10] H. Lee, J.C. Jung, H. Kim, Y.M. Chung, T.J. Kim, S.J. Lee, S.H. Oh, Y.S. Kim, I.K. Song, *Korean J. Chem. Eng.,* **26** (2009) 994-998

[11] H. Lee, J.C. Jung, H. Kim, Y.M. Chung, T.J. Kim, S.J. Lee, S.H. Oh, Y.S. Kim, I.K. Song, *Catal. Commun.,* **9** (2008) 1137-1142

[12] J.A. Toledo, P. Bosch, M.A. Valenzuela, A. Montoya, N. Nava, *J. Mol. Catal.,* **125** (1997) 53-62

[13] H. Armendariz, J.A. Toledo, G. Aguilar-Rios, M.A. Valenzuela, P. Salas, A. Cabral, H. Jimenez, I. Schifter, *J. Mol. Catal.,* **92** (1994) 325-332

[14] R.J. Rennard, W.L. Kehl, *J. Catal.*, **21** (1971) 282-293

[15] B.J. Liaw, D.S. Cheng, B.L. Yang, *J. Catal.*, **118** (1989) 312-326

[16] W.Q. Xu, Y.G. Yin, G.Y. Li, S. Chen, *Appl. Catal. A: Gen.,* **89** (1992) 131-142

[17] F.Y. Qiu, L.T. Weng, E. Sham, P. Ruiz, B. Delmon, *Appl. Catal.,* **51** (1989) 235-253

[18] Y.M. Chung, Y.T. Kwon, T.J. Kim, S.J. Lee, S.H. Oh, *Catal. Lett.,* **131** (2009) 579-586

[19] M.A. Gibson, J.W. Hightower, *J. Catal.,* **41** (1976) 431-439

[20] A. Dejoz, J.M. LoÂpez Nieto, F. MaÂrquez, M.I. VaÂzquez, *Appl. Catal. A. Gen.*, **180** (1999) 83-94

[21] J.K. Lee, H. Lee, U.G. Hong, J. Lee, Y.-J. Cho, Y. Yoo, H.S. Jang, I.K. Song, *J. Ind. Eng. Chem.,* **18** (2012) 1096-1101

[22] J.M. Lopez Nieto, P. Concepci, A. Dejoz, H. Knozinger, F. Melo, M.I. Vazquez., *J. Catal.,* **189** (2000) 147–157

[23] J.H. Park, H. Noh, J.W. Park, K. Row, K.D. Jung, C.-H. Shin, *Appl. Catal. A. Gen.,* **431** (2012) 137-143

[24] J.C. Jung, H. Lee, H. Kim, Y.M. Chung, T.J. Kim, S.J. Lee, S.H. Oh, Y.S. Kim, I.K. Song, *Catal. Commun.,* **9** (2008) 943–949

[25] J.C. Jung, H. Kim, Y.M. Chung, T.J. Kim, S.J. Lee, S.H. Oh, Y.S. Kim, I.K. Song, *J. Mol. Catal.*, **264** (2007) 237-240

[26] J.C. Jung, H. Kim, Y.M. Chung, T.J. Kim, S.J. Lee, S.H. Oh, Y.S. Kim, I.K. Song, *Appl. Catal. A: Gen.*, **317** (2007) 244-249

[27] A.P.V. Soares, L.D. Dimitrov, M.C.A. Oliveira, L. Hilaire, M.F. Portela, R.K. Grasselli, *Appl. Catal. A: Gen.,* **253** (2003) 191-200

[28] K. Fukudome, N. Ikenaga, T. Miyakke, T. Suzuki, *Catal. Sci. Technol.,* **1** (2011) 987-998

[29] N. Ikenaga, N. Chiyoda, H. Matsushima, T. Suzuki, *Fuel,* **81** (2002) 1569-1576

[30] Y. Wang, H. Zhao, M. Li, J. Fan, G. Zhao, *Appl. Catal. B: Environ.,* **147** (2014) 534-545

[31] C. Reitz, C. Suchomski, J. Haetge, T. Leichtweiss, Z. Jaglicic, I. Djerdj, T Brezesinski, *Chem. Commun.,* **48** (2012) 4471-4473

Chapter 3

Oxidative dehydrogenation of but-1-ene at low temperature with copper ferrite catalysts

1. Introduction

Buta-1,3-diene (BD) is prepared from the steam-cracking of naphtha, and it is an important material for polybutadiene rubber, styrene butadiene rubber, and ABS resin. However, there are problems with the steam-cracking of naphtha. For example, the process requires a high temperature of more than 700 ^{o}C, and uses a lot of energy because the reaction is endothermic. In addition, since many products are also produced, BD selectivity in this process is low. On the other hand, the dehydrogenation of n-butene has been proposed as a production process for BD, but this process is also an endothermic reaction that requires a lot of energy (Eq. (1)). Therefore, new alternative processes are needed.

$$1\text{-}C_4H_8 \rightarrow C_4H_6 + H_2 \qquad \Delta H^o = 112 \text{ kJ/mol} \qquad (1)$$

Recently, the oxidative dehydrogenation (ODH) of compared in C4 fraction with molecular O_2 (Eq. (2)) has attracted much attention as an alternative process for the production of BD. Since this reaction is an exothermic process, it is very useful from the viewpoint of energy conservation. Moreover, it allows BD to be produced with high selectivity.

$$1\text{-}C_4H_8 + 1/2O_2 \rightarrow C_4H_6 + H_2O \quad \Delta H^o = -132.1 \text{ kJ/mol} \qquad (2)$$

Various composite metal oxides, and metal oxides or metal-supported catalysts, have been investigated for the ODH of many hydrocarbons, including propane [1], ethylbenzene [2], ethane [3], n-butane [4], n-butene [5], and cyclohexane [6]. For the ODH of n-butene and n-butane, Pd-In catalyst [7], ferrite-type catalysts [5,8-21], V-containing catalysts [22-24], Bi-Mo catalysts [25-29], and CuO/Al_2O_3 catalyst [30] exhibited high activity.

As mentioned in Chapter 2, zinc ferrite-type catalysts such as Zn-Fe [5,8-13,19,20], Zn-Fe-Cr [15], and Zn-Fe-Al [14] have been widely studied for the ODH of n-butene. However, in the presence of O_2, the deep oxidation to CO and CO_2 proceeded easily during the ODH.

In order to inhibit the complete oxidation, ODH with a zinc ferrite catalyst has been carried out under an O_2 flow with steam. Because the latent heat of steam is large, excessive energy are necessary. Therefore, the supply of steam is undesirable. As a process to produce BD without forming CO_2, the ODH of propane or butene with the lattice oxygen of the catalyst has also been reported [30,31]. In these studies, the lattice oxygen of the metal oxide catalyst was used to inhibit the deep oxidation of the reactant and the product, and then molecular O_2 was supplied after the reaction to regenerate the used lattice oxygen (Eqs. (3), (4)). Moreover, the catalytic activity was maintained throughout repeated ODHs.

$$1\text{-}C_4H_8 + MO_x \rightarrow C_4H_6 + H_2O + MO_{x-1} \qquad (3)$$

$$MO_{x-1} + 1/2O_2 \rightarrow MO_x \qquad (4)$$

In Chapter 2, the copper ferrite catalyst prepared in the presence of activated carbon exhibited the high activity for the ODH of but-1-ene with the lattice oxygen at a temperature (270 ^oC) lower than those for various ferrite catalysts in the repeated studies.

Moreover, the copper ferrite catalyst could be used repeatedly for the ODH by the re-oxidation with O_2.

On the other hand, there are few reports on the continuous BD production over a long time in the ODH under O_2 flow at the temperature lower than 300 ^oC. Therefore, the objective of this chapter is to continuously produce BD at the low temperature.

In order to produce BD more efficiently, the ODH of but-1-ene was carried out under an O_2 flow, and the catalytic performance of the copper ferrite catalyst in the ODH at 270 ^oC over a long time was studied. Furthermore, the role of the copper ferrite phase and the optimum reaction conditions for the ODH of but-1-ene were examined.

2. Experimental Section

2.1 Materials

$Fe(NO_3)_3 \cdot 9H_2O$ (assay = min. 99.0%), $Cu(NO_3)_2 \cdot 3H_2O$ (assay = min. 99.0%), activated carbon (AC), citric acid (assay = min. 98.0%), and NaOH (assay = min. 93.0%) were purchased from Wako Pure Chemical Industry, and used for the preparation of copper oxide catalysts. But-1-ene (1-C_4H_8) (assay = min. 99.0%) was supplied from Sumitomo Seika Chemical.

2.2 Catalyst preparation

2.2.1 Preparation by the impregnation method

Copper ferrite catalysts were prepared by the impregnation method at a weight ratio of AC: composite metal oxides=4:1. An activated carbon was impregnated with an aqueous solution of $Fe(NO_3)_3 \cdot 9H_2O$ and $Cu(NO_3)_2 \cdot 3H_2O$ at a molar ratio of Cu:Fe=0.25, 0.5, 1, or 2:2 in 120 mL of water. After standing at room temperature overnight, water was evaporated to dryness under reduced pressure of 1 kPa. The resulting solid was dried at 70 ^oC overnight in vacuo. The catalyst precursor was calcined at 500 ^oC for 2 h in air. Hereafter, this material will be referred to as $CuFe_2O_4$(AC). Fe_2O_3(AC) and CuO(AC) were prepared by the same method. In a previous study, we reported that the carbon derived from AC does not remain in the copper ferrite. Moreover, according to TG-DTA analysis of Fe_2O_3(AC) and CuO(AC), AC was not observed in the catalyst calcined at 500 ^oC (Figure 3-1).

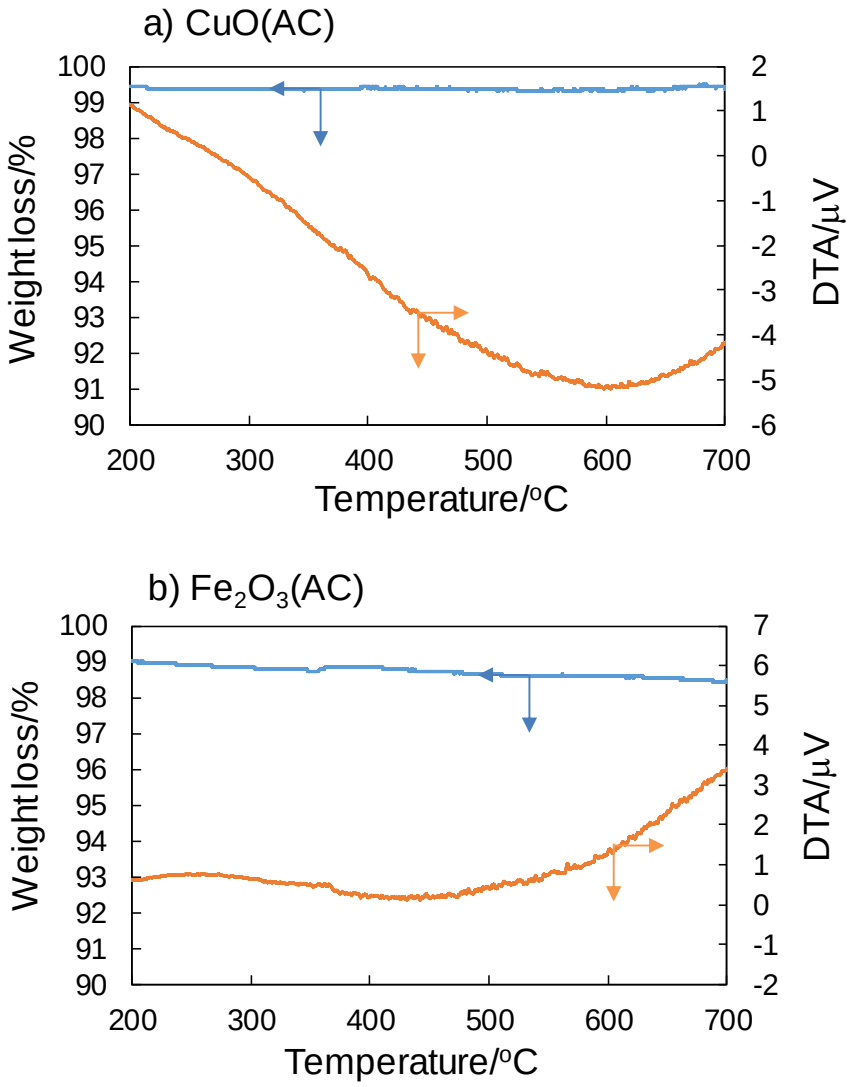

Fig. 3-1 TG-DTA profiles of CuO(AC) and Fe_2O_3(AC) catalysts

Substance: CuO(AC), Fe_2O_3(AC), Flow rate: air=100 mL/min (STP), Temperature ramp rate: 5 °C/min

2.2.2 Preparation by the citric acid complex method

Copper ferrite was prepared by the citric acid complex method. At a molar ratio of Cu:Fe=1:2, metal nitrates were dissolved in a citric acid aqueous solution in which the citric acid is equivalent to the sum of metals. The solution was stirred at room temperature overnight, and then water was evaporated under reduced pressure. The solid was calcined at 500 ^{o}C for 2 h in air. Hereafter, the notation for this substance will be $CuFe_2O_4$c.

2.2.3 Preparation by the co-precipitation method

Copper ferrite was prepared by the co-precipitation method. At a molar ratio Cu:Fe=1:2, metal nitrates of $Cu(NO_3)_2{\cdot}6H_2O$ (5 mmol) and $Fe(NO_3)_3{\cdot}9H_2O$ (10 mmol) were dissolved in 100 mL of pure water. The solution was stirred at room temperature for 1 h. After stirring, 1 mol/L of NaOH solution was added drop-wise to the solution under vigorous stirring until the pH reached 13. After stirring, the resultant precipitate was separated by centrifugation, and the solid was washed with a large amount of pure water until the pH reached 7-8, and then dried under vacuum. The solid was calcined at 500 ^{o}C for 2 h in air. Hereafter, the notation for this material will be $CuFe_2O_4$cop.

2.2.4 Cu_2O preparation by the precipitation method

Copper(I) oxide was prepared by the precipitation method. A amount of $Cu(NO_3)_2{\cdot}6H_2O$ (10 mmol) was dissolved in 100 mL of pure water. The solution was stirred at room temperature for 1 h. Then, 1 mol/L of NaOH solution was added drop-wise to the solution under vigorous stirring until the pH reached 13. After stirring, glycerin was added until the solution became a clear deep blue. The glucose solution (glucose/water=12 g/90 g) was then added to reduce the deep blue solution, and the

suspension was left to stand in the dark room overnight. The resulting precipitate was separated by centrifugation, and the solid was washed with a large amount of pure water. The red solid was obtained by drying under a vacuum. Hereafter, the notation for this material will be Cu_2O.

2.3 Catalyst characterization

X-ray diffraction (XRD) patterns of copper oxide catalysts were obtained using the powder method with a Shimadzu XRD-6000 diffractometer with monochromatic Cu Kα radiation under the following conditions: tube voltage 40 kV, tube current 30 mA, scan step 0.02^o, scan region $10\text{-}80^o$, and scan speed 2.0^o/min. X-ray photoelectron spectra (XPS) analyses were carried out with a JEOL model JPS-9010MX using Mg Kα radiation as an energy source.

2.4 Catalyst test

2.4.1 ODH of but-1-ene with lattice oxygen in ferrite catalyst

ODH of but-1-ene was carried out using a fixed-bed flow quartz reactor at 270 ^{o}C under atmospheric pressure. A 200 mg portion of the catalyst was placed in the reactor, and the reactor was heated to a reaction temperature of 270 ^{o}C under 25 mL/min of Ar flow. Then, 5 mL/min (STP) of but-1-ene and 25 mL/min (STP) of Ar were introduced for 8 min. The C4 compounds (1-C_4H_8, *cis*-2-C_4H_8, *trans*-2-C_4H_8, and C_4H_6) were analyzed by a flame ionization detector (FID) gas chromatograph (Shimadzu GC14B, column: Unicarbon A-400). CO and CO_2 were also analyzed by FID gas chromatograph (column: Activated carbon) equipped with a methanizer (Shimadzu MTN-1). H_2 was

analyzed by a thermal conductivity detector (TCD) gas chromatograph (Shimadzu GC8A, column: Activated carbon).

2.4.2 ODH of but-1-ene with ferrite catalyst under a molecular O_2 flow

The ODH of but-1-ene was carried out using the fixed-bed flow quartz reactor between 230-350 ^oC under atmospheric pressure for 100 min. A 200 mg portion of catalyst was placed in the reactor, and the reactor was preheated to a desired reaction temperature under 25 mL/min (STP) of Ar flow. Oxygen, 1-C_4H_8, and Ar were introduced at a flow rate of O_2/1-C_4H_8/Ar=(1, 2.5, 4 or 5)/5/(24, 22.5, or 21) mL/min (STP). Total gas flow rate was fixed at 30 mL/min. Quantification of the products was carried out using the same equipment as in Section 2.4.1.

3. Results and Discussion

3.1 Effect of reaction temperature on ODH of but-1ene

In order to investigate the optimum reaction temperature, ODH was conducted at reaction temperatures ranging from 230-350 ^oC. Figure 3-2 shows the effects of reaction temperature. When the ODH of but-1-ene was carried out at 270 ^oC, conversion was 19.5%, and the BD selectivity and yield were higher (43.7% and 8.5%, respectively). However, high CO_2 selectivity of 37.3% was also shown. On the other hand, because the lowest conversion of 1.5% was given at 230 ^oC, the reaction hardly progressed. At 260 ^oC, a lower conversion of 12.9% and lower BD yield of 5.9% were obtained, compared to those at 270 ^oC. BD selectivity and CO_2 selectivity were 46.1% and 39.8%, respectively. Therefore, the complete oxidation could not be suppressed by lowering the reaction temperature. When the ODH was carried out at 300 ^oC, the selectivities of BD and CO_2,

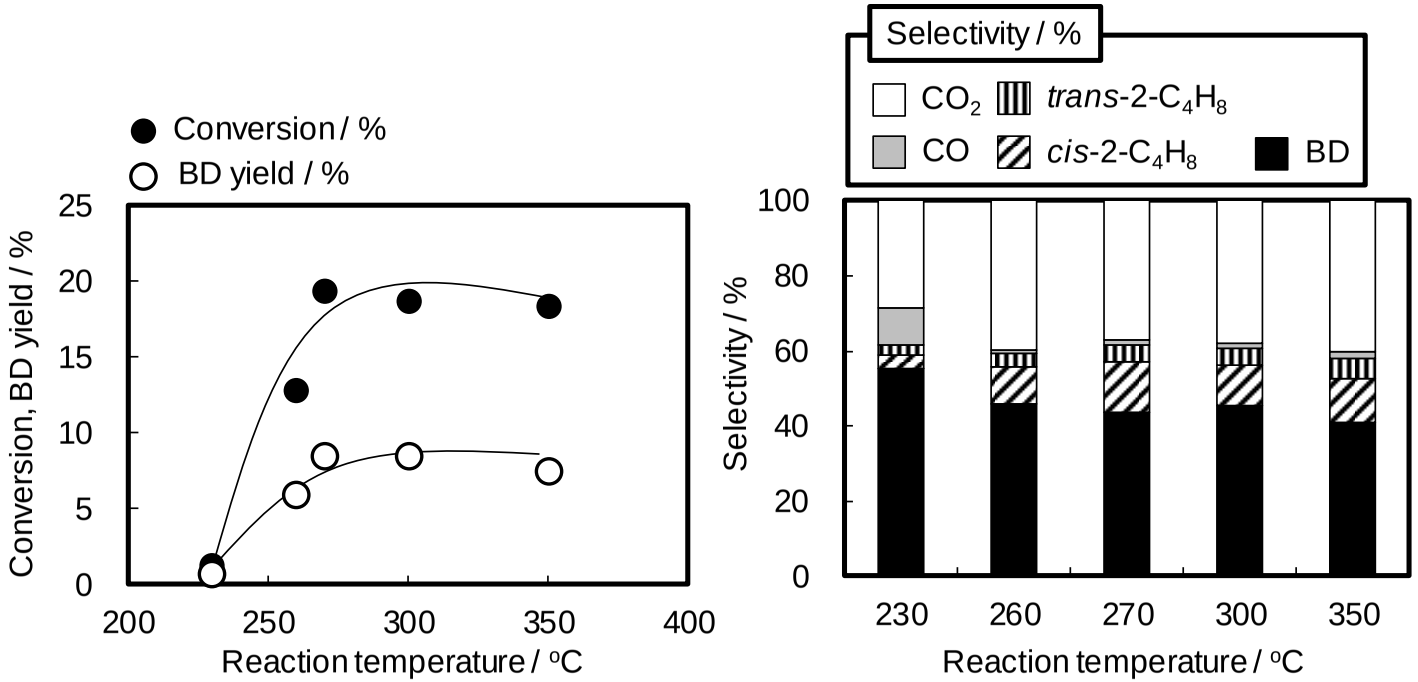

Fig. 3-2 Effect of reaction temperature on ODH of but-1-ene in the presence of O_2

Catalyst: $CuFe_2O_4$(AC), Catalyst weight: 200 mg,
Flow rate: 30 mL/min (1-C_4H_8 /O_2/Ar = 5/2.5/22.5), Reaction time: 100 min

the conversion, and the BD yield were almost the same as those at 270 °C. Meanwhile, also in the case of 350 °C, the same result (BD selectivity of 41% and BD yield of 7.5%) as 270 °C was obtained. Therefore, it was considered that the best reaction temperature for the ODH of but-1-ene under an O_2 atmosphere with $CuFe_2O_4$(AC) was 270 °C.

The usefulness of $CuFe_2O_4$ in the ODH at low temperature was examined. $ZnFe_2O_4$ catalyst as reference catalyst was used in the ODH of but-1-ene under O_2 flow at 270 °C. $ZnFe_2O_4$ was prepared as previously reported [13]. As the result, BD was not formed (Figure 3-3). Therefore, $CuFe_2O_4$(AC) catalyst was superior to $ZnFe_2O_4$ for the ODH activity at 270 °C.

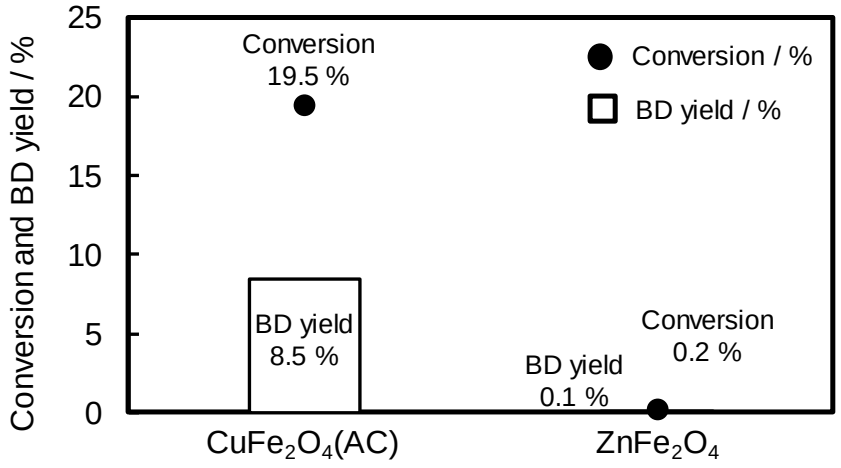

Fig. 3-3 ODH of but-1-ene in the presence of O_2 at 270 °C with ferrite catalysts

3.2 Effect of the catalyst preparation method on ODH of but-1-ene

To determine the best preparation method, the catalysts were prepared by different methods: impregnation in the presence of AC ($CuFe_2O_4$(AC)), the co-precipitation method ($CuFe_2O_4$cop), and the citric acid complex method ($CuFe_2O_4$c).

Figure 3-4 shows the XRD patterns of the copper ferrite catalysts prepared by the different methods. $CuFe_2O_4$(AC) indicated $CuFe_2O_4$ and a few CuO diffraction peaks (Figure 3-4a). $CuFe_2O_4$cop showed small CuO and Fe_2O_3 diffraction peaks in addition to main $CuFe_2O_4$ diffraction peaks (Figure 3-4b). In case of $CuFe_2O_4$c, $CuFe_2O_4$ diffraction peaks were observed (Figure 3-4c). In all the copper ferrite catalysts, the main structure was $CuFe_2O_4$. On the other hand, the specific surface area of catalyst was the order of $CuFe_2O_4$cop (43 m^2/g)>$CuFe_2O_4$(AC) (34 m^2/g)>$CuFe_2O_4$c (26 m^2/g).

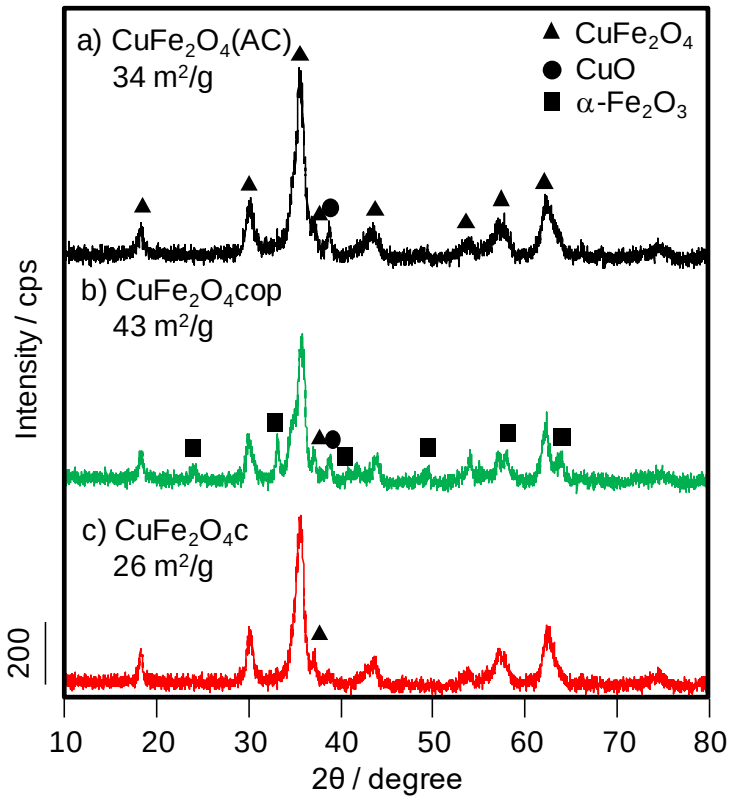

Fig. 3-4 XRD patterns of copper ferrite catalyst prepared by various methods

Figure 3-5 shows the results of the ODH of but-1-ene in the presence of O_2 with the copper ferrite catalysts. Although all the copper ferrite catalysts showed high CO_2 selectivity of about 30%, all catalysts formed BD during the 100 min reaction. $CuFe_2O_4$c showed the lowest BD yield of about 4%, and the lowest conversion of about 10%. Although $CuFe_2O_4$(AC) and $CuFe_2O_4$cop gave similarly high conversions of about 20%, $CuFe_2O_4$(AC) exhibited a higher BD yield (~8%) and higher BD selectivity (~40%) than $CuFe_2O_4$cop. Here, time course during ODH for 100 min with $CuFe_2O_4$(AC) was confirmed (Figure 3-6). Although the butene conversion and BD yield decreased between 20 and 40 min, the ODH activity was maintained after 40 min. In addition, the selectivities were not changed for 100 min. $CuFe_2O_4$(AC) catalyst would be able to generate BD for a long time.

To understand the effect of the different preparation methods on the ODH in the presence of O_2, the lattice oxygen mobility in the catalyst was noted. Table 3-1 presents the results of the ODH of but-1-ene with the lattice oxygen for 8 min. $CuFe_2O_4$(AC) had a low conversion of 21.3% and high BD selectivity of 39.9%. $CuFe_2O_4$cop showed a high conversion of 30.3% and medium BD selectivity of 27.0%. $CuFe_2O_4$c exhibited a medium conversion of 23.5% and low BD selectivity of 22.8%. The order of BD yield was $CuFe_2O_4$(AC) (8.5%, Run 1) ≈ $CuFe_2O_4$cop (8.2%, Run 2) > $CuFe_2O_4$c (5.4%, Run 3). These results were identical to those for the ODH in the presence of O_2. Therefore, the amount of lattice oxygen in the copper ferrite catalyst to form BD seems to be related to the ODH of but-1-ene in the presence of O_2.

Meanwhile, as shown in Fig. 3-4, $CuFe_2O_4$(AC) hardly had CuO and Fe_2O_3 phases, and had the high specific surface area. Therefore, it was suggested that pure $CuFe_2O_4$ phase which has high specific surface area were necessary to progress the ODH. The

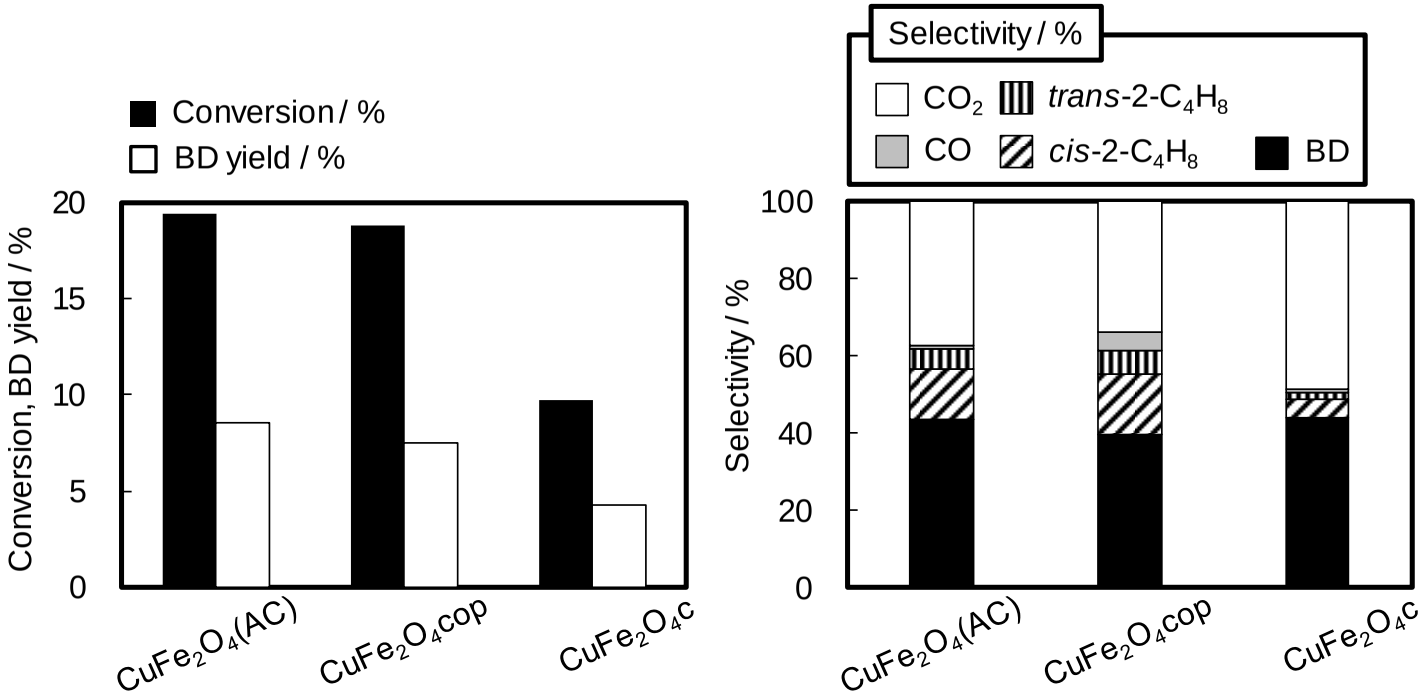

Fig. 3-5 Effect of various preparation methods on ODH of but-1-ene in the presence of O_2

Catalyst: 200 mg, Flow rate: 30 mL/min (1-C_4H_8 /O_2/Ar = 5/2.5/22.5)
Reaction temperature : 270 ^oC, Reaction time: 100 min

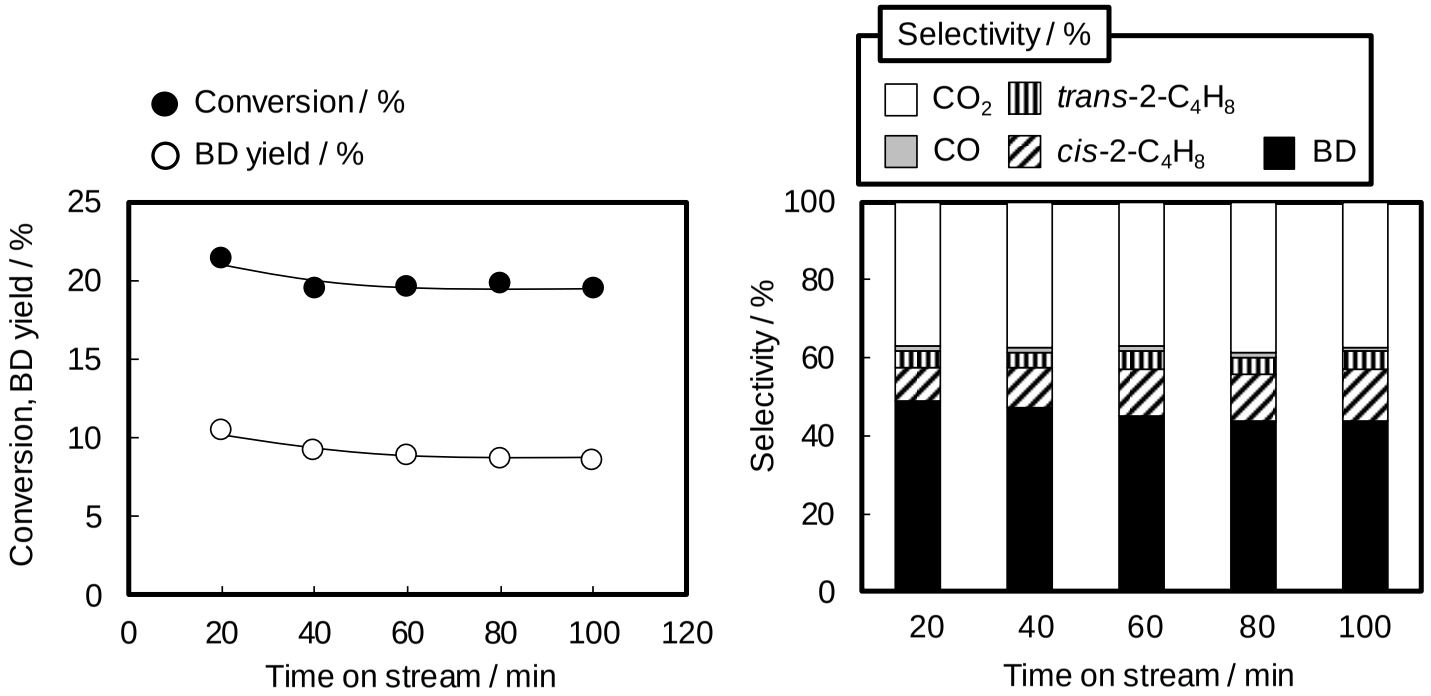

Fig. 3-6 Time course of ODH of but-1-ene in the presence of O_2 with $CuFe_2O_4$(AC)

impregnation method in the presence of AC was shown to be the best preparation method for the copper ferrite catalyst.

Table 3-1 Effect of preperation method on ODH of 1-C_4H_8 by the lattice oxygen of copper ferrite catalysts

Run	Catalyst	Conversion (%)	Selectivity(%)					Yield(%)
			C_4H_6	cis-C_4H_8	trans-C_4H_8	CO	CO_2	C_4H_6
1	$CuFe_2O_4$(AC)	21.3	39.9	34.2	23.1	0.7	2.1	8.5
2	$CuFe_2O_4$cop	30.3	27.0	44.0	26.9	0.2	1.9	8.2
3	$CuFe_2O_4$c	23.5	22.8	47.3	28.7	0.2	1.0	5.4

Calcination temp: 500 °C, Catalyst: 200mg, Flow rate: 1-C_4H_8/Ar=5/25 (mL/min)
Reaction temp.: 270 °C, Reaction time: 8 min

3.3 Effect of the Cu/Fe ratio

To determine the optimum Cu/Fe ratio of $CuFe_2O_4$(AC), various $CuFe_2O_4$(AC) catalysts were prepared by the impregnation method at various Cu/Fe ratios.

XRD analyses were carried out, and the results are shown in Figure 3-7. The catalyst prepared at Cu/Fe=1/8 showed mostly the α-Fe_2O_3 phase with a partial spinel phase (Figure 3-7a). The catalyst prepared at Cu/Fe=1/4 mainly showed $CuFe_2O_4$ diffraction peaks (Figure 3-7b). However, α-Fe_2O_3 diffraction peaks were also obtained in addition to $CuFe_2O_4$ diffraction peaks. When the catalyst was prepared at Cu/Fe=1/2 (Figure 3-7c), the spinel structure and a small amount of CuO diffraction peaks were observed. In the case of Cu/Fe=1/1(Figure 3-7d) a spinel structure was observed with more CuO diffraction peaks than in Cu/Fe=1/2. Thus, the amount of copper ferrite structure could be controlled by changing the Cu/Fe ratio.

Figure 3-8 shows the effect of Cu/Fe ratio on the ODH of but-1-ene in the presence of O_2. The catalyst prepared at Cu/Fe=1/8 showed low conversion (10%) and BD yield (5%), and high BD (48%) and CO_2 selectivities (42%). In the case of Cu/Fe=1/4, this

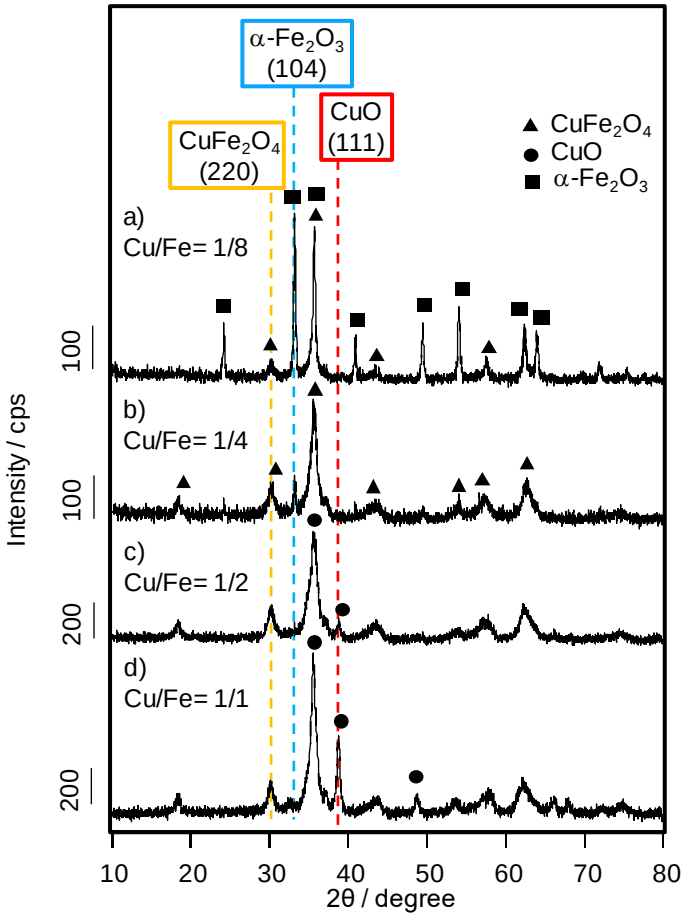

Fig. 3-7 XRD patterns of $CuFe_2O_4$(AC) catalysts prepared by various Cu/Fe ratios

catalyst showed a conversion of 14% and high BD yield of 8.0%. A high BD selectivity of 50% was also found. When the catalyst prepared at Cu/Fe=1/1 was used, a higher conversion of 15% was observed. However, the BD selectivity was lower than those of the other catalysts, and thus the BD yield was also lower (6.5%). Although the catalyst prepared at Cu/Fe=1/2 exhibited a lower BD selectivity (43.3%) than that prepared at Cu/Fe=1/4, the catalyst of Cu/Fe=1/2 showed the highest conversion and BD yield (20% and 8.5%, respectively). Therefore, the optimum Cu/Fe ratio was Cu/Fe=1/2.

The conversion of but-1-ene seems to be dependent on CuO content. However, the conversion decreased with an increase from Cu/Fe=1/2 to 1/1. In Chapter 2, in the case

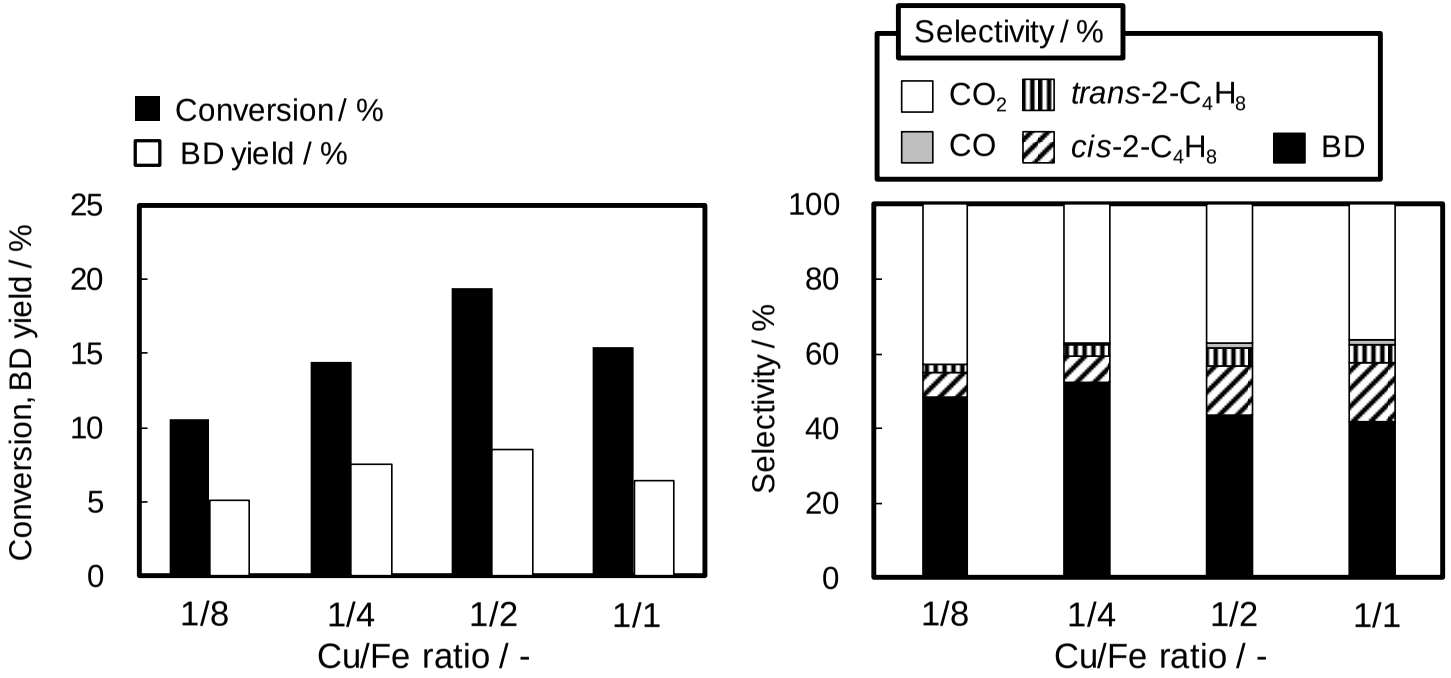

Fig. 3-8 Effect of Cu/Fe ratio on ODH of but-1-ene in the presence of O_2

Catalyst: $CuFe_2O_4$(AC) (Cu/Fe=1/8, 1/4, 1/2, 1/1), Catalyst weight: 200 mg,
Flow rate: 30 mL/min (1-C_4H_8 /O_2/Ar = 5/2.5/22.5) Reaction time: 100 min

of the ODH with lattice oxygen in CuO, the conversion was low. Therefore, it was considered that excessive CuO content led to the decline of conversion in the presence of O_2. On the other hand, high BD selectivity and yield were exhibited with the copper ferrite catalyst, which mainly had a spinel structure (Cu/Fe=1/2, 1/4). Therefore, the relation between the amount of $CuFe_2O_4$ and BD yield was investigated.

Table 3-2 shows the abundance ratios of the $CuFe_2O_4$ phase in the catalyst. The ratios of the $CuFe_2O_4$ phase ($(CuO+Fe_2O_3)/CuFe_2O_4$) were calculated from the diffraction intensity of CuO(111), Fe_2O_3(104), and $CuFe_2O_4$(220) diffraction peaks in these catalysts. The values of $(CuO+Fe_2O_3)/CuFe_2O_4$ were in the order of Cu/Fe=1/8(17.5)>1/1(2.5)>1/4(0.8)>1/2(0.5). Since a lower $(Fe_2O_3+CuO)/CuFe_2O_4$ value indicates the abundance of $CuFe_2O_4$ phase, these results show that the $CuFe_2O_4$(AC) catalyst prepared at Cu/Fe=1/2 contains the large amount of $CuFe_2O_4$ phase. Figure 3-9 shows the relation between the relative amount of $CuFe_2O_4$ and the BD yield. With a decrease in the $(CuO+Fe_2O_3)/CuFe_2O_4$ value, the BD yield tended to increase. Therefore, since the $CuFe_2O_4$(Cu/Fe=1/2) catalyst contained more $CuFe_2O_4$ phase than the other catalysts, the highest BD yield of 8.5% was obtained in the ODH of but-1-ene in the presence of O_2.

Table 3-2 Abundance ratio of $CuFe_2O_4$ calculated from intensity of XRD diffraction peaks

Cu/Fe ratio	Fe_2O_3(104) (%)	CuO (111) (%)	$CuFe_2O_4$(220) (%)	$(Fe_2O_3+CuO)/CuFe_2O_4$
1/8	94.6	0.0	5.4	17.5
1/4	43.3	0.0	56.7	0.8
1/2	0.0	34.8	65.2	0.5
1/1	0.0	71.4	28.6	2.5

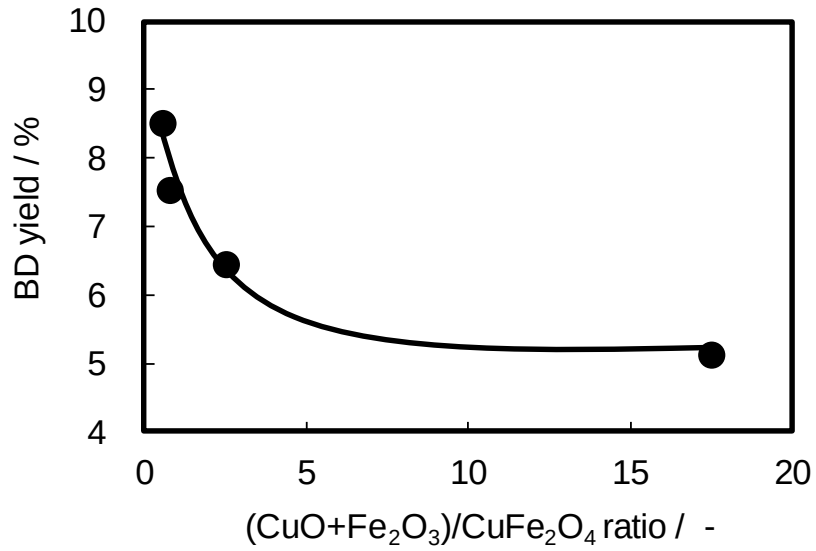

Fig. 3-9 Relationship between relative amount of $CuFe_2O_4$ phase and BD yield

On the other hand, CO_2 selectivities of about 40% were observed with all catalysts. The relationship between the complete oxidation reaction and CuO, Fe_2O_3, or $CuFe_2O_4$ phase could not be determined. Therefore, other factors should be considered for the complete oxidation of the C4 fraction.

3.4 Effect of the 1-C_4H_8/O_2 ratio on ODH

In order to elucidate the effect of the 1-C_4H_8/O_2 ratio on the ODH in the presence of O_2, O_2 flow rate was changed from 1 to 5 mL/min. Figure 3-10 shows the effect of the 1-C_4H_8/O_2 ratio on the ODH with $CuFe_2O_4$(AC) at 270 ºC. At 1-C_4H_8/O_2=5/1, the highest BD selectivity of 56.5% was obtained. However, the conversion and BD yield were low. In the cases of 1-C_4H_8/O_2=5/2.5, 4 and 5, BD selectivity tended to decline and CO_2 selectivity was slightly increased. Therefore, the complete oxidation of butene and/or BD was progressed. However, since the significant improvement of conversion was seen, the amount of O_2 seems to be related to the increase in conversion of but-1-ene. In other

words, both ODH and complete oxidation were increased with an increase in the amount of O_2. When the ODH of but-1-ene was carried out at 1-C_4H_8/O_2=5/5, the highest conversion of 30% and highest BD yield of 15% were obtained. In addition, but-1-ene

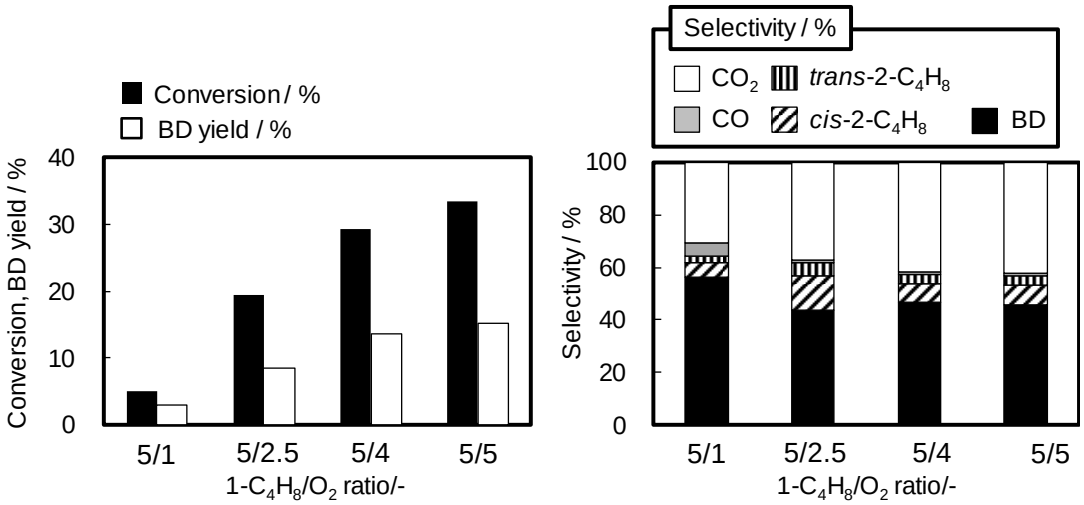

Fig. 3-10 Effect of 1-C_4H_8/O_2 ratio on ODH of but-1-ene in the presence of O_2

Catalyst: $CuFe_2O_4$(AC), Catalyst weight: 200 mg,
Flow rate: 30 mL/min (1-C_4H_8 /O_2/Ar = 5/1, 2.5, 4, 5/balance), Reaction time: 100 min

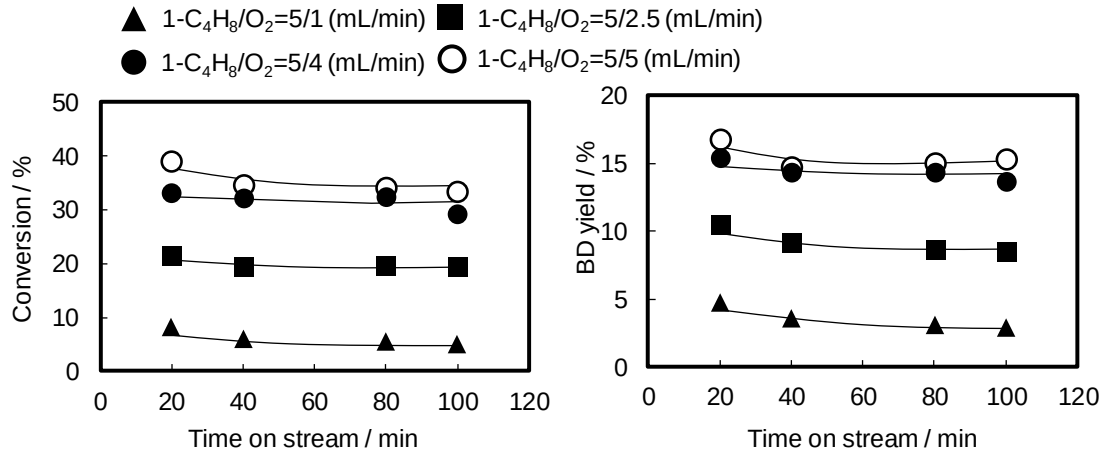

Fig. 3-11 Time course of ODH of but-1-ene under various 1-C_4H_8/O_2 ratio with $CuFe_2O_4$(AC)

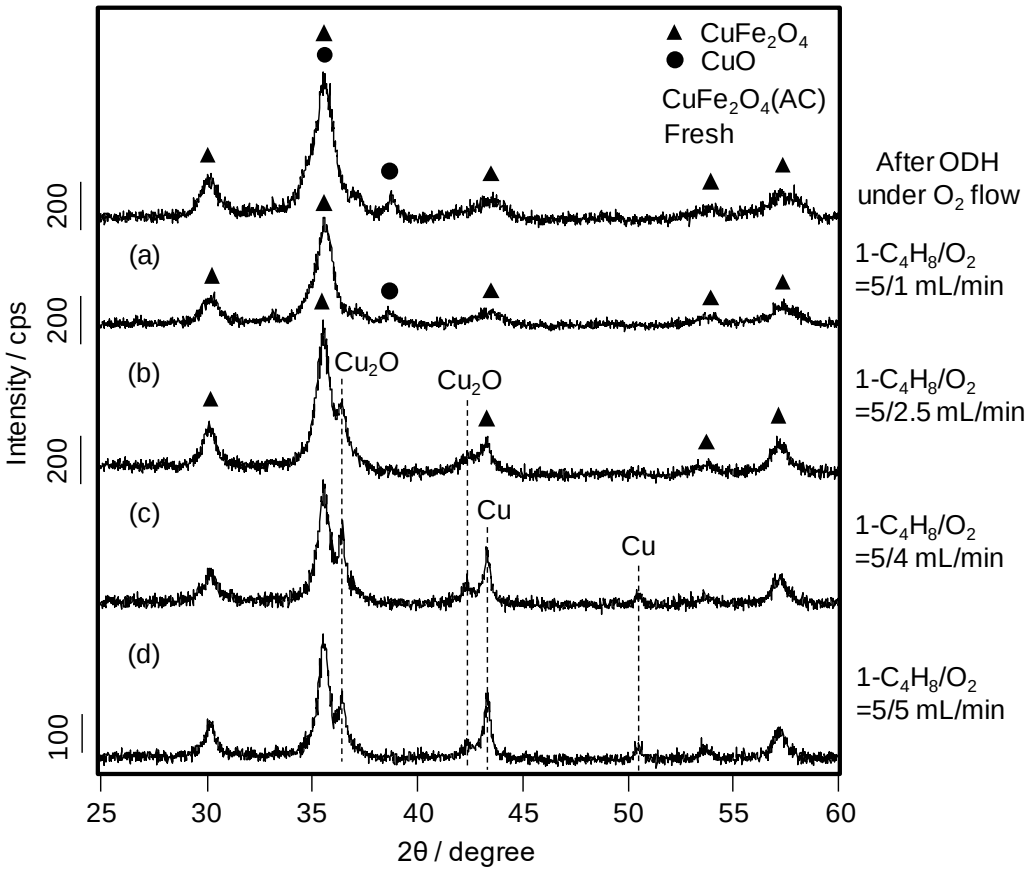

Fig. 3-12 XRD patterns of $CuFe_2O_4$(AC) catalyst after ODH at various 1-C_4H_8/O_2 ratios

conversion and BD yield were maintained for 100 min under all 1-C_4H_8/O_2 ratios (Figure 3-11). Therefore, $CuFe_2O_4$(AC) catalyst is possible to continuously produce BD for a long time at 270 °C. Figure 3-12 shows XRD patterns of the $CuFe_2O_4$(AC) catalyst after ODH at the different 1-C_4H_8/O_2 ratios. At the lower O_2 flow rates, the catalysts before and after the reaction showed only $CuFe_2O_4$ diffraction peaks (Figure 3-12a). In the catalysts after ODH under a 1-C_4H_8/O_2 ratio lower than 5/2.5, the small CuO diffraction peak disappeared and reduced Cu species such as Cu_2O and metallic Cu newly appeared (Figures 3-12b-d). Hence, the reduced copper species seems to cause the complete oxidation. On the other hand, the spinel structure could be maintained during ODH at all

1-C_4H_8/O_2 ratios (Figures 3-12a-d). It is considered that the maintenance of the $CuFe_2O_4$ structure is important to produce BD.

3.5 Oxidative dehydrogenation of but-1-ene with metal oxide catalysts under an O_2 atmosphere

It was clarified that $CuFe_2O_4$ catalyst could produce BD. However, high CO_2 selectivity was shown. In addition, Cu_2O appeared in the $CuFe_2O_4$ catalyst after ODH. In order to understand the role of copper oxide and iron oxide species for ODH, CuO(AC), Cu_2O, and Fe_2O_3(AC) catalysts were used for the ODH in addition to the $CuFe_2O_4$ catalyst.

Figure 3-13 shows the results of the ODH with CuO(AC), Cu_2O, and Fe_2O_3(AC). As mentioned in Section 3.1, $CuFe_2O_4$(AC) showed a high BD yield and higher CO_2 selectivity. Fe_2O_3(AC) showed the lowest conversion of 0.6%. Iron oxide species did not promote the ODH of but-1-ene. On the other hand, when CuO(AC) was used, a conversion of 9.1% and lower BD yield of 1.3% were obtained, along with the highest CO_2 selectivity in this study, 72.2%. Cu_2O exhibited a low conversion and BD yield of 13 and 1.3%, respectively. In addition, high CO_2 selectivity of 60% was obtained. It is considered that CuO phase included in $CuFe_2O_4$(AC) lead to decrease in BD selectivity in the ODH, because CuO promotes the complete oxidation.

The reactivity of the lattice oxygen in CuO(AC) and Cu_2O was also evaluated for the ODH (Table 3-3). CuO(AC) showed low BD yield and high CO_2 selectivity (Table 3-3, Run 1). The lattice oxygen in CuO(AC) caused complete oxidation, and Cu_2O was not used for the reaction because the formation of oxidation products such as BD and CO_x were hardly seen (Table 3-3, Run 2). It is suggested that complete oxidation on Cu_2O under an O_2 atmosphere did not progress through the lattice oxygen in the catalyst. On

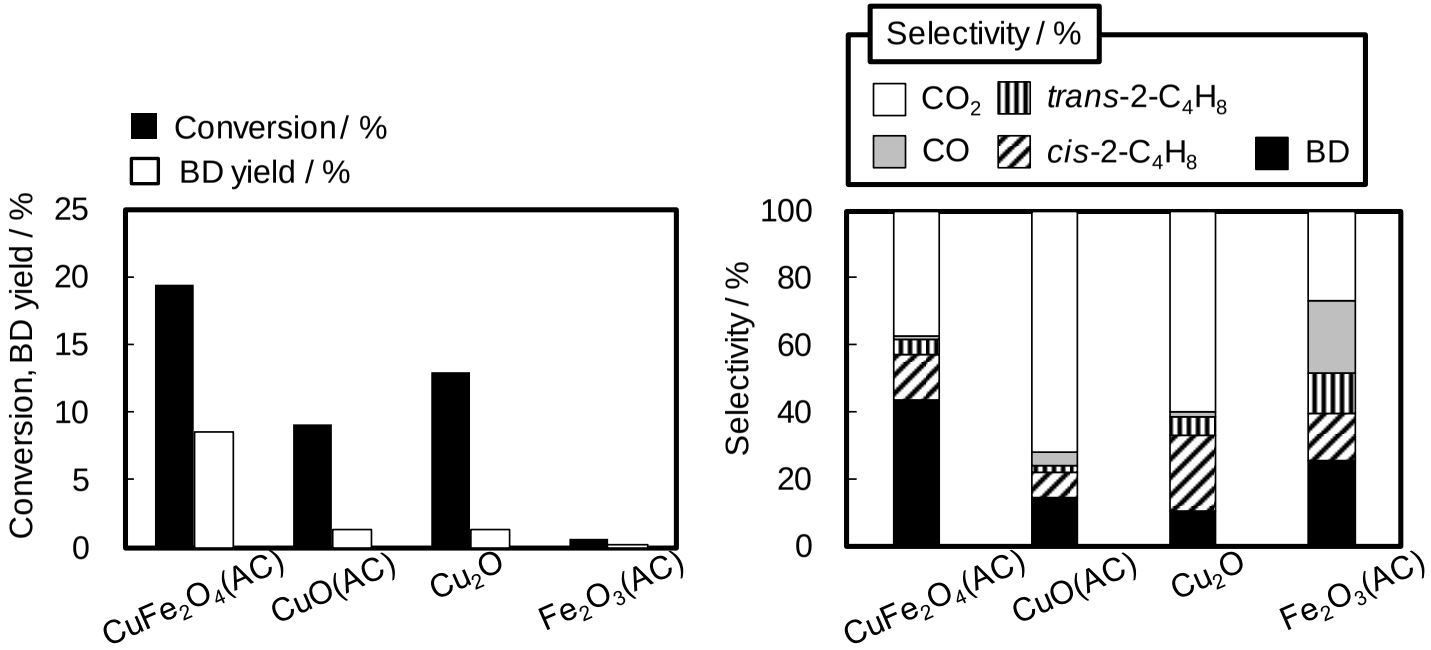

Fig. 3-13 ODH of but-1-ene in the presence of O_2 with copper and iron oxide catalysts

Catalyst: $CuFe_2O_4$(AC), CuO(AC), Fe_2O_3(AC), Catalyst weight: 200 mg,
Flow rate: 30 mL/min (1-C_4H_8 /O_2/Ar = 5/2.5/22.5), Reaction time: 100 min

the other hand, from these results, the $CuFe_2O_4$ structure generated by combining CuO with Fe_2O_3 was considered to be necessary to produce BD. The oxygen species of Cu-O bond in $CuFe_2O_4$ rather than that of CuO would be important to progress ODH even in the presence of O_2, since the lattice oxygen of $CuFe_2O_4$ was efficiently used for the ODH compared with the result of CuO(AC) (Table 3-1: Run 1, Table 3-3: Run 1).

Table 3-3 Result of ODH of 1-C_4H_8 with lattice oxygen in copper oxide catalyst

Catalyst	Conversion	Selectivity(%)					Yield(%)
	(%)	C_4H_6	*cis*-2-C_4H_8	*trans*-2-C_4H_8	CO	CO_2	C_4H_6
CuO(AC)	1.9	46.7	10.7	3.0	2.6	36.9	0.9
Cu_2O	1.7	8.9	64.6	15.7	3.3	7.5	0.2

$CuFe_2O_4$(AC) could produce BD, and CuO(AC) and Cu_2O mainly promoted complete oxidation. Hence, in order to elucidate the cause of the ODH and complete oxidation, XRD and XPS analyses were carried out for $CuFe_2O_4$(AC), CuO(AC), and Cu_2O. Figure 3-14 shows the XRD patterns. Although the CuO structure in $CuFe_2O_4$(AC) disappeared after the ODH, the $CuFe_2O_4$ structure was maintained (Figure 3-14a, a'). Meanwhile, the CuO diffraction peaks in CuO(AC) after the ODH almost disappeared, and the Cu_2O and Cu diffraction peaks became predominant (Figure 3-14b, b'). Here, CuO(AC) after the ODH with the lattice oxygen showed Cu_2O (Figure 3-15). Therefore, it is considered that the crystalline CuO in $CuFe_2O_4$(AC) and CuO(AC) was reduced to Cu_2O with but-1-ene. Because the XRD pattern of the Cu_2O catalyst after the ODH were similar to that of a fresh catalyst (Figure 3-14c, c'), the Cu_2O structure was maintained during the reaction and had high stability.

XPS spectra of $CuFe_2O_4$(AC), CuO(AC), and Cu_2O catalysts before and after ODH are shown in Figure 3-16. Generally, XPS spectra of Cu species appear near 934.0 and

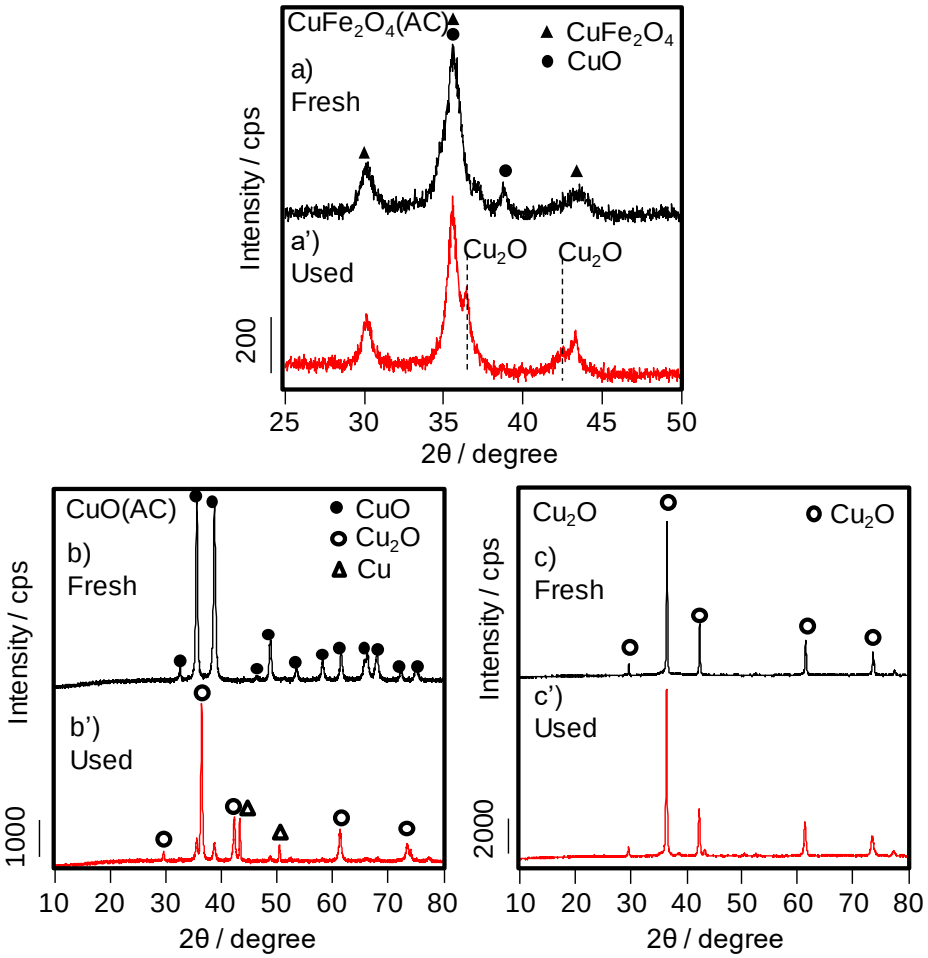

Fig. 3-14 XRD patterns of $CuFe_2O_4$(AC), CuO(AC) and Cu_2O catalysts before and after ODH

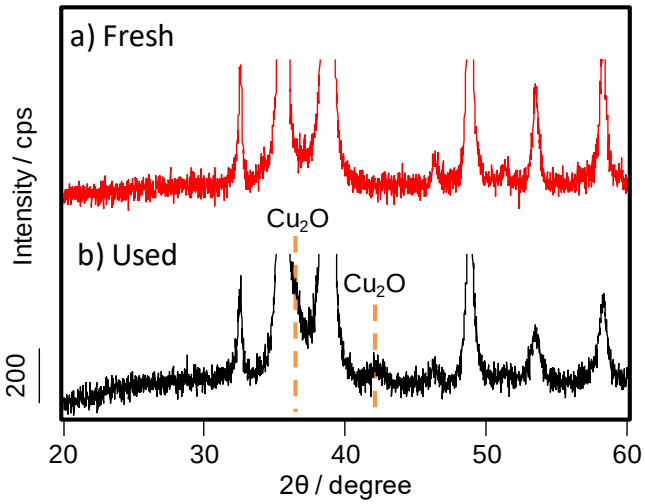

Fig. 3-15 XRD patterns of CuO(AC) catalyst after ODH of but-1-ene with lattice oxygen

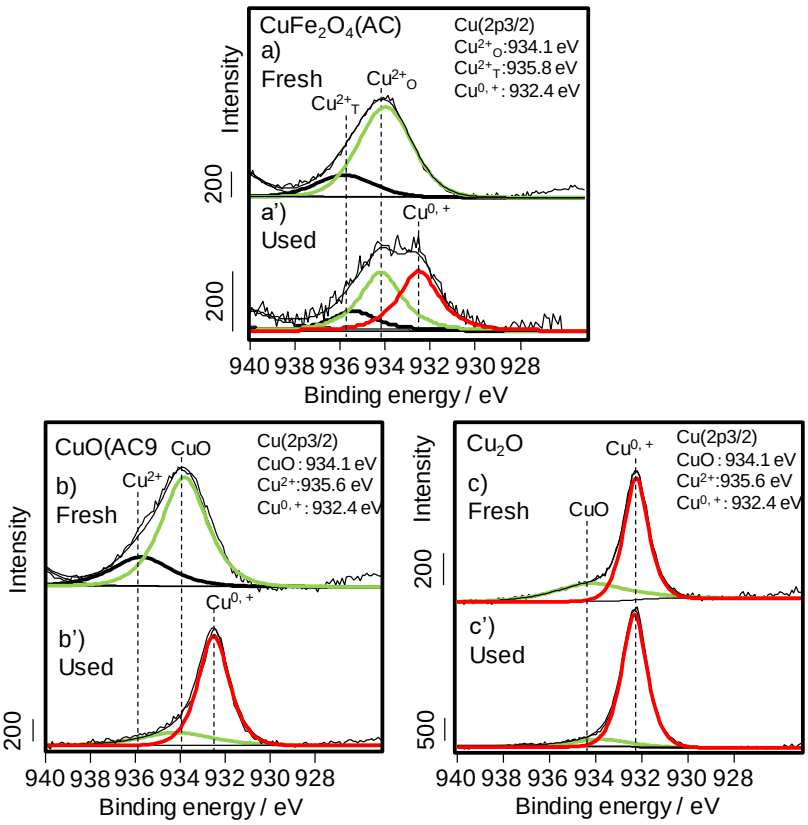

Fig. 3-16 XPS spectra of Cu species of $CuFe_2O_4$(AC), CuO(AC), and Cu_2O catalysts before and after ODH

935.6 eV and are assigned to copper (II) ion [33, 34]. XPS spectra of Cu^{2+} in copper ferrite can be separated into a tetrahedral site ($Cu^{2+}{}_T$: 935.8 eV) and octahedral site ($Cu^{2+}{}_O$: 934.1 eV) [35, 36]. The reduced Cu species such as Cu^0 and Cu^+ appear near 932.6 eV [33].

The XPS spectra of Cu species related to the Cu^{2+} species at 934.1 and 935.8 eV are observed in $CuFe_2O_4$(AC) and CuO(AC) before the ODH (Figure 3-16a, b). Cu_2O catalyst before the ODH showed the spectra of $Cu^{+\text{ or }0}$ at 932.4 eV (Figure 3-16c). In $CuFe_2O_4$(AC) after the ODH, although the XPS spectrum of $Cu^{+\text{ or }0}$ appeared at 932.4 eV, the Cu^{2+} species remained in $CuFe_2O_4$(AC) after the ODH (Figure 3-16a, a'). On the other hand, the XPS spectrum of CuO(AC) after the ODH indicated Cu^0 or Cu^+ at 932.4 eV without Cu^{2+} species. CuO(AC) could not maintain the divalent state during ODH

(Figure 3-16b, b'). The results of XPS analysis of the Cu_2O catalyst after the ODH showed Cu^+ similar to that of a fresh catalyst (Figure 3-16c, c').

According to XRD and XPS analyses of $CuFe_2O_4$(AC), CuO(AC), and Cu_2O catalysts before and after ODH, the spinel structure of $CuFe_2O_4$ and maintenance of divalent Cu are necessary to produce BD efficiently. Chapter 2 reported that the lattice oxygen in $CuFe_2O_4$ was used to produce BD in the ODH of but-1-ene, and was regenerated by molecular O_2 [32]. Therefore, it is considered that BD could be produced, and BD production could be maintained by keeping the $CuFe_2O_4$ phase and the divalent state, and that BD would be continuously produced with the lattice oxygen in copper oxide species in $CuFe_2O_4$(AC).

On the other hand, the lattice oxygen in CuO reacted with butene to produce CO_2 and Cu_2O. Cu_2O promoted the complete oxidation with molecular O_2. In the case of this complete oxidation, XRD and XPS analyses of Cu_2O after calcination at 270 °C in air revealed that the Cu_2O surface was oxidized, although bulk Cu_2O was not oxidized (Figure 3-17). In addition, it was also reported that molecular O_2 adsorbed on the Cu_2O

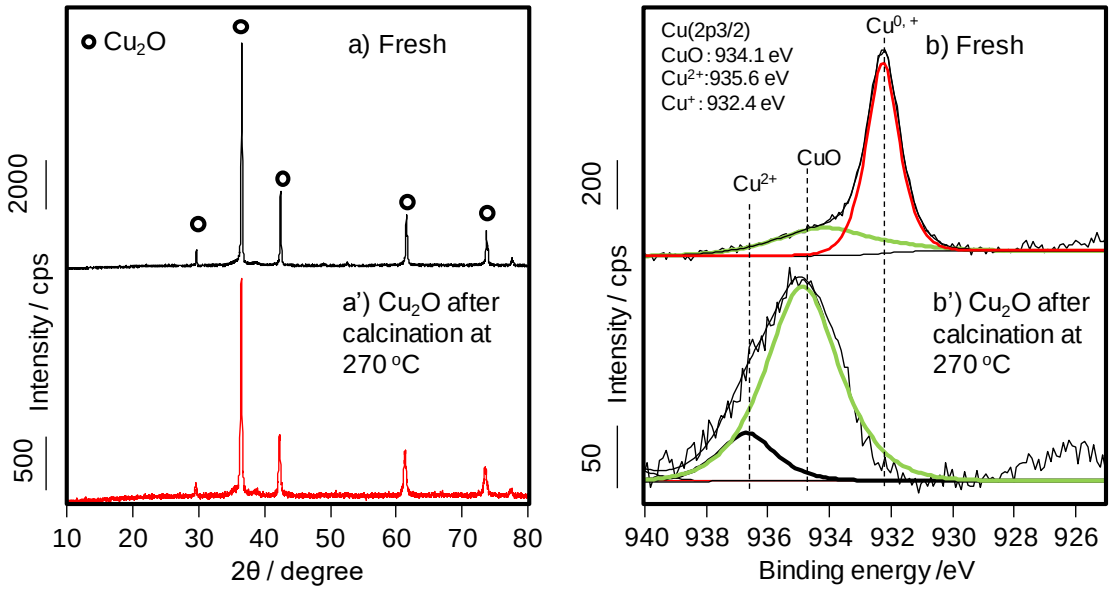

Fig. 3-17 XRD and XPS spectra of Cu_2O catalyst after calcination at 270 °C

surface forms active oxygen species such as O_2^{2-} [37]. Therefore, it is considered that the complete oxidation of the C4 compounds progressed through the lattice oxygen in CuO or by molecular oxygen species adsorbed on Cu_2O. If the inhibition of the formation of CuO in $CuFe_2O_4$(AC) is possible, $CuFe_2O_4$(AC) will be able to efficiently produce BD at 270 ^oC without Cu_2O and CO_2 production.

4. Conclusions

$CuFe_2O_4$(AC) prepared in the presence of AC and with Cu/Fe=1/2 gave a high BD yield of 8.5% in the ODH of but-1-ene under an O_2 atmosphere. The reaction temperature of 270 ^oC was optimum for the ODH. When the ODH was carried out at 1-C_4H_8/O_2=5/5, $CuFe_2O_4$(AC) gave the highest BD yield of 15% for 100 min. On the other hand, Fe_2O_3(AC) did not work as an oxidation catalyst. CuO(AC) and Cu_2O catalysts mainly promoted the complete oxidation. It was indicated that the $CuFe_2O_4$ phase was important for BD production, and $CuFe_2O_4$ had the potential to produce BD efficiently at the lower reaction temperature of 270 ^oC.

According to XRD and XPS analyses of the catalysts before and after ODH, the crystalline CuO was mostly reduced to Cu_2O during the reaction, and Cu_2O was maintained during the ODH. Therefore, it was considered that the complete oxidation proceeded on the reduced copper species such as Cu_2O.

On the other hand, although $CuFe_2O_4$(AC) after ODH showed the presence of Cu_2O and reduced Cu species such as $Cu^{+ \text{ or } 0}$, mostly $CuFe_2O_4$ structure and Cu^{2+} were maintained during the reaction by molecular O_2. The maintenance of the $CuFe_2O_4$ structure and Cu^{2+} is necessary to produce BD continuously in the ODH of but-1-ene in the presence of O_2.

In this paper, it was found that the $CuFe_2O_4$ catalyst enabled the ODH of but-1-ene at a temperature lower than 300 ^oC.

5. References

[1] F. Ma, S. Chem, Y. Li, H. Zhou, A. Xu, W. Lu, *Appl. Surf. Sci.*, **313** (2014) 654-659

[2] H. Fan, J. Feng, X. Li, Y. Guo, W. Li, K. Xie, *Chem. Eng. Sci.*, **135** (2015) 403-411

[3] I.A. Bakare, S.A. Mohamed, S. Al-Ghamdi, S.A. Razzak, M.M. Hossain, H.I. de Lasa, *Chem. Eng. J.*, **278** (2015) 207-216

[4] M. Setnicka, R. Bulanek, L. Capek, P. Cicmanec, *J. Mol. Catal.*, **344** (2011) 1-10

[5] J.A. Toledo, N. Nava, M. Martinez, X. Bokhimi, *Appl. Catal. A: Gen.*, **234** (2002) 137-144

[6] S. Lee, M.D. Vece, B. Lee, S. Seifert, R.E. Winans, S. Vajda, *Phys. Chem. Chem. Phys.*, **14** (2012) 9336-9342

[7] S. Furukawa, M. Endo, T. Komatsu, *ACS catal*., **4** (2014) 3533-3542

[8] H. Armendariz, G. Aguilar-Rios, P. Salas, M.A. Valenzuela, I. Schifter, H. Arriola, N. Nava, *Appl. Catal. A: Gen.*, **92** (1992) 29-38

[9] H. Lee, J.C. Jung, H. Kim, Y.M. Chung, T.J. Kim, S.J. Lee, S.H. Oh, Y.S. Kim, I.K. Song, *Catal. Lett.*, **131** (2009) 344-349

[10] Y.M. Chung, Y.T. Kwon, T.J. Kim, S.J. Lee, S.H. Oh, *Catal. Lett*., **130** (2009) 417-423

[11] H. Lee, J.C. Jung, I.K. Song, *Catal. Lett.*, **133** (2009) 321-327

[12] H. Lee, J.C. Jung, H. Kim, Y.M. Chung, T.J. Kim, S.J. Lee, S.H. Oh, Y.S. Kim, I.K. Song, *Korean J. Chem. Eng.*, **26** (2009) 994-998

[13] H. Lee, J.C. Jung, H. Kim, Y.M. Chung, T.J. Kim, S.J. Lee, S.H. Oh, Y.S. Kim, I.K. Song, *Catal. Commun.*, **9** (2008) 1137-1142

[14] J.A. Toledo, P. Bosch, M.A. Valenzuela, A. Montoya, N. Nava, *J. Mol. Catal.*, **125** (1997) 53-62

[15] H. Armendariz, J.A. Toledo, G. Aguilar-Rios, M.A. Valenzuela, P. Salas, A. Cabral, H. Jimenez, I. Schifter, *J. Mol. Catal.*, **92** (1994) 325-332

[16] R.J. Rennard, W.L. Kehl, *J. Catal.*, **21** (1971) 282-293

[17] B.J. LIAW, D.S. CHENG, B.L. YANG, *J. Catal.*, **118** (1989) 312-326

[18] W.Q. Xu, Y.G. Yin, G.Y. Li, S. Chen, *Appl. Catal. A: Gen.*, **89** (1992) 131-142

[19] F.Y. Qiu, L.T. Weng, E. Sham, P. Ruiz, B. Delmon, *Appl. Catal.*, **51** (1989) 235-253

[20] Y.M. Chung, Y.T. Kwon, T.J. Kim, S.J. Lee, S.H. Oh, *Catal. Lett.*, **131** (2009) 579-586

[21] M.A. Gibson, J.W. Hightower, *J. Catal.*, **41** (1976) 431-439

[22] A. Dejoz, J.M. LoÂpez Nieto, F. MaÂrquez, M.I. VaÂzquez, *Appl. Catal. A. Gen.*, **180** (1999) 83-94

[23] J.K. Lee, H. Lee, U.G. Hong, J. Lee, Y.-J. Cho, Y. Yoo, H.S. Jang, I.K. Song, *J. Ind. Eng. Chem.*, **18** (2012) 1096-1101

[24] J.M. Lopez Nieto, P. Concepci, A. Dejoz, H. Knozinger, F. Melo, M.I. Vazquez., *J. Catal.*, **189** (2000) 147–157

[25] J.H. Park, H. Noh, J.W. Park, K. Row, K.D. Jung, C.-H. Shin, *Appl. Catal. A. Gen.*, **431** (2012) 137-143

[26] J.C. Jung, H. Lee, H. Kim, Y.M. Chung, T.J. Kim, S.J. Lee, S.H. Oh, Y.S. Kim, I.K. Song, *Catal. Commun.*, **9** (2008) 943–949

[27] J.C. Jung, H. Kim, Y.M. Chung, T.J. Kim, S.J. Lee, S.H. Oh, Y.S. Kim, I.K. Song, *J. Mol. Catal.*, **264** (2007) 237-240

[28] J.C. Jung, H. Kim, Y.M. Chung, T.J. Kim, S.J. Lee, S.H. Oh, Y.S. Kim, I.K. Song, *Appl. Catal. A: Gen.,* **317** (2007) 244-249

[29] A.P.V. Soares, L.D. Dimitrov, M.C.A. Oliveira, L. Hilaire, M.F. Portela, R.K. Grasselli, *Appl. Catal. A: Gen.,* **253** (2003) 191-200

[30] S. Gong, S. Park, W.C. Choi, H. Seo, N.Y. Kang, M.Wan. Han, Y.K. Park, *J. Mol. Catal. A: Chem.,* **391** (2014) 19-24

[31] K. Fukudome, N. Ikenaga, T. Miyakke, T. Suzuki, *Catal. Sci. Technol.,* **1** (2011) 987-998

[32] T. Kiyokawa, N. Ikenaga, *Appl. Catal. A: Gen.,* **536** (2017) 97-103

[33] G. Zhang, J. Long, X. Wang, W. Dai, Z. Li, L. Wu, X. Fu, *New J. Chem.,* **33** (2009) 2044-2050

[34] O. Akhavan, R. Azimirad, S. Safa, E. Hasani, *J. Mater. Chem.,* **21** (2011) 9634-9640

[35] Y. Wang, H. Zhao, M. Li, J. Fan, G. Zhao, *Appl. Catal. B: Environ.,* **147** (2014) 534-545

[36] C. Reitz, C. Suchomski, J. Haetge, T. Leichtweiss, Z. Jaglicic, I. Djerdj, T. Brezesinski, *Chem. Commun.,* **48** (2012) 4471-4473

[37] R. Zhang, H. Liu, H. Zheng, L. Ling, Z. Li, B. Wang, *Appl. Surf. Sci.*, **257** (2011) 4787-4794

Chapter 4

Selective buta-1,3-diene production via oxidative dehydrogenation of but-1-ene with CuO-loaded catalyst

1. Introduction

Buta-1,3-diene (BD) has attracted interest as a monomer of petrochemical products such as polybutadiene rubber, styrene butadiene rubber, and ABS resin. Almost BD is produced by the endothermic steam-cracking of naphtha. However, this process produces many petrochemicals such as ethylene and propylene at the same time and needs a high temperature more than 700 ^{o}C. Therefore, this process consumes a lot of energy and can not produce BD efficiently. As the other problem, naphtha cracker tend to decrease because of spread of shale-gas.

Recently, oxidative dehydrogenation (ODH) of the C4 compounds with molecular O_2 (Eq. (1)) has attracted attention from the perspective of energy saving, because it is an exothermic process and can more efficiently produce BD at a lower temperature than the current process. Moreover, since this is single process to produce BD, BD can be produced with high selectivity without by-products.

$$1\text{-}C_4H_8 + 1/2O_2 \rightarrow C_4H_6 + H_2O \ \Delta H^{o}=\text{-}132.1 \text{ kJ/mol} \qquad (1)$$

For the ODH of n-butene and n-butane, ferrite-type catalysts [1-15], V-containing catalysts [16-18], and Bi-Mo catalysts [19-24] have been proposed as the good catalyst. Among these catalysts, $ZnFe_2O_4$ and Bi-Mo catalysts are especially investigated. The ODH of n-butene with these catalysts is known to proceed through the Mars−van Krevelen mechanism using redox cycle with the lattice oxygen in the metal oxide catalyst

[3-5, 24].

On the other hand, under an O_2 atmosphere, the deep oxidation to CO and CO_2 proceeded easily during the ODH (Eq. (2), (3)).

$$C_4H_8 + 6O_2 \rightarrow 4CO_2 + 4H_2O \qquad \Delta H^o = -2717 \text{ kJ/mol} \qquad (2)$$

$$C_4H_6 + 11/2O_2 \rightarrow 4CO_2 + 3H_2O \qquad \Delta H^o = -2540 \text{ kJ/mol} \qquad (3)$$

Therefore, in order to inhibit the complete oxidation, the ODH with zinc ferrite catalyst has been carried out under an O_2 flow with excess steam. Since the latent heat of steam is large, excessive energy is necessary. Therefore, the supply of steam lead to a lot of energy consumption. As a means to produce BD without forming CO_2, the ODH of propane or butene with the lattice oxygen in metal oxide has also been reported [25, 26]. In these previous studies, the lattice oxygen of the metal oxide catalyst was used to inhibit the deep oxidation of the reactant and the product, and then molecular O_2 was supplied after the reaction to regenerate the used lattice oxygen. Moreover, the catalytic activity was maintained throughout repeated ODHs. However, the repeated ODH process can not continuously produce BD because the regeneration of the spent catalyst is necessary.

Thus, operating the ODH under O_2 flow without steam is essential to realize high efficiency process and energy saving process. Hence, the development of catalyst which can inhibit the complete oxidation under O_2 flow is necessary. To achieve the inhibition of complete oxidation, the author have focused on the catalyst that can show the ODH activity at the low temperature.

In Chapter 3, the author have found that copper ferrite catalyst can show the ODH activity at the low temperature of 270 °C. Moreover, it is also clarified that the ODH proceed on the copper oxide species in the copper ferrite [27]. To progress the ODH, it

was important to combine CuO with Fe_2O_3. The author expected that oxidation performance would change due to the interaction between CuO and metal oxide.

Therefore, in this Chapter, copper oxide-loaded catalyst was focused. The effects of various metal oxide supports, copper oxide loading level, and the catalyst calcination temperature were investigated. In addition, the detailed catalyst analyses were conducted to examine the copper oxide species related to the ODH and the complete oxidation.

2. Experimental

2.1 Materials

Catalyst supports such as ZnO, MgO, Ga_2O_3, Y_2O_3, La_2O_3, α-Fe_2O_3, CeO_2, and ZrO_2 used in this study were prepared by the precipitation method. Each metal nitrate was dissolved in 100 mL of pure water. The solution was stirred at a room temperature for 1 h. After stirring, 1 mol/L of NaOH solution was added drop-wise to the solution under vigorous stirring until pH reached 13. After adding, the resultant precipitate was separated by centrifugation, and the solid was washed with a large amount of pure water until pH reached 7-8, and then was dried at 110 ºC. TiO_2 was prepared by hydrolysis of $[(CH_3)_2CHO]_4Ti$ in ethanol using 1 mol/L NH_3aq. These solids were calcined at 500 ºC for 2 h in air. The obtained materials, γ-Al_2O_3 (Merck) and SiO_2 (Fuji Silicia Chemical Ltd., Q-3 (550 m^2/g, notation: HS), Q-6 (450 m^2/g, MS), Q-10 (300 m^2/g, LS)) were used as catalyst supports.

$Cu(NO_3)_2{\cdot}3H_2O$ (assay = min. 99.0%), $Zn(NO_3)_2{\cdot}6H_2O$ (assay = min. 99.0%), $Mg(NO_3)_2{\cdot}6H_2O$ (assay = min. 99.0%), $Fe(NO_3)_3{\cdot}9H_2O$ (assay = min. 99.0%), $Ce(NO_3)_3{\cdot}6H_2O$ (assay = min. 98.0%), $ZrO(NO_3)_2{\cdot}2H_2O$ (assay = min. 97.0%), NaOH

(assay = 97.0%) were purchased from Wako Pure Chemical Industry. $La(NO_3)_3 \cdot 6H_2O$ (assay = 99.9%) was purchased from Nacalai Tesque, Inc. $Ga(NO_3)_3 \cdot 8H_2O$ (assay = 99.0%) was purchased from Kishida Chemical Co.,Ltd. $Y(NO_3)_3 \cdot 6H_2O$ (assay = 99.8%) was purchased from Aldrich. But-1-ene (1-C_4H_8) (assay = min. 99.0%) was supplied from Sumitomo Seika Chemical.

2.2 Catalyst preparation

Preparation by impregnation method

Various copper oxide-loaded catalysts were prepared by the impregnation method. Each metal oxide support was impregnated with an aqueous solution of $Cu(NO_3)_2 \cdot 3H_2O$ to give 10 wt% of CuO. After the mixture was allowed to stand at the room temperature for 2 h, water was evaporated to dryness under a reduced pressure. The solid was then dried at 110 ºC for 1 h. These solids were calcined at 400 ºC for 2 h in air. CuO-loaded SiO_2(HS) catalyst was prepared at various loadings (1-20 wt%) and calcined at the range of 400-700 ºC for 2 h in air. CuO was prepared by the precipitation method. Hereafter, the notation is CuO(A)/MOx-B, where A is loading, MOx is support, and B is calcination temperature.

2.3 Catalyst characterization

X-ray diffraction (XRD) patterns of copper oxide catalysts were obtained using the powder method with a Shimadzu XRD-6000 diffractometer with monochromatic Cu Kα radiation under the following conditions: tube voltage 40 kV, tube current 30 mA, scan step 0.02º, scan region 10-80º, and scan speed 2.0º/min. X-ray photoelectron spectra (XPS) analyses were carried out with a JEOL model JPS-9010MX using Mg Kα radiation

as an energy source. N_2O titration method to obtain the copper surface area was conducted with a BelCat-B-ISP (Microtrac BEL) as follows; CuO-loaded catalyst was reduced at 300 ºC under H_2 flow. After H_2 reduction, temperature was lowered up to 150 ºC under He flow. Then, N_2O gas was pulsed at 150 ºC. Then, the generated N_2 and unreacted N_2O were separated, and copper surface area was calculated from the amount of N_2 generated.

2.4 Catalyst test

ODH of but-1-ene with copper oxide loaded catalyst under a molecular O_2 atmosphere

The ODH of but-1-ene was carried out using a fixed-bed flow quartz reactor at 270 ºC for 20 min under atmospheric pressure. After 200 mg of catalyst was placed in the reactor, the reactor was preheated to a reaction temperature of 270 ºC under 22.5 mL/min (STP) of Ar flow. Oxygen, 1-C_4H_8, and Ar were introduced at a flow rate of O_2/1-C_4H_8/Ar=2.5/5/22.5 mL/min (STP). Total gas flow rate was fixed at 30 mL/min.

1-C_4H_8, *cis*-2-C_4H_8, *trans*-2-C_4H_8, and C_4H_6 were analyzed by a flame ionization detector (FID) gas chromatograph (Shimadzu GC14B, column: Unicarbon A-400). CH_4, CO, and CO_2 were also analyzed by a thermal conductivity detector (TCD) gas chromatograph (Shimadzu GC8A, column: activated carbon). O_2 and H_2 was analyzed by TCD gas chromatograph (Shimadzu GC8A, column: molecurar sieve 5A)

3. Results and discussion

3.1 Effect of catalyst support on the ODH of but-1-ene

In order to determine the optimum catalyst support, the effect of support on the ODH of but-1-ene was examined. Table 4-1 shows the results. When ZnO, MgO, Ga_2O_3, Y_2O_3, La_2O_3, and α-Fe_2O_3 were used as the catalyst support (Table 4-1: entries 1-6), CuO loaded on these supports showed a low but-1-ene conversion less than 5% and a low BD yield less than 1%. CuO loaded on γ-Al_2O_3, TiO_2, CeO_2, and ZrO_2 catalysts exhibited a high O_2 conversion more than 90% and a relatively high but-1-ene conversion of 12-16% (Table 4-1: entries 7-10). However, a low BD selectivity of less than 25% and a high CO_2 selectivity of more than 50% were given, and a low BD yield about 3% was obtained. Therefore, these catalysts mainly progressed the complete oxidation. When CuO loaded on SiO_2 catalyst was used for the ODH (Table 4-1: entry 11), this catalyst showed high O_2 and but-1-ene conversions of 93.6% and 15%, respectively. In addition, a high BD selectivity of 50% and a high BD yield of 8.1% were obtained. SiO_2 used in this reaction had the high specific surface area (550 m^2/g). Hence, the effect of SiO_2 surface area on the ODH was investigated (Table 4-1: entries 12, 13). Since CuO-loaded SiO_2 catalyst having a low surface area (450 or 300 m^2/g) showed low O_2 and but-1-ene conversions of less than 1%, and therefore the high specific surface area SiO_2 is necessary to progress the ODH reaction. However, since the BD selectivity decreased from 100 to 50.2% and the CO_2 selectivity increased from 0 to 38.8% with an increase in the specific surface area of SiO_2 support, an increase in the specific surface area of support also promoted the complete oxidation in addition to the ODH reaction.

In the case of the other supports, the reactivity may also be improved by increasing the specific surface area of the supports. However, CuO loaded on the other supports

Table 4-1 Effect of catalyst support on ODH of but-1-ene under O_2 flow

Entry no.	Catalyst	O_2 conv.	But-1-ene conv.	Selectivity(%)					Yield(%)
		(%)	(%)	C_4H_6	*cis*-2-C_4H_8	*trans*-2-C_4H_8	CO	CO_2	C_4H_6
1	CuO(10)/ZnO-400	16.5	0.4	24.1	16.1	0.0	0.0	59.8	0.1
2	CuO(10)/MgO-400	23.3	0.5	11.5	0.0	0.0	11.9	76.5	0.1
3	CuO(10)/Ga_2O_3-400	5.3	1.4	58.2	5.0	5.1	1.7	29.9	0.8
4	CuO(10)/Y_2O_3-400	19.4	2.4	13.9	10.3	3.0	0.7	72.1	0.3
5	CuO(10)/La_2O_3-400	24.8	3.4	13.2	13.0	4.2	3.6	65.9	0.4
6	CuO(10)/α-Fe_2O_3-400	15.8	1.1	17.0	0.0	0.0	0.0	83.0	0.2
7	CuO(10)/γ-Al_2O_3-400	94.0	13.7	26.4	15.4	5.7	3.2	49.4	3.6
8	CuO(10)/TiO_2-400	98.6	13.1	22.2	5.5	1.9	7.8	62.6	2.9
9	CuO(10)/CeO_2-400	98.8	15.8	21.5	18.8	5.6	0.0	54.2	3.4
10	CuO(10)/ZrO_2-400	91.8	12.0	29.3	3.9	1.5	1.8	63.6	3.5
11	CuO(10)/SiO_2(HS)-400	93.6	16.2	50.2	3.7	2.7	4.6	38.8	8.1
12	CuO(10)/SiO_2(LS)-400	0.2	0.2	100.0	0.0	0.0	0.0	0.0	0.2
13	CuO(10)/SiO_2(MS)-400	0.7	0.8	100.0	0.0	0.0	0.0	0.0	0.8

Catalyst: 200 mg

Flow rate: 1-C_4H_8/O_2/Ar=5/2.5/22.5 mL/min

Reaction temperature: 270 ^oC

Reaction time: 20 min

showed high O_2 conversion and CO_2 selectivity (Table 4-1: entries 1-10). Although CuO-loaded SiO_2 (MS, LS) showed low but-1-ene and O_2 conversion less than 1%, the formation of CO_2 was not seen. Since the improvement of the complete oxidation activity was seen in the case of SiO_2 support, the further promotion of the complete oxidation can be expected by increasing the specific surface area in the case of the other support.

From these results, the high specific surface area SiO_2(HS) was decided as the optimum catalyst support. In addition, it is considered that CuO well dispersed on SiO_2 may be necessary to produce BD by the ODH.

3.2 Effect of copper oxide loading on the ODH of but-1-ene

The effect of CuO loading on the ODH of but-1-ene was investigated and the results are shown in Fig. 4-1. By increasing CuO loading level up to 5 wt%, an increase in the O_2 conversion from 22.3 to 91.5% and the but-1-ene conversion from 5.2 to 16.5% were observed. Although the CO_2 selectivity increased from 11.8% to 30.2%, the BD yield also improved from 4 to 9.8%. At CuO loading over 10 wt%, the CO_2 selectivity further increased from 30.2% to 58.6%, and the BD yield decreased from 9.8% to 3.5%. It is considered that excessive amount of CuO would progress the complete oxidation. Therefore, the optimum loading level was determined as 5 wt%.

According to these results, it was suggested that the copper oxide species might relate to the ODH (1-5 wt%) and the complete oxidation (10 wt%-). Therefore, it is considered that the copper oxide species mainly having the complete oxidation activity might be formed with increasing the CuO loading.

In order to examine the change in selectivities with an increase in CuO-loading, XRD and XPS analyses were carried out. Figure 4-2 shows the result of XRD

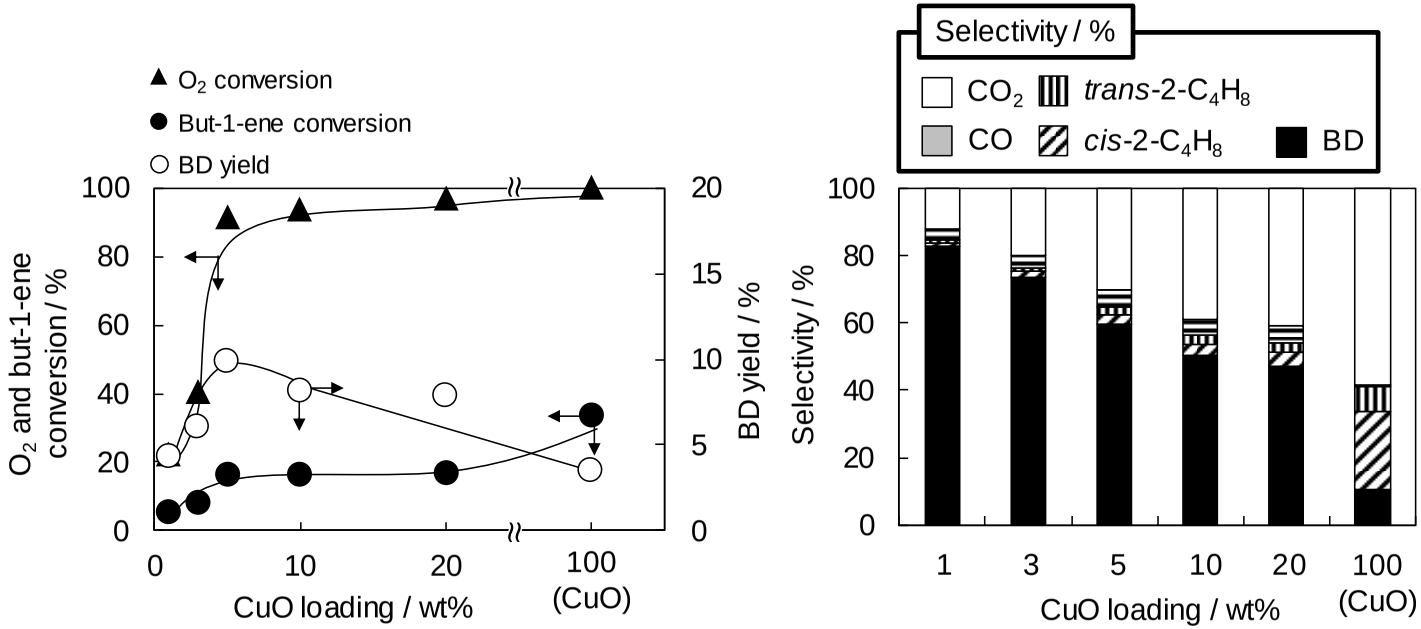

Fig. 4-1 Effect of CuO loading on ODH of but-1-ene

Catalyst weight: 200 mg,
Flow rate: 30 mL/min (1-C_4H_8 /O_2/Ar = 5/2.5/22.5),
Reaction temperature: 270 °C, Reaction time: 20 min

analyses of CuO-loaded SiO_2 catalysts. With an increase of CuO loading, CuO diffraction peaks were seen (Fig. 4-2(a)-(d)). Over 10 wt%, the crystalline CuO diffraction peaks were shown, and it was clearly appeared in CuO(20)/SiO_2(HS)-400 catalyst (Fig. 4-2(d), (e)). It is considered that the copper oxide species in the range of 1-5 wt% of CuO loading were loaded as amorphous CuO. In addition, over 10 wt%, the copper oxide species also existed as crystalline CuO. On the other hand, although the CuO diffraction peaks were clearly appeared in CuO(20)/SiO_2(HS)-400 catalyst compared with that of

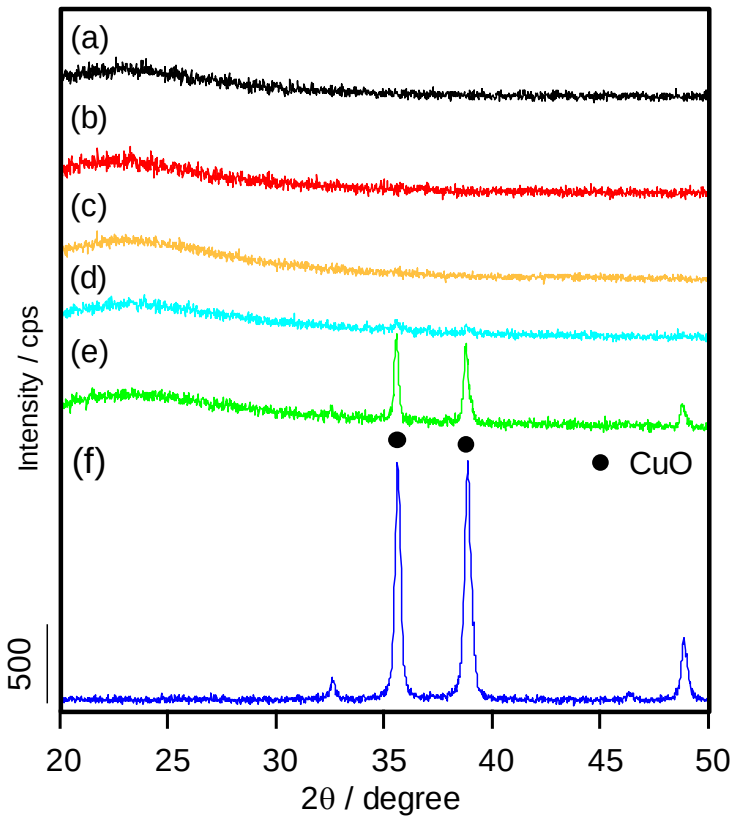

Fig. 4-2 XRD patterns of various CuO-loaded SiO_2 catalysts
(a) CuO(1)/SiO_2(HS)-400, (b) CuO(3)/SiO_2(HS)-400,
(c) CuO(5)/SiO_2(HS)-400, (d) CuO(10)/SiO_2(HS)-400,
(e) CuO(20)/SiO_2(HS)-400, (f) CuOp

CuO(10)/SiO_2(HS)-400, the same catalytic performance was seen. Therefore, XPS analysis was conducted to evaluate the catalyst surface state.

Figure 4-3 illustrates the XPS spectra of CuO-loaded catalysts, and Table 4-2 shows the ratio of various copper oxide species. The CuO-loaded SiO_2 catalyst showed three main peaks at 933.5, 935.4, and 936.4 eV (Fig. 4-3 (a)-(e)). According to a review of XPS for the copper species, the peak at around 933.5 eV is related to Cu^{2+} of bulk CuO [28, 29]. The copper oxide species observed at 935.4 eV is ascribed to $Cu(OH)_2$ or copper oxide species having the strong interaction between the copper oxide and SiO_2 such as copper silicate [29, 30]. The presence of copper silicate was expected, because the thermal stability of $Cu(OH)_2$ was low. Furthermore, the peak appearing the high oxidation state near 936.4 eV is reported as mono-(μ-oxo)-dicopper species [29, 31].

Bulk CuO and the other copper oxide species were seen in all the CuO-loaded catalysts (Fig. 4-3(a)-(e)). Here, as shown also in the result of XRD analysis, the amorphous CuO (the low loading level) and crystalline CuO (the high loading) were existed in the CuO-loaded catalyst. Therefore, the bulk CuO species shown in range of 1-5 wt% of CuO loading level are derived from amorphous CuO, and over 10 wt% of CuO loading level, the bulk CuO is attributed to the crystalline CuO.

As the result of XPS analysis, for CuO(1)/SiO_2(HS)-400, the abundance rate of the mono-(μ-oxo)-dicopper species was 0.45% and the highest $Cu(OH)_2$ and copper silicate rate (34.7%) and the high bulk CuO rate (64.8%) were obtained. CuO(3)/SiO_2(HS)-400 showed the mono-(μ-oxo)-dicopper species rate of 7.5%, $Cu(OH)_2$ and copper silicate rate of 23.8%, and the bulk CuO rate of 68.6%. On the other hand, the formation of the high oxidation state copper oxide species was clearly observed in the catalysts with CuO

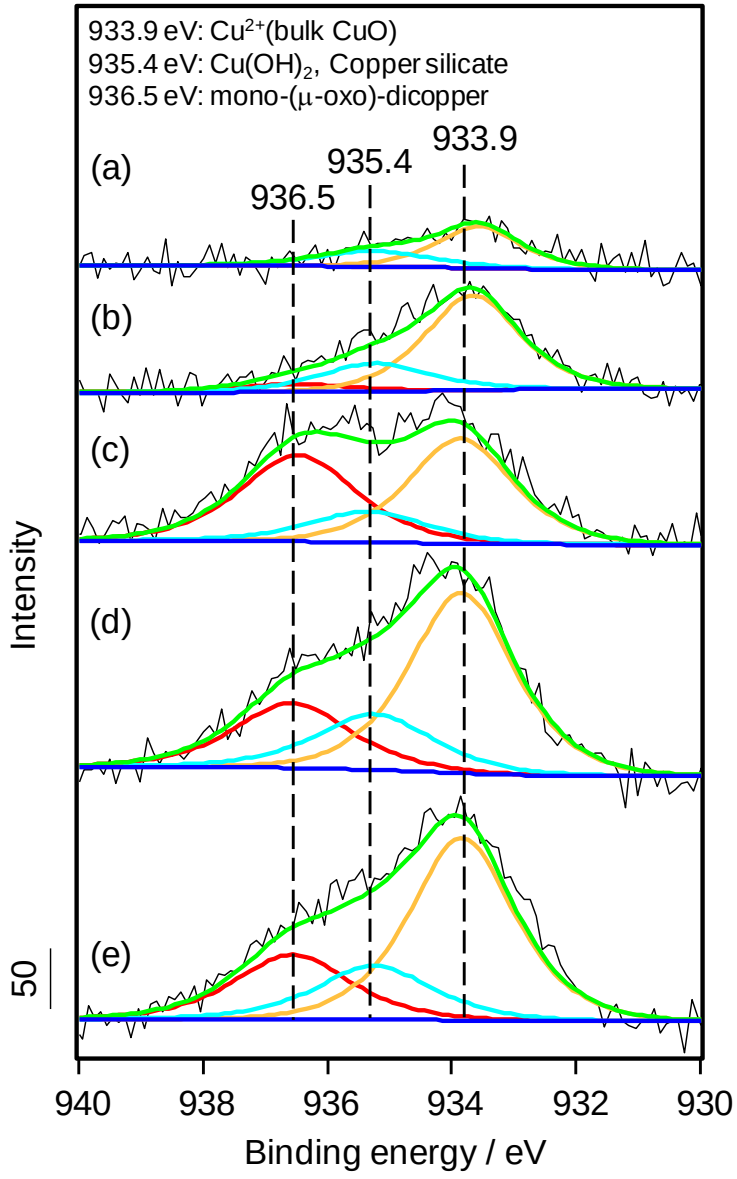

Fig. 4-3 XPS spectra of various CuO-loaded SiO_2 catalysts
(a) CuO(1)/SiO_2(HS)-400, (b) CuO(3)/SiO_2(HS)-400,
(c) CuO(5)/SiO_2(HS)-400, (d) CuO(10)/SiO_2(HS)-400,
(e) CuO(20)/SiO_2(HS)-400

loading over 5 wt% (Fig. 4-3(c)-(e)). CuO(5)/SiO_2(HS)-400 showed the highest mono-(μ-oxo)-dicopper species rate of 40.4% (Table 4-2). In addition, the low bulk CuO species rate of 44.9% and $Cu(OH)_2$ and copper silicate rate of 14.7% were observed. At CuO loading level more than 10 wt%, the high bulk CuO rate of about 58%, $Cu(OH)_2$ and copper silicate rate of about 20%, and the mono-(μ-oxo)-dicopper species rate of 22.8% were exhibited.

Table 4-2 Copper species rate calculated from XPS analysis (Cu2p3/2) of CuO-loaded SiO_2 catalyst

Catalyst	Copper species rate / %		
	936.5 eV mono-(μ-oxo)-dicopper	935.4 eV $Cu(OH)_2$, Copper silicate	933.9 eV Cu^{2+}(bulk CuO)
CuO(1)/SiO_2(HS)-400	0.45	34.7	64.8
CuO(3)/SiO_2(HS)-400	7.6	23.8	68.6
CuO(5)/SiO_2(HS)-400	40.4	14.7	44.9
CuO(10)/SiO_2(HS)-400	22.8	19.6	57.7
CuO(20)/SiO_2(HS)-400	22.8	18.9	58.3

According to the results of ODH, XRD, and XPS analyses, it is considered that the formation of the high oxidation state copper species like the mono-(μ-oxo)-dicopper can improve the reactivity between but-1-ene and oxygen, because the but-1-ene and O_2 conversions drastically increased until CuO loading level of 5wt%. CuO(1, 3)/SiO_2(HS)-400 catalysts showed the high BD selectivity in the substantial absence of the high oxidation copper oxide. The high oxidation copper oxide species seems to be related to the promotion of the complete oxidation rather than the improvement of the ODH activity. On the other hand, the formation of crystalline CuO was confirmed by XRD, when CuO more than 10 wt% was supported on SiO_2. Since the crystalline CuO catalyst showed the high O_2 conversion and the high CO_2 selectivity (Fig. 4-1), the presence of the crystalline CuO contributed to the complete oxidation of butenes and BD. Furthermore, it is

considered that amorphous CuO and/or $Cu(OH)_2$ and copper silicate are related to the ODH, but these copper oxide species were lost by the formation of crystalline CuO.

3.3 Effect of calcination temperature of CuO-loaded SiO_2 catalyst

The effect of calcination temperature of 5 wt%CuO/SiO_2(HS) catalyst on the ODH of but-1-ene was investigated. Figure 4-4 shows the results of the ODH reaction. With increasing the calcination temperature from 400 to 700 ºC, the O_2 conversion significantly decreased from 91.5 to 23.4%, the CO_2 selectivity decreased from 30.2 to 5.9%, the but-1-ene conversion slightly decreased from 16.5 to 12.3%, and the BD selectivity drastically increased from 59.6 to 92.8%. The BD yield of about 11% was kept. That is to say, the complete oxidation was selectively inhibited without suppression of the ODH reaction, and this result suggested that it might be possible to extinguish the active site associated with the complete oxidation.

Meanwhile, the CuO-loaded SiO_2 catalyst calcined at 800 ºC showed low but-1-ene and O_2 conversions of 1.8% and 6.5%, respectively. This catalyst did not progressed the reactions. It is most notable that CuO(5)/SiO_2(HS)-700 catalyst showed the highest BD selectivity of 92.8% and the high BD yield of 11.4%. Thus, that the calcination temperature of 700 ºC was determined as the best calcination temperature. In addition, the catalyst which can selectively produce BD without steam at the low temperature (270 ºC) could be proposed, and this catalyst will contribute for an energy saving process.

In order to examine the difference in the activity of the catalysts calcined at different temperatures, the catalysts were characterized by N_2O titration, XPS, and XRD. Table 4-3 shows Si/Cu ratio calculated from XPS analysis and Cu surface area determined by N_2O

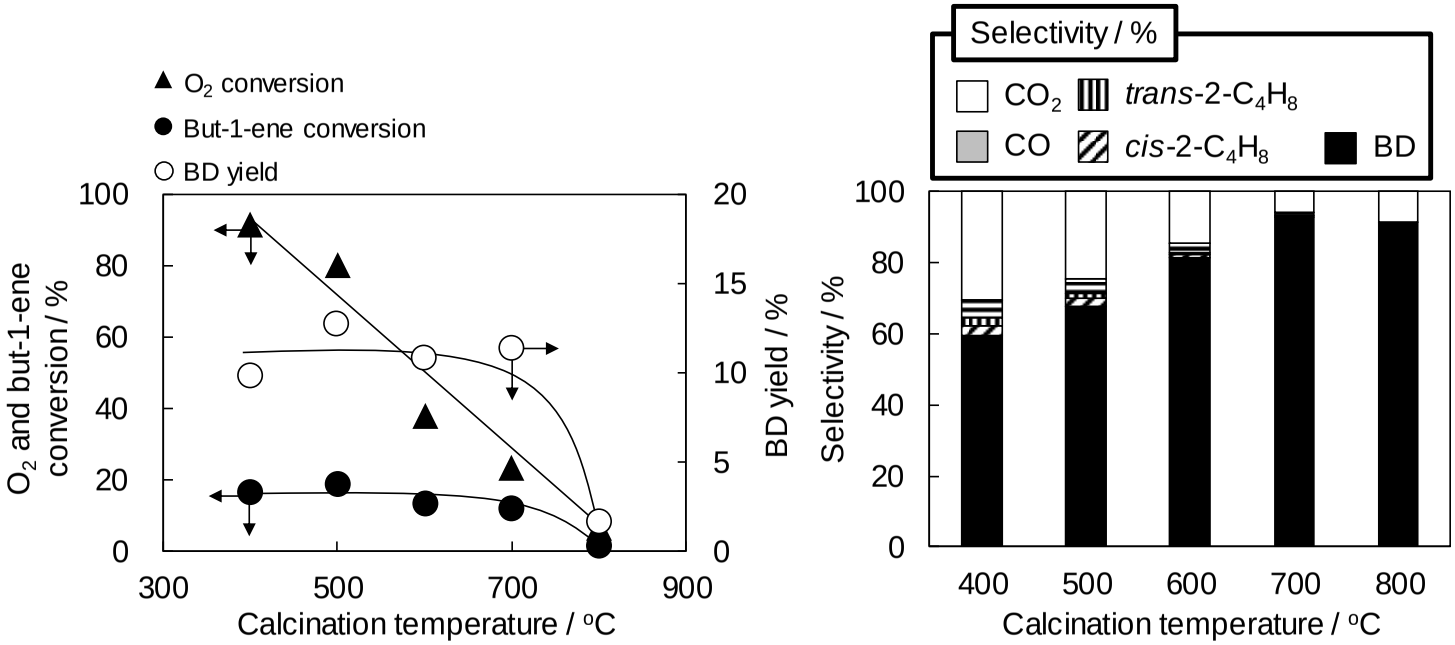

Fig. 4-4 Effect of calcination temperature of 5%CuO/SiO_2(HS) catalyst on ODH

Catalyst weight: 200 mg,
Flow rate: 30 mL/min (1-C_4H_8 /O_2/Ar = 5/2.5/22.5),
Reaction temperature: 270 °C, Reaction time: 20 min

Table 4-3 Copper surface area and Si/Cu ratio

Catalyst	Cu surface area m^2/g	Atomic ratio / - Si/Cu
$CuO(5)/SiO_2(HS)$-400	35	36.0
$CuO(5)/SiO_2(HS)$-500	33	35.9
$CuO(5)/SiO_2(HS)$-600	31	39.9
$CuO(5)/SiO_2(HS)$-700	34	41.0
$CuO(5)/SiO_2(HS)$-800	9	76.4

titration. The CuO-loaded catalyst calcined at 800 ºC exhibited the high Si/Cu ratio of 76.4 and the low Cu surface area of 9 m^2/g. It is considered that copper oxide species was covered by SiO_2 or sintered during the calcination. From XRD analyses for the CuO-loaded catalysts calcined at various temperatures, the diffraction peaks related to copper species was not seen in the catalysts calcined in the range of 400-600 ºC. Small CuO diffraction peaks were shown in CuO-loaded catalyst calcined at 700 ºC (Fig. 4-5(a)-(c)). On the other hand, the catalyst calcined at 800 ºC showed highly crystalline CuO as compared to the other CuO-loaded catalysts (Fig. 4-5(d)). These results suggested that the CuO crystallite grew by thermal sintering at 800 ºC. Therefore, the low Cu surface area was obtained. Moreover, it is considered that the amounts of the active copper species such as amorphous CuO and the mono-(μ-oxo)-dicopper species were reduced by the formation of crystalline CuO. Hence, the reaction can not be proceeded with this catalyst. On the other hand, the catalyst calcined in the range of 400-700 ºC showed the low Si/Cu ratio of ca.40 and the high copper surface area of about 30 m^2/g. Therefore, the ODH and the complete oxidation were progressed. In addition, the copper surface area may be related to BD yield rather than selectivities.

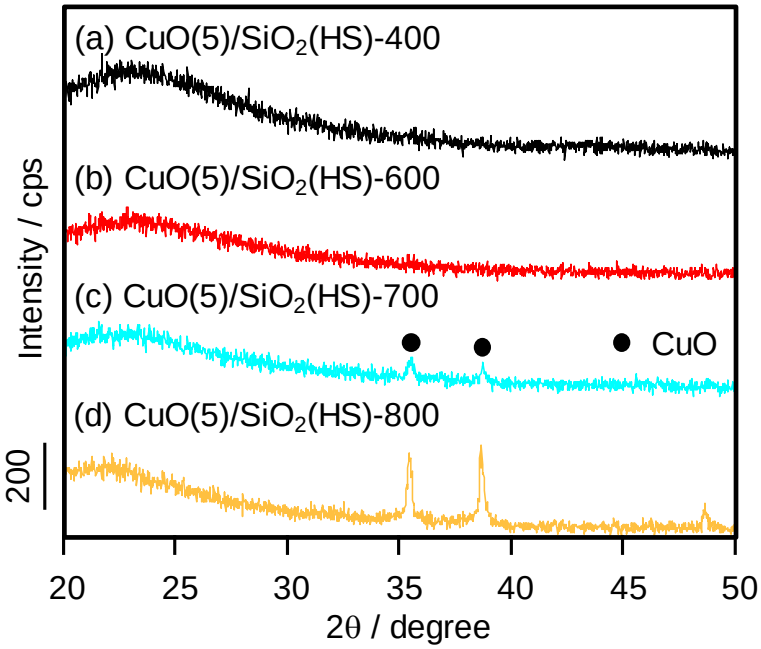

Fig. 4-5 XRD patterns of $CuO(5)/SiO_2$ catalysts calcined at various temperature

As shown in section 3.2, it was suggested that the copper oxide surface states is related to the ODH and the complete oxidation. Therefore, XPS analyses of $CuO(5)/SiO_2$(HS) catalysts calcined at various temperatures were conducted. Figure 4-6 illustrates XPS spectra of catalysts (Cu2p3/2). The abundance rates of copper oxide species are exhibited in Table 4-4.

From these XPS spectra, the presences of the bulk CuO, $Cu(OH)_2$ or copper silicate, and mono-(μ-oxo)-dicopper species were observed in all the CuO-loaded catalysts (Fig. 4-6). The abundance rate of the high oxidation state copper oxide such as mono-(μ-oxo)-dicopper oxide clearly decreased from 40.4 to 4.8% with increasing the calcination temperature (Table 4-4). This result showed that the high oxidation copper oxide is related to the complete oxidation, because the decrease in the CO_2 selectivity was seen with the decrease in this copper oxide species rate. On the other hand, Cu2p3/2 and O1s atomic

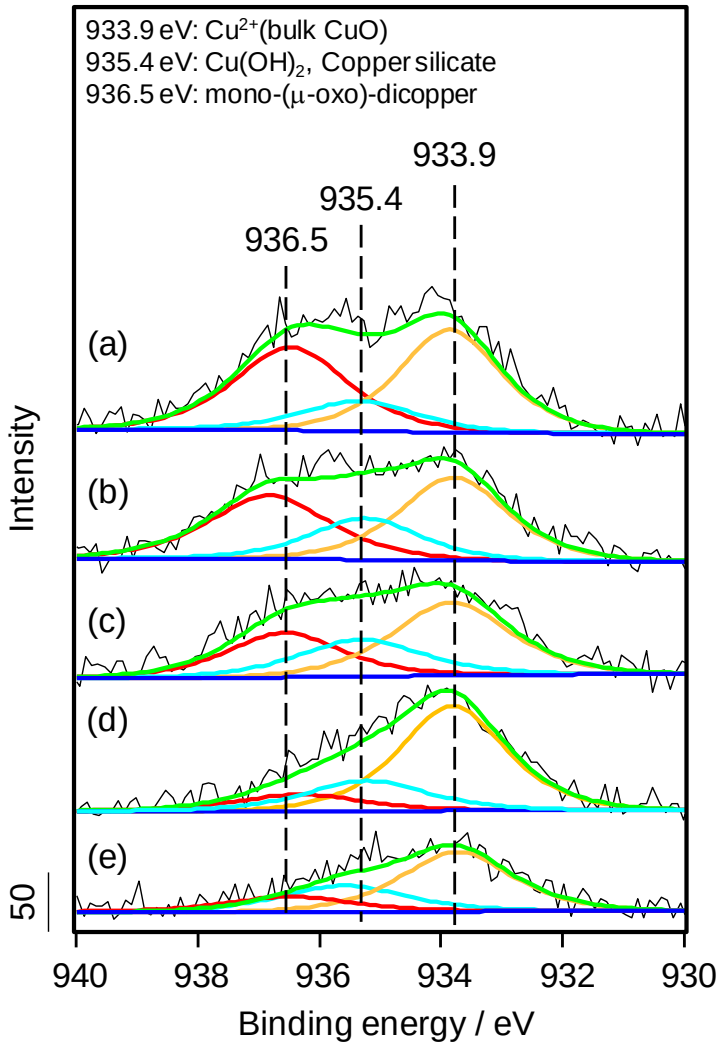

Fig. 4-6 XPS spectra of $CuO(5)/SiO_2$ catalysts calcined at various temperature
(a) $CuO(5)/SiO_2$(HS)-400, (b) $CuO(5)/SiO_2$(HS)-500, (c) $CuO(5)/SiO_2$(HS)-600, (d) $CuO(5)/SiO_2$(HS)-700, (e) $CuO(5)/SiO_2$(HS)-800

Table 4-4 Copper species and O1s ratios calculated from XPS spectra of CuO-loaded SiO_2 catalyst

Catalyst	Copper species rate / %			Atomic rate / %	
	936.5 eV mono-(μ-oxo)-dicopper	935.4 eV $Cu(OH)_2$, Copper silicate	933.9 eV Cu^{2+}(bulk CuO)	O 1s	Cu 2p3/2
CuO(5)/SiO_2(HS)-400	40.4	14.7	44.9	98.8	1.23
CuO(5)/SiO_2(HS)-500	35.7	21.6	42.6	98.7	1.27
CuO(5)/SiO_2(HS)-600	28.2	25.2	46.6	99.0	1.01
CuO(5)/SiO_2(HS)-700	11.8	21.8	66.4	99.0	1.04
CuO(5)/SiO_2(HS)-800	4.8	33.0	62.2	99.5	0.54

rates did not changed significantly to 700 ºC (Table 4-4). Hence, it was considered that the copper oxide species related to complete oxidation of C4 compounds were transformed to inactive copper oxide species.

As shown from these results, since CuO(5)/SiO_2(HS)-700 catalyst has the high copper surface area and the high oxidation state copper oxide species was not formed, the selective BD production was realized under O_2 flow.

4. Conclusions

The effects of catalyst supports, CuO-loading, and calcination temperature on the ODH of but-1-ene under O_2 flow were investigated. The high surface area SiO_2 was suitable as the catalyst support, and CuO(5)-loaded SiO_2 catalyst calcined at 700 ºC showed the highest BD selectivity of 92.8% and the high BD yield of 11.4%. CuO-loaded SiO_2 was proposed as the good catalyst which can more efficiently produce BD at the low temperature, because the production of CO_2 was limited even under O_2 flow.

According to N_2O titration, XRD, and XPS, copper surface area seems to be related to the reactivity between O_2 and the substrate. In addition, it was clarified that the high oxidation state copper oxide species such as mono-(μ-oxo)-dicopper and the crystalline CuO would progress the complete oxidation of C4 compounds. The formation of these copper oxide species could be inhibited by controlling the loading and calcination temperature.

Thus, it was indicated that the CuO-loaded SiO_2 catalyst having the high copper surface area in absence of crystalline CuO and the high oxidation state copper oxide species is valid to produce BD efficiently.

5. References

[1] J.A. Toledo, N. Nava, M. Martinez, X. Bokhimi, *Appl. Catal. A: Gen.,* **234** (2002) 137-144

[2] H. Armendariz, G. Aguilar-Rios, P. Salas, M.A. Valenzuela, I. Schifter, H. Arriola, N. Nava, *Appl. Catal. A: Gen.,* **92** (1992) 29-38

[3] H. Lee, J.C. Jung, H. Kim, Y.M. Chung, T.J. Kim, S.J. Lee, S.H. Oh, Y.S. Kim, I.K. Song, *Catal. Lett.,* **131** (2009) 344-349

[4] Y.M. Chung, Y.T. Kwon, T.J. Kim, S.J. Lee, S.H. Oh, *Catal. Lett*., **130** (2009) 417-423

[5] H. Lee, J.C. Jung, I.K. Song, *Catal. Lett.,* **133** (2009) 321-327

[6] H. Lee, J.C. Jung, H. Kim, Y.M. Chung, T.J. Kim, S.J. Lee, S.H. Oh, Y.S. Kim, I.K. Song, *Korean J. Chem. Eng.,* **26** (2009) 994-998

[7] H. Lee, J.C. Jung, H. Kim, Y.M. Chung, T.J. Kim, S.J. Lee, S.H. Oh, Y.S. Kim, I.K. Song, *Catal. Commun.*, **9** (2008) 1137-1142

[8] J.A. Toledo, P. Bosch, M.A. Valenzuela, A. Montoya, N. Nava, *J. Mol. Catal.*, **125** (1997) 53-62

[9] H. Armendariz, J.A. Toledo, G. Aguilar-Rios, M.A. Valenzuela, P. Salas, A. Cabral, H. Jimenez, I. Schifter, *J. Mol. Catal.*,, **92** (1994) 325-332

[10] R.J. Rennard, W.L. Kehl, *J. Catal.,* **21** (1971) 282-293

[11] B.J. Liaw, D.S. Cheng, B.L. Yang, *J. Catal.,* **118** (1989) 312-326

[12] W.Q. Xu, Y.G. Yin, G.Y. Li, S. Chen, *Appl. Catal. A: Gen.,* **89** (1992) 131-142

[13] F.Y. Qiu, L.T. Weng, E. Sham, P. Ruiz, B. Delmon, *Appl. Catal.,* **51** (1989) 235-253

[14] Y.M. Chung, Y.T. Kwon, T.J. Kim, S.J. Lee, S.H. Oh, *Catal. Lett.*, **131** (2009) 579-586

[15] M.A. Gibson, J.W. Hightower, *J. Catal.*, **41** (1976) 431-439

[16] A. Dejoz, J.M. LoÂpez Nieto, F. MaÂrquez, M.I. VaÂzquez, *Appl. Catal. A. Gen.*, **180** (1999) 83-94

[17] J.K. Lee, H. Lee, U.G. Hong, J. Lee, Y.-J. Cho, Y. Yoo, H.S. Jang, I.K. Song, *J. Ind. Eng. Chem.*, **18** (2012) 1096-1101

[18] J.M. Lopez Nieto, P. Concepci, A. Dejoz, H. Knozinger, F. Melo, M.I. Vazquez., *J. Catal.*, **189** (2000) 147–157

[19] J.H. Park, H. Noh, J.W. Park, K. Row, K.D. Jung, C.-H. Shin, *Appl. Catal. A. Gen.*, **431** (2012) 137-143

[20] J.C. Jung, H. Lee, H. Kim, Y.M. Chung, T.J. Kim, S.J. Lee, S.H. Oh, Y.S. Kim, I.K. Song, *Catal. Commun.*, **9** (2008) 943-949

[21] J.C. Jung, H. Kim, Y.M. Chung, T.J. Kim, S.J. Lee, S.H. Oh, Y.S. Kim, I.K. Song, *J. Mol. Catal.*, **264** (2007) 237-240

[22] J.C. Jung, H. Kim, Y.M. Chung, T.J. Kim, S.J. Lee, S.H. Oh, Y.S. Kim, I.K. Song, *Appl. Catal. A: Gen.*, **317** (2007) 244-249

[23] A.P.V. Soares, L.D. Dimitrov, M.C.A. Oliveira, L. Hilaire, M.F. Portela, R.K. Grasselli, *Appl. Catal. A: Gen.*, **253** (2003) 191-200

[24] J.C. Jung, H. Lee, H. Kim, Y.M. Chung, T.J. Kim, S.J. Lee, S.H. Oh, Y.S. Kim, I.K. Song, *Catal. Lett.*, **124** (2008) 262-267

[25] S. Gong, S. Park, W.C. Choi, H. Seo, N.Y. Kang, M.Wan. Han, Y.K. Park, *J. Mol. Catal. A: Chem.*, **391** (2014) 19-24

[26] K. Fukudome, N. Ikenaga, T. Miyakke, T. Suzuki, *Catal. Sci. Technol.,* **1** (2011) 987-998

[27] T. Kiyokawa, N. Ikenaga, *ChemistrySelect*, **3** (2018) 6426-6433

[28] J. Koo, S. Kwon, N.R. Kim, K. Shin, H.M. Lee, *J. Phys. Chem. C*, **120** (2016) 3334-3340

[29] F. Teng, L. Zheng, K. Hu, H. Chen, Y. Li, Z. Zhang, X. Fang, *J. Mater. Chem. C*, **4** (2016) 8416-8421

[30] W. Di, J. Cheng, S. Tian, J. Li, J. Chen, Q. Sun, *Appl. Catal. A: Gen.,* **510** (2016) 244-259

[31] A.S. Vidal, J. Balmaseda, L.L. Rojas, E. Reguera, *Microporous Mesoporous Mater.,* **185** (2014) 113-120

Chapter 5

Oxidative dehydrogenation of n-butene with novel iron oxide based catalyst

1. Introduction

One of principal intermediate products in the petrochemical industry is buta-1,3-diene (BD), and BD demand is increasing. BD as a major building block in the petrochemical industry is almost produced by steam cracking of naphtha. However, this process is operated at a high temperature over 700 ^{o}C, and the high energy is required because of the endothermic reaction. In addition, the steam cracking of naphtha can not selectively produce BD, because this process mainly produce the light hydrocarbons such as ethene and propylene. As the other problem, due to the shale gas revolution, ethane can be cheaply supplied. To produce ethene cheaply, the substrate used in cracking transfers from naphtha to ethane derived from the shale gas. Therefore, the supply of BD in the near future are concerned, and an alternative process to produce BD is required.

Recently, the oxidative dehydrogenation (ODH) of C4 fraction (Eq. (1)), which is an exothermic reaction, has attracted much attention. This reaction is very useful from a viewpoint of energy saving and is proposed as the process which can efficiently produce BD.

$$C_4H_8 + 1/2O_2 \rightarrow C_4H_6 + H_2O \qquad \Delta H^o = -132.1 \text{ kJ/mol} \quad (1)$$

However, the ODH has a serious problem that the complete oxidation of reactant and product to CO_2 proceeds easily (Eqs. (2), (3)).

$$C_4H_8 + 6O_2 \rightarrow 4CO_2 + 4H_2O \qquad \Delta H^o = -2540.8 \text{ kJ/mol} \quad (2)$$

$$C_4H_8 + 4O_2 \rightarrow 4CO + 4H_2O \qquad \Delta H^o = -1409.0 \text{ kJ/mol} \quad (3)$$

In order to inhibit the complete oxidation, the ODH of n-butene has been carried out under an O_2 flow with a large amount of steam [1]. However, since the latent heat of steam is large, a lot of energy are necessary. The supply of steam will be undesirable. In another way, the ODHs of n-butene and propane have been performed with the lattice oxygen of the catalyst in order to prevent the complete oxidation of the substrates (Eqs. (4), (5)) [2, 3]. However, it is not suitable for the continuous BD production for a long time, because this process require the regeneration step of the used catalyst.

$$C_4H_8 + MO_x \rightarrow C_4H_6 + H_2O + MO_{x-1} \qquad (4)$$

$$MO_{x-1} + 1/2O_2 \rightarrow MO_x \qquad (5)$$

For the effective and continuous BD production, the ODHs of n-butane and n-butene are preferable to apply under O_2 flow without of steam.

Various effective catalysts such as Bi-Mo composite oxide [4-13], ferrite type [14-27], and V-containing catalysts [28-30] have been proposed for the ODH of n-butene and n-butane. Among them, Bi-Mo composite oxide and ferrite type catalysts are widely studied. It has been reported that the ODH reaction with these catalysts proceeds through the Mars-van Krevelen mechanism [4, 5]. This mechanism is a redox cycle with the lattice oxygen in the metal oxide, and the reactivity of lattice oxygen in metal oxide during the ODH reaction is crucial factor to determine the catalytic performance. On the other hand, the effect of crystalline structure of catalyst on the ODH is often discussed [7, 17, 19]. Bi-Mo complex oxide has α-$Bi_2Mo_3O_{12}$, β-$Bi_2Mo_2O_9$, and γ-Bi_2MoO_6. Generally, the catalytic activity for the ODH of n-butene is the order of $\gamma > \alpha$ [7]. β-$Bi_2Mo_2O_9$ is inappropriate for the ODH, because it decompose to α and γ at the reaction temperature of 400–550 °C [6]. It is indicated that this order is consistent with the lattice oxygen

reactivity [31]. In the case of iron oxide catalyst, it is reported that ferrite type catalyst having the spinel structure can exhibit the high ODH activity, and the presence of α-Fe_2O_3 leads the low ODH performance [17, 19].

Thus, extensive study on the effect of the crystallite structure on the ODH is important to perform the development of the catalyst which can show the high catalytic performance. Iron oxide has various crystalline structures such as α-, β-, γ-, and ε-Fe_2O_3, and each crystalline structure can be easily synthesized in the single phase. Meanwhile, in various ODH reactions, the detailed investigation of the crystalline phase of iron oxide is not conducted yet.

Therefore, in this study, the effect of crystalline structure of iron oxide on the ODH of n-butene was examined. The effective iron oxide catalyst for the ODH reaction was proposed in this Chapter. In order to achieve the efficient BD production, the ODH of butene was carried out under O_2 flow without steam, and the catalytic performance stability during the ODH was also investigated.

2. Experimental

2.1 Materials

$Fe(NO_3)_3{\cdot}9H_2O$ (assay = min. 99.0%), $FeSO_4{\cdot}7H_2O$ (assay = 99-102%), $Fe_2(SO_4)_3{\cdot}nH_2O$ (assay = 60-80%), $Zn(NO_3)_2{\cdot}6H_2O$ (assay = min. 99.0%), NaOH (assay = min. 97.0%), 28%NH_3 solution, n-octane (assay = min. 98%), 1-butanol (assay = min. 99%), acetone (assay = min. 99.5%), methanol (assay = min. 99.8%), NaCl (assay = 99.5%), cetyltrimethylammonium bromide (CTAB), tetraethyl orthosilicate (TEOS) (assay = min. 95.0%), and Fe_3O_4 were purchased from Wako Pure Chemical Industry and were used for the preparation of iron oxide catalysts. But-1-ene (1-C_4H_8) (assay = min. 99.0%) was supplied from Sumitomo Seika Chemical. *Cis*-but-2-ene (*cis*-2-C_4H_8) (assay = min. 99.0%) was supplied from Takachiho Chemical Industrial Co.,Ltd.

2.2 Preparation of various iron oxide catalysts

α-Fe_2O_3 were prepared by the precipitation method. $Fe(NO_3)_3{\cdot}9H_2O$ (10 mmol) was dissolved in 100 mL of pure water. The solution was stirred at room temperature for 1 h. After stirring, 1 mol/L of NaOH solution was added to the solution under vigorous stirring until the pH reached 10. After stirring for 1 h, the resultant precipitate was separated by the centrifugation, the solid was washed with a large amount of pure water until the pH reached 7-8, and then it was dried at 110 ºC in oven overnight. The solid was calcined at 500 ºC for 2 h in air. γ-Fe_2O_3 was prepared by the same method as α-Fe_2O_3. $FeSO_4{\cdot}7H_2O$ (10 mmol) as precursor was used, and the calcination was carried out at 400 ºC.

β-Fe_2O_3 was prepared according to the previous reports [32, 33]. Firstly, $Fe_2(SO_4)_3$ was prepared by calcining $Fe_2(SO_4)_3{\cdot}nH_2O$ at 400 ºC under N_2 flow. $Fe_2(SO_4)_3$ and NaCl with molar ratio of 1:2 were mixed in a mortar for 30 min. Mixed material was calcined

at 550 ºC for 2 h in air. Calcined product was added into pure water, and stirred at the room temperature overnight. After stirring, the solid was filtered, washed with a large amount of pure water, and dried at 110 ºC in oven overnight.

Firstly, ε-Fe_2O_3-SiO_2 was prepared referring to previous reports [34-36]. Namely, ε-Fe_2O_3-SiO_2 was prepared by the reverse micelle method. $Fe(NO_3)_3{\cdot}9H_2O$ was dissolved in mixed solution of pure water, n-octane, and 1-butanol. CTAB at H_2O/CTAB=30/1 (mol/mol) was added into the mixed solution containing $Fe(NO_3)_3{\cdot}9H_2O$, and stirred until dissolved (Solution 1). Next, a solution containing 28% NH_3aq was prepared with the same method as Solution 1 (Solution 2). Solution 2 was added drop-wise to Slution 1, and the slurry obtained here was stirred for 30 min. Then, TEOS was added into the slurry to yield weight ratio of $(Fe_2O_3)/(SiO_2+Fe_2O_3)$=0.1, 0.2, 0.5, and stirred overnight. After stirring, this slurry was separated by the centrifugation. The solid obtained was washed with mixed solvent of acetone and methanol (volume ratio=1/1), and then it was dried at 60 ºC in oven for 5 h. The solid was calcined at 1050 ºC for 4 h in air. The different Fe_2O_3 containing catalysts were prepared by varying the amount of $Fe(NO_3)_3{\cdot}9H_2O$. Here, notation is ε-Fe_2O_3(X)-SiO_2, where X is Fe_2O_3 content (wt%). Pure ε-Fe_2O_3 was obtained by the following process. SiO_2 in ε-Fe_2O_3(50)-SiO_2 was dissolved in 1 mol/L NaOH solution at 60 ºC for overnight, and the solid was filtered, washed with a large amount of pure water, and dried at 110 ºC in oven for overnight.

$ZnFe_2O_4$ was prepared as previously reported [19]. $Fe(NO_3)_3{\cdot}9H_2O$ and $Zn(NO_3)_2{\cdot}6H_2O$ were dissolved in 100 mL of pure water. The mixed solution was stirred at the room temperature for 1 h. After stirring, 3 mol/L of NaOH solution was added to the solution under vigorous stirring until the pH 9. After stirring at the room temperature for 12 h, it was aged overnight. The resultant precipitate was separated by centrifugation,

the solid was washed with a large amount of pure water until the pH 7-8, and then it was dried at 175 ºC for 16 h. The solid was calcined at 650 ºC for 2 h in air.

2.3 Catalyst characterization

X-ray diffraction (XRD) patterns of iron oxide catalysts were obtained by the powder method with a Rigaku RINT-TTRIII diffractometer using monochromatic Cu Kα radiation under the following conditions: tube voltage 40 kV, tube current 30 mA, scan step 0.02 º, scan region 10-80 º, and scan speed 4.0 º/min.

2.4 Catalyst test

2.4.1 ODH of n-butene with iron oxide catalyst under O_2 atmosphere

The ODH of but-1-ene was carried out using a fixed-bed flow quartz reactor at 450 ºC under atmosphere pressure. After 200 mg of catalyst was placed in the reactor, the reactor was preheated until reaction temperature at 450 ºC under 22.5 mL/min (STP) of Ar flow. Oxygen, 1-C_4H_8 or *cis*-2-C_4H_8, and Ar were introduced at a flow rate of O_2/1-C_4H_8 or *cis*-2-C_4H_8/Ar=2.5/5/22.5 mL/min (STP). Total gas flow rate was fixed at 30 mL/min.

The C4 fractions (1-C_4H_8, *cis*-2-C_4H_8, *trans*-2-C_4H_8, and C_4H_6) were analyzed by a flame ionization detector (FID) gas chromatograph (Shimadzu GC14B, column: Unicarbon A-400). CH_4, CO, and CO_2 were also analyzed by a thermal conductivity detector (TCD) gas chromatograph (column: activated carbon). O_2 and H_2 was analyzed by TCD gas chromatograph (Shimadzu GC8A, column: molecular sievs 5A).

2.4.2 ODH of but-1-ene with lattice oxygen in iron oxide catalyst

The ODH of but-1-ene was carried out using the fixed-bed flow quartz reactor at 450 ºC under atmospheric pressure. After 200 mg of the catalyst was placed in the reactor, the reactor was preheated until reaction temperature at 450 ºC under 25 mL/min (STP) of Ar flow. Then, 5 mL/min of but-1-ene and 25 mL/min of Ar were introduced for 5 min. Re-oxidation after the reaction was carried out under 5 mL/min of O_2 and 25 mL/min of Ar for 10 min at 450 ºC. Quantification of the products were carried out using the same equipment as section 2.4.1.

3. Results and discussion

3.1 Effect of crystal phase of iron oxide on the ODH

Figure 5-1 shows XRD patterns of various iron oxide catalysts. α-Fe_2O_3 and γ-Fe_2O_3 indicated α-Fe_2O_3 and γ-Fe_2O_3 diffraction peaks, respectively (Fig. 5-1 (a), (d)). Also, formation of ε-Fe_2O_3 and β-Fe_2O_3 in the single phase could be confirmed with the diffraction peaks matching with peaks reported in the literature (Fig. 5-1 (b), (c)) [33, 36, 37].

Table 5-1 shows the effect of crystallite structure of various iron oxides on the ODH reaction. Although all the iron oxide catalysts showed a high O_2 conversion of more than 95%, the different catalytic performances in each iron oxide catalyst were given (Table 5-1: entries 1-4). α-Fe_2O_3 catalyst mainly progressed the complete oxidation, showing the high CO_2 selectivity of 47.6% and the lowest BD yield of 2.8% (Table 5-1: entry 1). When γ- and β-Fe_2O_3 were used for the ODH reaction, these catalysts exhibited the high but-1-ene conversion of more than 20% and BD yield of more than 10%. Hence, the better catalytic performance than that of α-Fe_2O_3 was obtained (Table 5-1: entries 2, 3). In the case of ε-Fe_2O_3, this catalyst showed the highest but-1-ene conversion of 43.5% and the

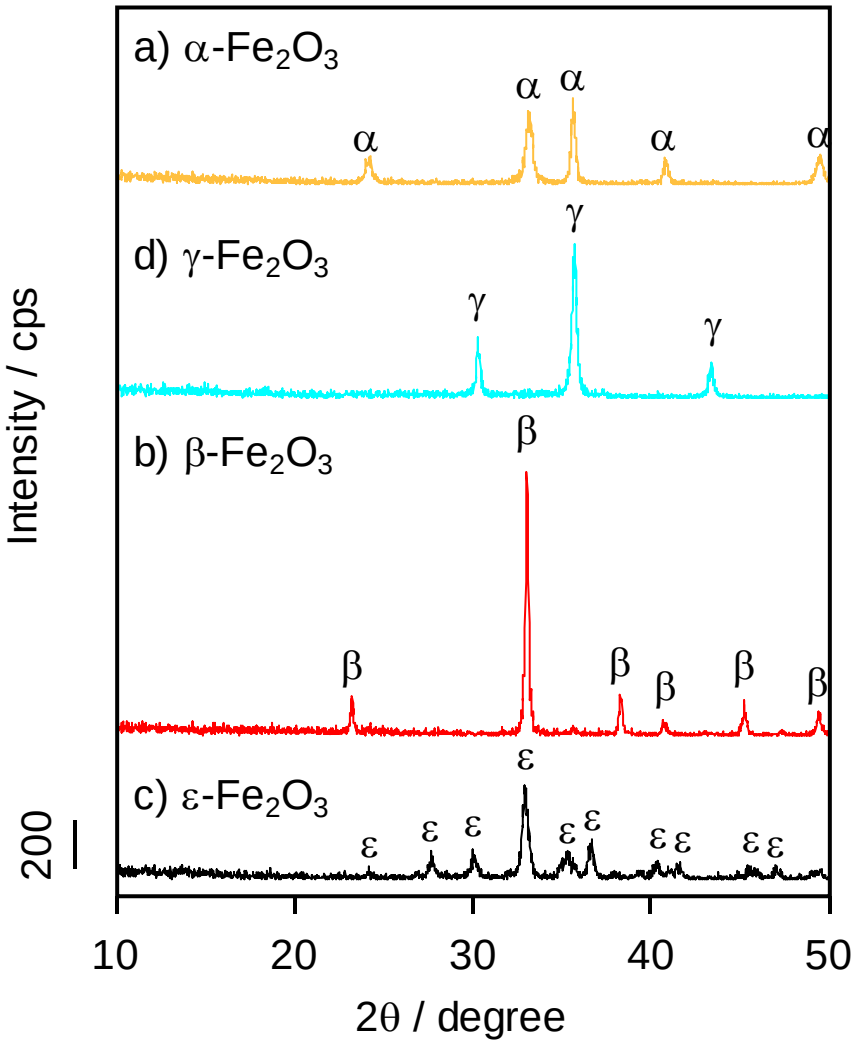

Fig. 5-1 XRD patterns of various iron oxides

Table 5-1 Effect of crystalline structure of iron oxide on ODH of but-1-ene

Entry	Catalyst	O_2 convesion	But-1-ene conversion.	Selectivity(%)					BD yield(%)
		(%)	(%)	C_4H_6	cis-2-C_4H_8	trans-2-C_4H_8	CO	CO_2	C_4H_6
1	α-Fe_2O_3	100.0	18.0	15.3	20.9	16.2	0.0	47.6	2.8
2	γ-Fe_2O_3	100.0	25.0	49.9	9.2	7.6	3.5	29.8	12.5
3	β-Fe_2O_3	98.0	20.6	52.0	3.6	3.1	4.2	37.1	10.7
4	ε-Fe_2O_3	100.0	43.5	39.3	21.5	22.0	0.6	16.6	17.1
5	Fe_3O_4	99.9	29.1	35.0	21.2	17.4	0.7	25.7	10.2
6	$ZnFe_2O_4$ ref	99.2	33.9	31.1	26.6	21.1	2.6	18.7	10.5

Catalyst: 200 mg
Flow rate: 1-C_4H_8/O_2/Ar=5/2.5/22.5 mL/min
Reaction temperature: 450 °C
Reaction time: 30 min

lower CO_2 selectivity of 16.6% than those of the other iron oxides, and the highest BD yield of 17.1% was obtained (Table 5-1: entry 4). The Fe_3O_4 catalyst gave the lower but-1-ene conversion of 29.1% and BD yield of 10.2% than those of ε-Fe_2O_3 (Table 5-1: entry 5). In addition, ε-Fe_2O_3 showed the higher catalytic activity as compared with $ZnFe_2O_4$ already reported in thesis (Table 5-1: entry 6). Among various iron oxide catalysts, ε-Fe_2O_3 exhibited the highest ODH activity.

As far as I know, this is the fruitful result that ε-Fe_2O_3 could show the high activity for the ODHs of various substrate such as propane and but-1-ene.

In order to understand the effect of crystalline structure of iron oxide on the ODH in the absence of gas-phase O_2, the ODH with lattice oxygen in iron oxide was carried out. Table 5-2 shows the result. α-Fe_2O_3 showed low but-1-ene conversion of 9.9% and low BD selectivity of 15.6%. γ-Fe_2O_3 showed high conversion of 24.4%. However, this catalyst exhibited high CO_2 selectivity of 22.1%. Therefore, γ-Fe_2O_3 progressed the complete oxidation. Although β-Fe_2O_3 indicated low conversion of 13.8%, the highest BD selectivity of 56.9% was obtained. Surprisingly, ε-Fe_2O_3 showed the highest conversion of 46.4%, and the high BD selectivity of 49.9%.

Table 5-2 Oxidative dehydrogenation of but-1-ene with lattice oxygen in various iron oxide

Catalyst	But-1-ene conversion (%)	Selectivity(%)					yield(%)
		C_4H_6	*cis*-2-C_4H_8	*trans*-2-C_4H_8	CO	CO_2	C_4H_6
α-Fe_2O_3	9.9	15.6	37.9	26.8	0.0	19.6	1.6
γ-Fe_2O_3	24.4	22.7	24.8	26.4	4.1	22.1	5.5
β-Fe_2O_3	13.8	56.9	11.2	10.7	0.5	20.7	7.9
ε-Fe_2O_3	46.4	49.9	24.1	23.0	0.0	3.0	23.2

Catalyst: 200 mg, Flow rate: 1-C_4H_8/Ar=5/25 (mL/min), Reaction temperature: 450°C

The order of BD yield was ε-Fe_2O_3 (23.2%)>β-Fe_2O_3 (7.9%)>γ-Fe_2O_3 (5.5%)>α-Fe_2O_3 (1.6%). From this result, it was clarified that the lattice oxygen in ε-Fe_2O_3 was effectively used for the ODH of but-1-ene. This unique performance of ε-Fe_2O_3 seems to be related to the ODH of but-1-ene in the presence of O_2.

3.2 Stability of ε-Fe_2O_3 catalyst

The catalytic performance stability for the ODH reaction is an important factor to continuously produce BD. Therefore, the stability test of ε-Fe_2O_3 was carried out. The result is shown in Table 5-3: entry 7. Although ε-Fe_2O_3 showed the high BD yield of 17.1% for 30 min, after 60 min the but-1-ene conversion decreased from 34.3 to 27.8% and the CO_2 selectivity increased from 20.5 to 25.5%. Unfortunately, the BD yield decreased from 17.1% to 13.7%.

To examine the reason for the decrease in the ODH activity, XRD analyses of the catalyst before and after the ODH were conducted. The XRD patterns before and after the ODH are shown in Figure 5-2. As shown in this figure, ε-Fe_2O_3 diffraction peaks observed before the ODH disappeared after the reaction and Fe_3O_4 diffraction peaks appeared after the reaction for 2 h. In the ODH of but-1-ene, it has been reported that the ODH activity of iron oxide-based catalyst was declined by the formation of divalent iron oxide species during the reaction [26, 27]. Actually, Fe_3O_4 catalyst showed the low ODH activity (Table 5-1: entry 5). Therefore, it is considered that the catalytic performance was decreased by changing from ε-Fe_2O_3 to the reduced iron oxide such as Fe_3O_4 during the ODH. In addition, the crystallite diameter of ε-Fe_2O_3 after the ODH grown from 25.4 to 31.4 nm. The sintering of the catalyst might also be related to the decline of the ODH activity.

On the other hand, Wan *et al*. has reported that the catalytic activity for the ODH of

Table 5-3 Effect of e-Fe_2O_3 containing level on ODH of but-1-ene under O_2 atmosphere

Entry	Catalyst	Reaction time	O_2 conversion	But-1-ene conversion	Selectivity(%)					BD yield(%)
		(min)	(%)	(%)	C_4H_6	*cis*-2-C_4H_8	*trans*-2-C_4H_8	CO	CO_2	C_4H_6
7	ε-Fe_2O_3	30	100.0	43.5	39.3	21.5	22.0	0.6	16.6	17.1
		60	100.0	34.3	41.2	19.5	17.9	1.0	20.5	14.1
		90	100.0	30.5	45.8	15.5	13.5	1.2	24.0	13.9
		120	100.0	27.8	49.4	13.0	10.8	1.3	25.5	13.7
8	ε-Fe_2O_3(50)-SiO_2	30	64.1	22.5	58.0	14.0	11.4	4.2	12.5	13.0
		60	75.9	24.6	63.4	9.5	7.8	4.5	14.9	15.6
		90	79.1	25.5	65.1	8.3	6.9	4.5	15.3	16.6
		120	81.4	25.9	66.1	7.5	6.2	4.5	15.7	17.1
		180	89.9	26.7	66.3	6.4	5.3	4.7	17.4	17.7
		210	89.1	27.0	67.6	6.1	5.0	4.5	16.8	18.2
		240	89.0	21.9	86.1	7.6	6.3	-	-	18.8
9	ε-Fe_2O_3(20)-SiO_2	30	73.0	27.6	60.0	12.0	10.0	5.5	12.5	16.5
		60	69.8	25.3	60.4	11.4	9.4	5.5	13.3	15.3
		90	70.5	25.5	61.6	10.2	8.5	5.7	14.0	15.7
		120	72.9	26.5	62.8	9.0	7.5	5.9	14.7	16.6
		180	78.4	26.6	67.4	8.1	6.8	5.6	12.1	17.9
		240	82.8	28.2	64.2	6.7	9.3	5.7	14.1	18.1
10	ε-Fe_2O_3(10)-SiO_2	30	61.7	24.6	63.7	11.1	9.4	5.0	10.8	15.6
		60	59.9	23.6	59.9	13.0	11.0	4.9	11.3	14.1
		90	61.0	22.6	62.9	11.4	9.5	4.9	11.2	14.2
		120	57.2	22.2	64.1	10.8	8.9	5.0	11.3	14.2

Catalyst: 200 mg

Flow rate: 1-C_4H_8/O_2/Ar=5/2.5/22.5 mL/min

Reaction temperature: 450 °C

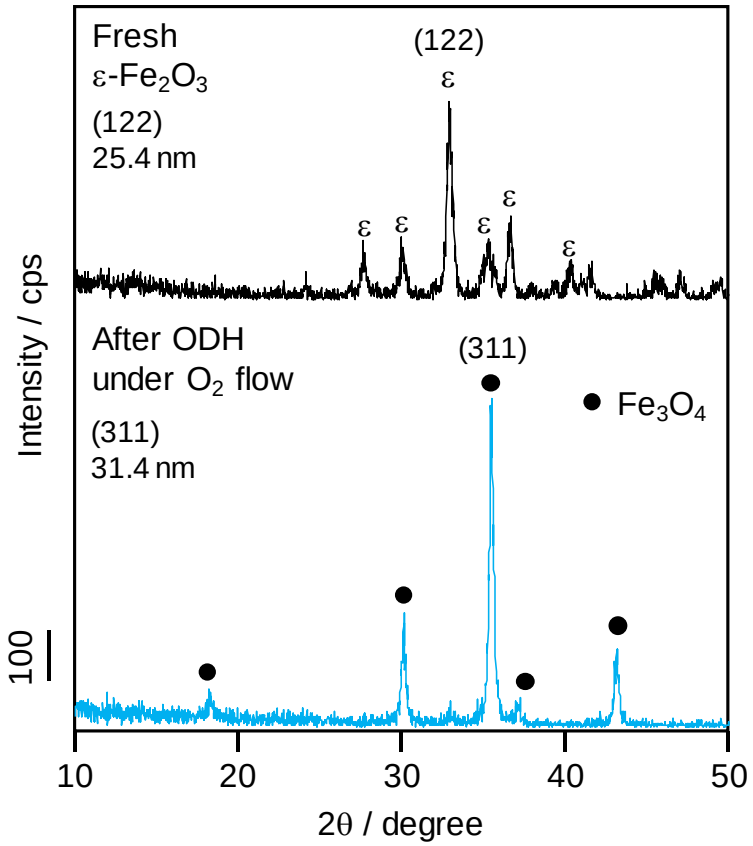

Fig. 5-2 XRD patterns of ε-Fe_2O_3 before and after ODH of but-1-ene under O_2 flow

n-butene is related to the oxidation and reduction cycle (redox cycle) through the lattice oxygen in the metal oxide [11]. Hence, the ODH with the lattice oxygen in the catalyst and the regeneration with O_2 were carried out using ε-Fe_2O_3. The results are indicated in Fig. 5-3 (a). In the first ODH reaction, the high BD yield of 23% was obtained. Although the but-1-ene conversion (53.7%) of the second reaction was higher than that (46.4%) of the first reaction, the low BD selectivity of 19. 2% and BD yield of 10.3% were observed

From these results, the lattice oxygen in ε-Fe_2O_3 could be used to produce BD, but the used lattice oxygen in ε-Fe_2O_3 could not be re-generated with O_2, showing that the BD yield decreased in the second ODH. According to XRD analysis of ε-Fe_2O_3 after the

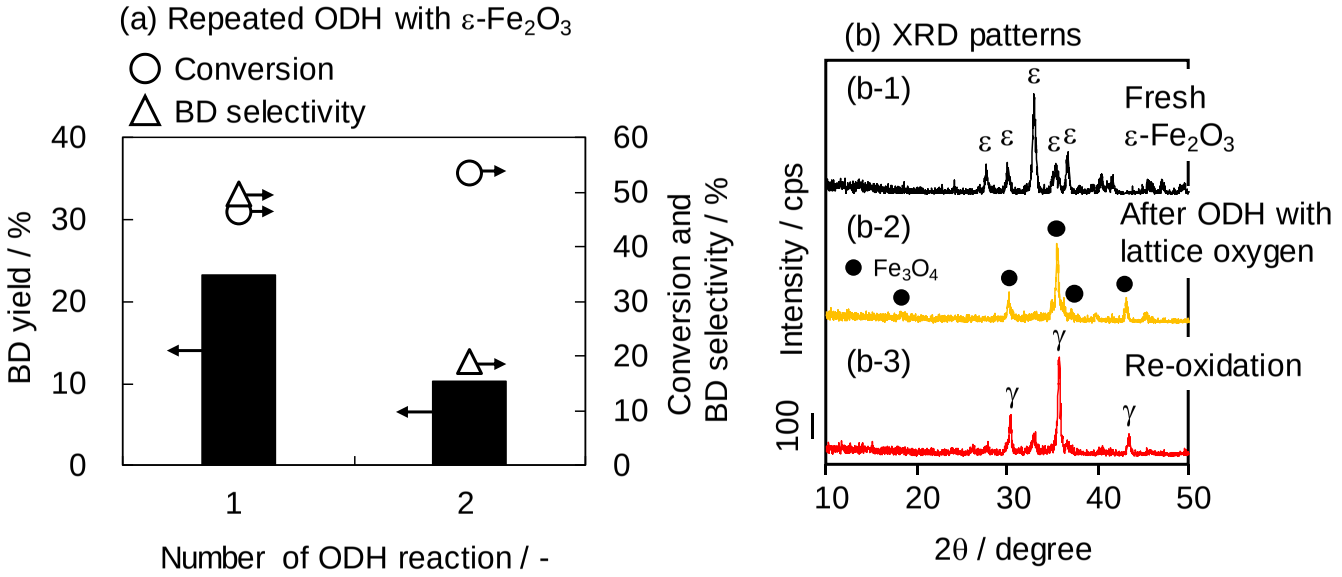

Fig. 5-3 (a) Repeated ODH of but-1-ene and re-oxidation with ε-Fe_2O_3,
(b) XRD patterns of ε-Fe_2O_3 after the ODH with lattice oxygen and re-oxidation with O_2

Catalyst: 200 mg,
ODH: 30 mL/min (1-C_4H_8 /Ar = 5/25 mL/min),
ODH temperature: 450 °C , ODH time: 5 min,
Re-oxidation: O_2/Ar=5/25 mL/min,
Re-oxidation temperature: 450 °C, Re-oxidation time: 10 min

ODH using the lattice oxygen and the regeneration using O_2, diffraction peaks attributable to Fe_3O_4 were shown in the catalyst (Fig. 5-3(b-2)), and the diffraction peaks of γ-Fe_2O_3 were seen in the catalyst after the regeneration with O_2 (Fig. 5-3(b-3)). Therefore, this result clearly indicates that ε-Fe_2O_3 reduced to Fe_3O_4 can not be regenerated to ε-Fe_2O_3 by O_2.

It is suggested that keeping the redox property of the lattice oxygen of ε-Fe_2O_3 phase is most important to maintain the ODH activity under O_2 flow.

3.3 Effect of SiO_2 contained in the catalyst on the ODH

As mentioned in section 3.2, the ε-Fe_2O_3 catalyst showed the higher ODH activity than those of the other iron oxide catalysts, and was proposed as a novel catalyst. However, this catalyst was deactivated due to the change in the crystalline structure during the reaction and the failure of redox cycle. Therefore, the improvement of catalytic performance stability was tried.

Fe_2O_3/SiO_2 is proposed as the good catalyst which shows the high catalytic performance for high temperature sulfuric acid decomposition [37, 38]. According to these literatures, it is indicated that the redox property of metal oxide is important factor to determine the reaction rate, and it has been reported that Fe_2O_3/SiO_2 showed the better redox property among various iron oxide-based catalysts. It is also reported that Fe_2O_3 containing Al_2O_3, CaO, and SiO_2 showed the high redox cycle stability for cyclic water gas shift process. Then, SiO_2 seems to be related to inhibition of iron species sintering by physical blocking [39]. The improvement of the redox property is expected by including SiO_2 in iron oxide.

On the other hand, ε-Fe_2O_3 can be formed by calcining iron oxide (γ-Fe_2O_3) coated

with SiO_2 at 1050 ºC [36]. Hence, to maintain the catalytic activity in the ODH, the effect of containing SiO_2 to ε-Fe_2O_3 on the ODH of but-1-ene under O_2 flow was investigated. ε-Fe_2O_3(50 wt%)-containing SiO_2 catalyst (ε-Fe_2O_3(50)-SiO_2) was used for the reaction.

The results of ODH with ε-Fe_2O_3(50)-SiO_2 catalyst are indicated in Table 5-3: entry 8. Although ε-Fe_2O_3(50)-SiO_2 catalyst showed the low O_2 conversion of 64.1%, high but-1-ene conversion of 22.5% and the BD yield of 13.0% were obtained in the reaction for 30 min. After 60 min, this catalyst showed the higher BD yield of ca.18% and the lower CO_2 selectivity of 17% than those of pure ε-Fe_2O_3. In addition, although the improvement of CO_2 selectivity was seen with the course of the reaction time, deactivation was not seen during the reaction for 4 h. Therefore, ε-Fe_2O_3 containing SiO_2 catalyst indicated the higher catalytic performance as compared to pure ε-Fe_2O_3. When XRD analyses of ε-Fe_2O_3(50)-SiO_2 catalyst before and after the ODH were carried out, ε-Fe_2O_3 diffraction peaks were observed in the catalyst even after the ODH (Fig. 5-4). In addition, the growth of the crystallite diameter of ε-Fe_2O_3 after the ODH was not seen. It was considered the presence of SiO_2 inhibited the sintering of ε-Fe_2O_3 during the ODH. Unlike pure ε-Fe_2O_3, it is indicated that the stability of ε-Fe_2O_3 phase could be improved by containing SiO_2 and the maintenance of ε-Fe_2O_3 phase led to the increase in the ODH activity and the stability during the reaction.

Therefore, the redox property of the lattice oxygen in ε-Fe_2O_3(50)-SiO_2 catalyst was examined by the repeated ODH. The results are shown in Fig. 5-5(a). The low but-1-ene conversion of 22.4%, the high BD selectivity of 49.2%, and the low BD yield of 11% were obtained in the first ODH reaction. The lower lattice oxygen reactivity in ε-Fe_2O_3(50)-SiO_2 than that of pure ε-Fe_2O_3 was shown. This is because the amount of lattice oxygen that can be used for the ODH is probably half of that of pure ε-Fe_2O_3.

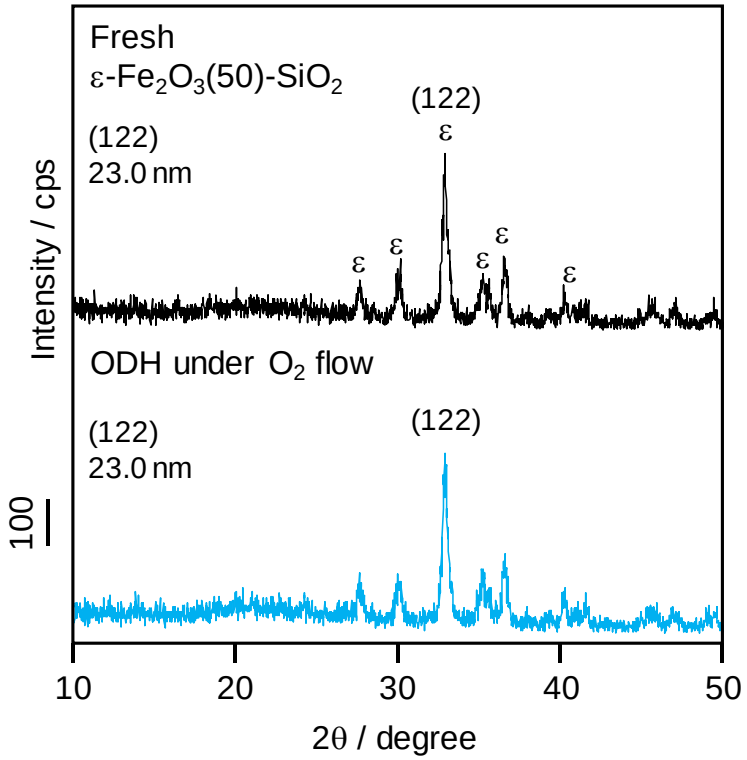

Fig. 5-4 XRD patterns of ε-Fe_2O_3(50)-SiO_2 before and after the ODH of but-1-ene under O_2 flow

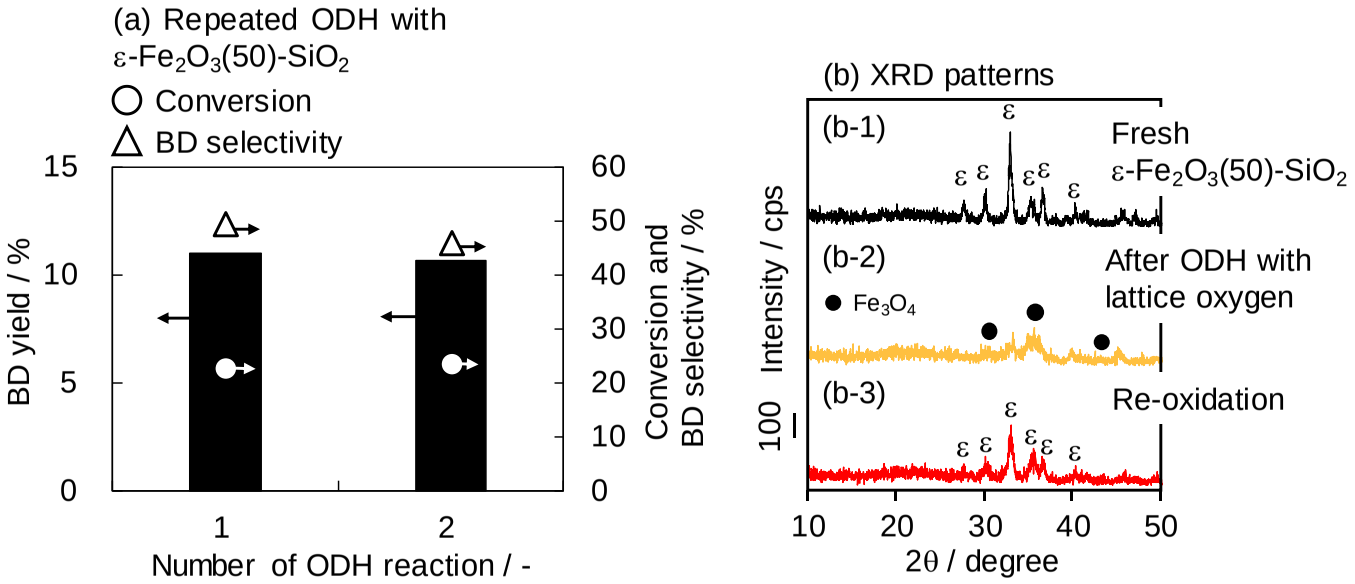

Fig. 5-5 (a) Repeated ODH of but-1-ene and re-oxidation with ε-Fe_2O_3(50)-SiO_2,
(b) XRD patterns of ε-Fe_2O_3(50)-SiO_2 after the ODH with lattice oxygen and re-oxidation with O_2

Catalyst: 200 mg,
ODH: 30 mL/min (1-C_4H_8 /Ar = 5/25 mL/min),
ODH temperature: 450 °C , ODH time: 5 min,
Re-oxidation: O_2/Ar=5/25 mL/min,
Re-oxidation temperature: 450 °C, Re-oxidation time: 10 min

Meanwhile, when the ODH with the lattice oxygen in the re-oxidized ε-Fe_2O_3(50)-SiO_2 was carried out, the but-1-ene conversion of 23.3%, the BD selectivity of 45.7%, and the BD yield of 10.7% were similar to the results in the first ODH. This result indicated that the used lattice oxygen in ε-Fe_2O_3 containing SiO_2 could be easily regenerated by molecular O_2.

According to XRD (Fig. 5-5(b)), ε-Fe_2O_3 diffraction peaks were not seen in ε-Fe_2O_3(50)-SiO_2 after the reaction with the lattice oxygen, and the small diffraction peaks related to Fe_3O_4 were also observed (Fig. 5-5(b-2)). Surprisingly, the catalyst after the re-oxidation with O_2 showed ε-Fe_2O_3 diffraction peaks (Fig. 5-5(b-3)). Therefore, ε-Fe_2O_3(50)-SiO_2 after the ODH with the lattice oxygen could be restructured to ε-Fe_2O_3 phase by O_2. The improvement of the redox property of ε-Fe_2O_3 by the presence of SiO_2 was revealed.

From the results of the XRD analyses and the repeated ODH, by containing SiO_2, the sintering of ε-Fe_2O_3 during the ODH was inhibited and the redox property of the lattice oxygen in ε-Fe_2O_3 was improved as compared to that of pure ε-Fe_2O_3. Therefore, it is considered that this catalyst exhibited the high catalytic activity and the stability during the ODH under O_2 flow.

3.4 Effect of content of ε-Fe_2O_3 on the ODH

The usefulness of containing ε-Fe_2O_3 in SiO_2 for the ODH was suggested. Therefore, the effect of content of ε-Fe_2O_3 on the ODH was investigated. ε-Fe_2O_3(10, 20, 50)-SiO_2 and pure ε-Fe_2O_3 were used for the ODH.

XRD analyses were carried out, and the results are shown in Fig. 5-6. The ε-Fe_2O_3 diffraction peaks appeared in all the catalysts, and the amorphous SiO_2 was observed in

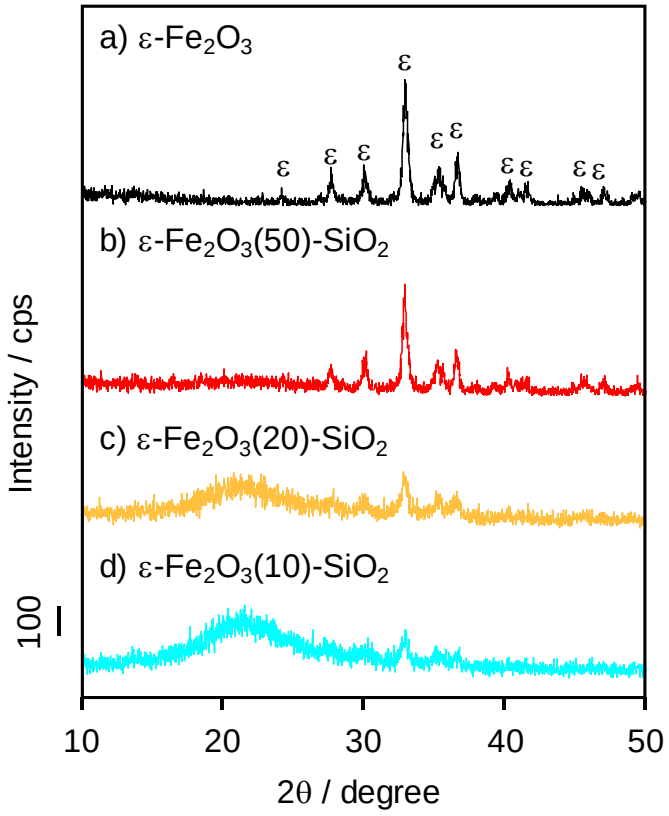

Fig. 5-6 XRD patterns of ε-Fe_2O_3 catalysts containing SiO_2

ε-Fe_2O_3(10, 20, 50)-SiO_2.

The results of the ODH using ε-Fe_2O_3 (10, 20, 50)-SiO_2 are shown in Table 5-3. As mentioned in sections 3. 2 and 3. 3, pure ε-Fe_2O_3 catalyst gave the high O_2 and but-1-ene conversions and the high BD yield of 17.1% for 30 min. However, after 30 min, the decrease in the BD selectivity and the increase in the CO_2 selectivity were seen, and the BD yield declined to 13.7% (Table 5-3: entry 7). Meanwhile, although ε-Fe_2O_3(50)-SiO_2 catalyst showed lower O_2 and but-1-ene conversions and lower BD yield than those of pure ε-Fe_2O_3 until 30 min, after 60 min the BD yield increased to about 18.0% during 4 h (Table 5-3: entry 8). In the ODH with ε-Fe_2O_3(20)-SiO_2 catalyst (Table 5-3: entry 9),

although this catalyst showed the low O_2 conversion of 80% for 4 h, the CO_2 selectivity of about 14% was lower than that of ε-Fe_2O_3(50)-SiO_2. In addition, the high BD yield of ca.18% was obtained, and the ODH activity of ε-Fe_2O_3(20)-SiO_2 catalyst was also maintained during the reaction for 4 h similarly to ε-Fe_2O_3(50)-SiO_2 catalyst. ε-Fe_2O_3(10)-SiO_2 catalyst showed the lowest CO_2 selectivity of 11% in this study. The low O_2 conversion of about 60% and the but-1-ene conversion of 22% were exhibited, showing the lower BD yield of ca.14% than those of the other ε-Fe_2O_3 containing SiO_2 catalysts. However, the catalytic performance was the most stable for ε-Fe_2O_3(10)-SiO_2 catalyst.

As shown in these results, all ε-Fe_2O_3 containing SiO_2 exhibited the high stability in comparison with pure ε-Fe_2O_3. Although the BD yield improved with increasing the ε-Fe_2O_3 content, the BD yield was plateau over 20 wt% of ε-Fe_2O_3. In addition, the CO_2 selectivity did not increase in the reaction with the catalyst containing ε-Fe_2O_3 over 20 wt%. Therefore, 20 wt% of ε-Fe_2O_3 was decided as the best content.

Finally, *cis*- or *trans*-but-2-ene is also important as a raw material to produce BD by the ODH. Therefore, the ODH of *cis*-but-2-ene with ε-Fe_2O_3(20)-SiO_2 catalyst was carried out. The result is shown in Fig. 5-7. The high *cis*-but-2-ene conversion of ca.30%, the high BD selectivity of about 63%, and the high BD yield of about 19% were obtained similarly to the case of ODH of but-1-ene. In addition, the ODH activity was maintained for 4 h. From these results, it is indicated that cis-but-2-ene can be used as a new material for BD with ε-Fe_2O_3(20)-SiO_2 catalyst.

Therefore, ε-Fe_2O_3 catalyst containing SiO_2 can be proposed as the novel iron oxide catalyst which shows the high catalytic performance for the ODH of n-butene.

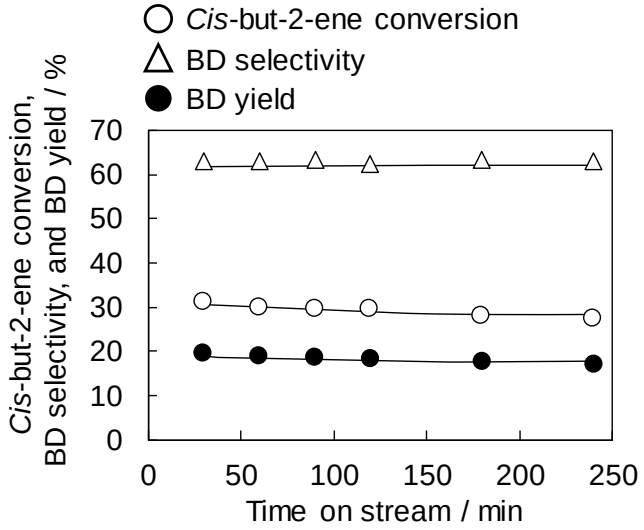

Fig. 5-7 ODH of *cis*-but-2-ene under O_2 flow with ε-Fe_2O_3(20)-SiO_2

Catalyst: 200 mg, Flow rate: 30 mL/min (*cis*-2-C_4H_8 /O_2/Ar = 5/2.5/22.5), Reaction temperature : 450 ^oC

4. Conclusions

In this study, the effect of crystalline structure of iron oxide catalyst on the ODH of but-1-ene was investigated. The ε-Fe_2O_3 catalyst showed the highest ODH activity (BD yield of 17.1%) among various iron oxide catalysts, and was proposed as the novel and excellent catalyst. Although ε-Fe_2O_3 showed the high ODH activity, the activity could not be maintained because of the transformation of crystalline structure.

In order to improve the catalyst stability, ε-Fe_2O_3 containing SiO_2 (ε-Fe_2O_3-SiO_2) was used in this reaction. The ε-Fe_2O_3(50)-SiO_2 catalyst indicated the high BD yield of 18% and the deactivation was not seen during 4 h. It was found that containing SiO_2 improved the maintenance of crystalline structure and the redox property of lattice oxygen in ε-Fe_2O_3. The effect of ε-Fe_2O_3 content on the ODH was also investigated. When ε-Fe_2O_3(20)-SiO_2 catalyst was used for the ODH, the high BD yield of 18% was obtained during 4 h. The optimum ε-Fe_2O_3 content was determined as 20 wt%. In addition, this catalyst could be used for the ODH of *cis*-but-2-ene, and the same BD yield (17%) as for but-1-ene and the high stability were shown. This suggested that cis- and trans-but-2-ene could be recycled, which means the substantial selectivity of BD is higher than these indicated in the Tables and Figures in this thesis.

5. References

[1] J.H. Park, C.H. Snin, *Appl. Catal. A: Gen.,* **495** (2015) 1-7

[2] K. Fukudome, N. Ikenaga, T. Miyakke, T. Suzuki, *Catal. Sci. Technol.,* **1** (2011) 987- 998

[3] S. Gong, S. Park, W.C. Choi, H. Seo, N.Y. Kang, M.Wan. Han, Y.K. Park, *J. Mol. Catal. A: Chem.,* **391** (2014) 19-24

[4] M.F. Portela, *Top. Catal.,* **15** (2001) 241-245,

[5] J.C. Jung, H. Lee, H. Kim, Y.M. Chung, T.J. Kim, S.J. Lee, S.H. Oh, Y.S. Kim, I.K. Song, *Catal. Lett.,* **124** (2008) 262-267

[6] J.C. Jung, H. Kim, Y.M. Chung, T.J. Kim, S.J. Lee, S.H. Oh, Y.S. Kim, I.K. Song, *J. Mol. Catal. A: Chem.,* **264** (2007) 237-240

[7] J.C. Jung, H. Lee, I.K. Song, *Catal. Surv. Asia,* **13** (2009) 78-93

[8] J.C. Jung, H. Lee, H. Kim, Y.M. Chung, T.J. Kim, S.J. Lee, S.H. Oh, Y.S. Kim, I.K. Song, *J. Mol. Catal. A: Chem.,* **271** (2007) 261-265

[9] J.H. Park, H. Noh, J.W. Park, K. Row, K.D. Jung, C.H. Shin. *Appl. Catal. A: Gen.,* **431-432** (2012) 137-143

[10] J.C. Jung, H. Kim, Y.S. Kim, Y.M. Chung, T.J. Kim, S.J. Lee, S.H. Oh, I.K. Song, *Appl. Catal. A: Gen.,* **317** (2007) 244-249

[11] C. Wan, D. Cheng, F. Chen, X. Zhan, *Chem. Eng. Sci.,* **135** (2015) 553-558

[12] C. Wan, D. Cheng, F. Chen, X. Zhan, *J. Chem. Technol. Biotechnol.,* **91** (2016) 353-358

[13] H. Armendariz, G. Aguilar-Rios, P. Salas, M.A. Valenzuela, I. Schifter, H. Arriola, N. Nava, *Appl. Catal. A: Gen.,* **92** (1992) 29-38

[14] J.A. Toledo, N. Nava, M. Martinez, X. Bokhimi, *Appl. Catal. A: Gen.,* **234** (2002)

137-144

[15] H. Lee, J.C. Jung, H. Kim, Y.M. Chung, T.J. Kim, S.J. Lee, S.H. Oh, Y.S. Kim, I.K. Song, *Catal. Lett.,* **131** (2009) 344-349

[16] Y.M. Chung, Y.T. Kwon, T.J. Kim, S.J. Lee, S.H. Oh, *Catal. Lett.,* **130** (2009) 417-423

[17] H. Lee, J.C. Jung, I.K. Song, *Catal. Lett.,* **133** (2009) 321-327

[18] H. Lee, J.C. Jung, H. Kim, Y.M. Chung, T.J. Kim, S.J. Lee, S.H. Oh, Y.S. Kim, I.K. Song, *Korean J. Chem. Eng.,* **26** (2009) 994-998

[19] H. Lee, J.C. Jung, H. Kim, Y.M. Chung, T.J. Kim, S.J. Lee, S.H. Oh, Y.S. Kim, I.K. Song, *Catal. Commun.,* **9** (2008) 1137-1142

[20] J.A. Toledo, P. Bosch, M.A. Valenzuela, A. Montoya, N. Nava, *J. Mol. Catal.,* **125** (1997) 53-62

[21] H. Armendariz, J.A. Toledo, G. Aguilar-Rios, M.A. Valenzuela, P. Salas, A. Cabral, H. Jimenez, I. Schifter, *J. Mol. Catal.,* **92** (1994) 325-332

[22] R.J. Rennard, W.L. Kehl, *J. Catal.,* **21** (1971) 282-293

[23] B.J. Liaw, D.S. Cheng, B.L. Yang, *J. Catal.,* **118** (1989) 312-326

[24] W.Q. Xu, Y.G. Yin, G.Y. Li, S. Chen, *Appl. Catal. A: Gen.* **89** (1992) 131-142

[25] F.Y. Qiu, L.T. Weng, E. Sham, P. Ruiz, B. Delmon, *Appl. Catal.* **51** (1989) 235-253

[26] Y.M. Chung, Y.T. Kwon, T.J. Kim, S.J. Lee, S.H. Oh, *Catal. Lett.,* **131** (2009) 579-586

[27] M.A. Gibson, J.W. Hightower, *J. Catal.,* **41** (1976) 431-439

[28] A. Dejoz, J.M. LoÂpez Nieto, F. MaÂrquez, M.I. VaÂzquez, *Appl. Catal. A: Gen.,* **180** (1999) 83-94

[29] J.K. Lee, H. Lee, U.G. Hong, J. Lee, Y.-J. Cho, Y. Yoo, H.S. Jang, I.K. Song, *J. Ind.*

Eng. Chem., **18** (2012) 1096-1101

[30] J.M. Lopez Nieto, P. Concepci, A. Dejoz, H. Knozinger, F. Melo, M.I. Vazquez., *J. Catal.,* **189** (2000) 147-157

[31] E. Ruckenstein, R. Krishnan, K.N. Rai, *J. Catal.,* **45** (1976) 270-273

[32] R. Zboril, M. Mashlan, D. Krausova, *Mossbauer Spectroscopy in Materials Science,* 49-56

[33] Y. Ikeda, M. Takano, Y. Bando, *Bull. Inst. Chem. Res., Kyoto Univ.,* **64** (1986) 249-258

[34] S. Ohkoshi, S. Sakurai, S. Sasaki, K. Sato, J. Shimoyama, *Japan patent,* JP5124825B2

[35] S. Ohkoshi, S. Kuroki, S. Sakurai, K. Matumoto, K. Sato, S. Sasaki, *Angew. Chem. Int. Ed.* **46** (2007) 8392-8395

[36] V.N. Nikolic, V. Spasojevic, M. Panjan, L. Kopanja, A. Mrakovic, M. Tadic, *Ceramics International,* **43** (2017) 7497-7507

[37] A. Nadar, A.M. Banerjee, M.R. Pai, S.S. Meena, R.V. Pai, R. Tewari, S.M. Yusuf, A.K. Tripathi, S.R. Bharadwaj, *Appl. Catal. B: Environ.,* **217** (2017) 154–168

[38] A. Nadar, A.M. Banerjee, M.R. Pai, R.V. Pai, S.S. Meena, R. Tewari, A.K. Tripathi, *Int. J. Hydrogen Energy.* **43** (2018) 37-52

[39] P. Datta, *Mater. Res. Bull.,* **48** (2013) 4008–4015

Chapter 6

General conclusions

This thesis has proposed the effective metal oxide catalyst to efficiently produce BD in the ODH of n-butene under O_2 flow without the supply of steam. The author conducted the development of the copper oxide-based catalysts that could show the high ODH activity at the low reaction temperature and the high BD selectivity. The author also attempted the development of the novel and effective iron oxide catalyst from the viewpoint of crystalline structure. The obtained results in this work are summarized as general conclusions.

Chapter 1 indicates general introduction as the background of this study.

In Chapter 2, the author investigated the ODH of but-1-ene with the lattice oxygen in ferrite catalysts. Among various ferrite catalysts, $CuFe_2O_4$ catalyst showed the highest ODH activity at the low reaction temperature of 270 ^oC. When the ODH of but-1-ene was carried out at 270 ^oC with the lattice oxygen in $CuFe_2O_4$ catalyst, the high BD yield of 8.5% was given. Moreover, $CuFe_2O_4$ after the ODH with the lattice oxygen was regenerated by the re-oxidation with O_2, and the regenerated $CuFe_2O_4$ could be reused for the reaction. From the results of XRD and XPS analyses of $CuFe_2O_4$ after the ODH and the re-oxidation, it was found that the ODH was progressed by using the lattice oxygen of Cu-O in Cu^{2+}_T.

Chapter 3 described the ODH of but-1-ene with the $CuFe_2O_4$ catalyst. In this chapter, to continuously produce BD, the ODH of but-1-ene was carried out under O_2 flow. When the effect of preparation method of $CuFe_2O_4$ on the ODH was investigated, $CuFe_2O_4$

prepared by the impregnation method in the presence of activated carbon and at Cu/Fe (molar ratio)=1/2 gave the high BD yield of 8.5% for 100 min. In addition, under following reaction conditions; flow rate: Ar/1-C_4H_8/O_2=20/5/5 (mL/min) and reaction temperature: 270 ^oC, this catalyst gave the highest BD yield of 15.3% for 100 min. It was indicated that $CuFe_2O_4$ has the potential to produce BD efficiently at 270 ^oC.

According to XRD and XPS analyses of the catalyst before and after the ODH, the complete oxidation proceeded on the reduced copper species such as Cu_2O, and it was clarified that the maintenance of the $CuFe_2O_4$ structure and Cu^{2+} species were important to produce BD continuously in the ODH of but-1-ene under O_2 flow.

In Chapter 4, the improvement of the ODH activity of the copper oxide-based catalyst was studied. The effects of the catalyst supports, CuO loading, and the calcination temperature on the ODH of but-1-ene under O_2 flow were investigated. 5 wt% of CuO loaded on the high specific surface area SiO_2 catalyst calcined at 700 ^oC showed the highest BD selectivity of 92.8% and the high BD yield of 11.4%. It was indicated that the CuO-loaded SiO_2 catalyst was the good catalyst which can more efficiently produce BD at 270 ^oC. From N_2O titration, XRD, and XPS analyses, the copper surface area seemed to be related to the reactivity between O_2 and but-1-ene, and the presences of the copper oxide species such as mono-(μ-oxo)-dicopper and crystalline CuO promoted the complete oxidation of n-butenes and BD. As the result, it was indicated that the CuO-loaded SiO_2 catalyst having the high copper surface area without crystalline CuO and mono-(μ-oxo)-dicopper species is necessary to produce BD efficiently.

Chapter 5 described the effect of iron oxide crystalline structure on the ODH of n-butene at 450 ^oC. When ε-Fe_2O_3 was used for the ODH, this catalyst showed the highest BD yield of 17.1% among various iron oxide catalysts. However, the ODH activity of

this catalyst could not be maintained due to the transformation of crystalline structure. To maintain the catalytic activity, the effect of SiO_2 addition to ε-Fe_2O_3 (ε-Fe_2O_3-SiO_2) on the ODH of but-1-ene was investigated. ε-Fe_2O_3-SiO_2 catalysts indicated the high BD yield of about 18% and the high stability during the reaction for 4 h. SiO_2 was related to the maintenance of crystalline structure and the improvement of redox property of ε-Fe_2O_3. In addition, this catalyst showed the high BD yield (ca.17%) and the high stability for the ODH of *cis*-but-2-ene. Therefore, ε-Fe_2O_3 was proposed as a novel and excellent catalyst for the ODH of n-butene.

In summary, the copper oxide-based catalyst showed the high ODH activity at the low reaction temperature, and CuO-loaded catalyst realized the selective BD production via the ODH of but-1-ene under O_2 flow. The author believes that the copper oxide-based catalyst will be expected as the effective catalyst for the ODH of n-butene.

On the other hand, ε-Fe_2O_3 was proposed as the novel iron oxide-based catalyst in the ODH of n-butene at the high reaction temperature. Then, but-1-ene conversion of ca.30%, BD selectivity of ca.65%, and BD yield of ca.18% were obtained for 4h. There is no report that this catalyst was used for the ODH reaction. ε-Fe_2O_3 might be applicable as the novel and excellent catalyst for the ODH of the other organic compounds such as propane, n-butane, and ethylbenzene.

List of publications

Chapter 2

"Oxidative dehydrogenation of but-1-ene with lattice oxygen in ferrite catalysts"

T. Kiyokawa, N. Ikenega

Applied Catalysis A: General, **536** (2017) 97-103

Chapter 3

"Oxidative Dehydrogenation of But-1-ene at Low Temperature with Copper Ferrite Catalysts"

T. Kiyokawa, N. Ikenega

ChemistrySelect, **3** (2018) 6426-6433

Chapter 4

"Selective buta-1,3-diene production via oxidative dehydrogenation of but-1-ene with CuO-loaded catalyst"

In preparation

Chapter 5

"Oxidative dehydrogenation of n-butene with novel iron oxide based catalyst"

In preparation

Acknowledgments

The author's studies in this thesis are the summaries of present author's work carried out during 2014-2019 at Graduate School of Science and Engineering, Kansai University.

The author would like to acknowledge Professor Naoki Ikenaga of Kansai University for his instructive guidance, suggestions and innumerable instructions throughout the course of this study.

The author is sincerely grateful to Assistant Professor Kojiro Fuku of Kansai University for his kind help, valuable advice, and warm encouragement.

The author is grateful to Mr. Takaya Shizuma, Mr. Takashi Hagihara, Mr. Junsuke Hatayama, Mr. Masahiro Asada, Mr. Kazuki Hoshita, and Mr. Shun Machida for their cooperation in carrying out this study.

The author is also thankful to all the member of Catalysis Engineering Laboratory of Kansai University.

The author is grateful for a Research Assistantship from Graduate School of Science and Engineering, Kansai University.

The author deeply thanks his parents and all of his family for their continuous understanding and support.

Takayasu Kiyokawa

2019